ABSTRACT

CHANG, DAVID W. Investigation of Interfacial Interactions in Surfactant-mediated Shear Protection of Animal Cell Culture (under the direction of Dr. Orlin D. Velev).

The biotechnology industry has rapidly developed over the past few decades as innovative treatments for diseases and conditions emerge. This progress has led to rapid expansion of technologies to support the large scale (>10000L) production of therapeutics from microbial, fungal, mammalian, and insect cell culture. Progress in strain engineering and media optimization has led to more than hundred-fold increases in yield and productivity. However, significant gaps in knowledge still exist on the physical and interfacial phenomena involved during the upstream production process. These include fundamental understanding of interactions between cells, surfactants, and proteins, as well as the formation and mitigation of foams stabilized by bioparticles. Improper control of these interactions can hinder cell growth through shear damage, mass transfer limitations, and cell aggregation.

This dissertation investigates the impact of surfactants (Poloxamers) on the gas, liquid, and cell membrane interfaces to elucidate the mechanism of surfactant-mediated protection of cell culture. We then apply this knowledge to improve bioreactor performance in a commercial Chinese Hamster Ovary (CHO) cell process. First, we characterize the foam stability and equilibrium surface tension of pure and mixed Poloxamer systems in correlation with their ability to mitigate shear damage to cells in a turbulent environment. We demonstrate that while Poloxamer 188 (P188) can function as a highly effective shear protectant, the presence of a surface-active contaminant can greatly hinder its protective characteristics. Poloxamer 407 (P407) was found to function as such a surface active “impurity,” disrupting shear protection when mixed with P188 by preferentially adsorbing to the gas-liquid and membrane-liquid interface. The mechanism of

disruption by P407 was determined to be independent of cell-to-bubble attachment, suggesting that Poloxamer adsorption to and subsequent reinforcement of the cell membrane may play a key role in protecting cells in high shear environments. To support this hypothesis, we quantified the effect of these surfactants on cell membrane fluidity using two complementary methods: fluorescence anisotropy for rotational fluidity, and pyrene excimer fluorescence for lateral fluidity. We demonstrate that shear sensitivity is a function of membrane fluidity not only with different surfactants, but also among different cell lines. These findings demonstrate that membrane properties are key to surfactant-mediated shear protection of cell culture.

To apply this knowledge to cell culture processes, we developed an assay to quantify shear sensitivity of a cell suspension using a turbulent concentric mixer. Using this method to investigate a commercial CHO cell process, we determined that cell sensitivity steadily increased during protein production, resulting in unexpected shear damage during the latter half of the process. Simple addition of P188 resulted in significantly higher cell viability and decreased cell debris in the supernatant. The additional surfactant also improves the colloidal stability of the cell suspension by preventing cell aggregation and adhesion to surfaces. The principles and methods developed in this dissertation provide physiological insight into surfactant-mediated cell protection, and enable rational development towards new generations of materials for future bioprocess intensification.

© Copyright 2018 by David Chang

All Rights Reserved

Investigation of Interfacial Interactions in Surfactant-mediated Shear Protection of Animal Cell Culture

by
David Chang

A dissertation submitted to the Graduate Faculty of
North Carolina State University
in partial fulfillment of the
requirements for the degree of
Doctor of Philosophy

Chemical Engineering

Raleigh, North Carolina

2018

APPROVED BY:

_____	_____
Orlin D. Velev Committee Chair	Michael C. Flickinger
_____	_____
Balaji Rao	Saad Khan

DEDICATION

This dissertation is dedicated to my wife and family, for all their support and love.

BIOGRAPHY

David W. Chang was born in San Jose, California to Chein Ling Chang and Theresa Hsue. After growing up with his older brother Jefferson in Saratoga, CA, he attended the University of California at Berkeley for his undergraduate degree, where he obtained a B.S. in Chemical Engineering. Following his undergraduate career, he spent two years working in Santa Barbara, CA before beginning his graduate studies at North Carolina State University in Raleigh, NC in 2013. There, he performed research under Dr. Orlin D. Velev to apply the group's expertise in colloidal principles to the field of biotechnology. Following completion of his doctorate, David will pursue a career in the biopharmaceutical industry.

ACKNOWLEDGMENTS

The work in this dissertation would not have been possible without the personal and professional help of many individuals. First and foremost, I would like to thank my wife Christine, my parents, and my brother for their constant encouragement in my academic and professional pursuits. Their unconditional support has enabled me in all my accomplishments.

I would like to thank my advisor, Dr. Orlin D. Velev, whose guidance has shaped me into the scientist I am today. His mentorship, positive attitude, and intellectual support have all contributed to my personal and professional development and consistently maintained my motivation to pursue excellence.

I would also like to thank Biogen in Research Triangle Park, NC for supporting this work. A significant portion of the experiments in this dissertation were conducted with help from the Cell Culture Development team at Biogen. I am grateful to Weiwei Hu and Kelly Wiltberger, who envisioned this project, Douglas Osborne and Kevin Chang, who supervised and guided my research, An Zhang, who has served as a mentor, Vivian Shen, Marshall Bowden, and Alex Vaca, who significantly helped with bioreactor experiments, and all the other individuals who have supported me. Finally, I would like to thank all my friends and colleagues, scattered throughout the country, for keeping my spirits up during the challenging times of my graduate career.

TABLE OF CONTENTS

LIST OF TABLES

LIST OF FIGURES

Chapter 1 – Introduction to interfacial interactions in mammalian cell bioreactor operation

1.1 Background

The past five decades have seen unrivaled progress in therapeutic innovations for humans. Solutions for previously incurable diseases are rapidly emerging and expanding in scope. Many of these products are cell-derived biologics with complex functionality, from allogeneic recombinant proteins to autologous T-cell therapies. The commercial success of biologics can partly be attributed to their broad scope of high-value applications. Additionally, these therapeutics can be produced from a variety of cell types including mammalian, plant, fungal, and bacterial cells. With the wide array of available expression platforms and recombinant DNA technology, biologics can be tailored to treat various diseases, making an immense impact on society. Examples of products manufactured from biological origin include natural proteins (e.g., insulin, interferons, cytokines), vaccines, nucleic-acid based materials (e.g., RNA, DNA, gene therapies), recombinant therapeutic proteins, and monoclonal antibodies (mAbs). While simple microbes such as *E.Coli* and *S.cerevesiae* are well established in producing relatively simple proteins such as insulin, treatments of complex diseases including cancer often call for large biomolecules that can only be produced by intricate metabolic machinery. For this reason, mammalian cells are the preferred host organisms for protein therapeutics, with 60-70% of all recombinant protein pharmaceuticals produced from mammalian cells [1]. However, mammalian cells have low protein expression levels and are highly susceptible to physical damage compared to their prokaryotic counterparts, resulting in a large research space for process optimization. Efforts in maximizing productivity can be broken down into several broad categories: host cell engineering, growth medium development, cell line screening, and process engineering and development. Combined progress

in these areas has led to the achievement of gram-per-liter product titers in mammalian cell bioreactors, a more than 100-fold yield improvement over similar processes in the 1980s [1].

Recombinant therapeutic proteins produced with large scale (>10,000L) animal cell cultures in stirred tank reactors generate more than $200 billion in sales globally, and are projected to reach $500 billion by 2020 [2]. The complete process of commercializing a biopharmaceutical product for therapeutic use can take years to decades: from initial drug discovery, cell line development, media formulation, bioreactor process development, downstream purification, and finally to clinical trials and FDA approval, the cost to market averages $2.9 billion per drug [3]. Additionally, 87% of drugs which reach Phase 1 clinical stage fail to launch [4], so drug developers must maintain a robust pipeline and develop multiple drug candidates simultaneously to mitigate risk. Therefore, process development for each drug candidate must be efficient to rapidly scale-up and generate material for patients in clinical trials. Despite the risks and technical challenges, societal and financial incentives drive the industry forward, and scientists continue to push bioprocesses to higher cell density, productivity, and yield.

Culturing animal cells in bioreactors is a complex and intricate art. The process can be operated in batch, fed-batch, or continuous modes. Although protein expression and cell metabolism are primarily achieved via biological pathways, the interfacial and colloidal interactions within a stirred tank bioreactor can impede or even prevent upstream bioprocessing if they are poorly understood and controlled. These include shear forces, which can be lethal to cells, foam buildup, which can inhibit mass transfer (through antifoam addition), and surfactant or protein interactions with gas/liquid, cell/liquid, and cell/gas interfaces, all of which can be detrimental to the process. The main objectives of this thesis are to expand the fundamental knowledge of interfacial interactions within modern bioreactors by focusing on the effect of

surfactants on the gas, liquid, and cell interface. We then apply this knowledge to develop strategies to control these interactions to improve the operation of stirred tank bioreactors. The first chapter of this thesis provides a foundational background of bioreactor operation and the relevant interfacial interactions between components in the bioreactor.

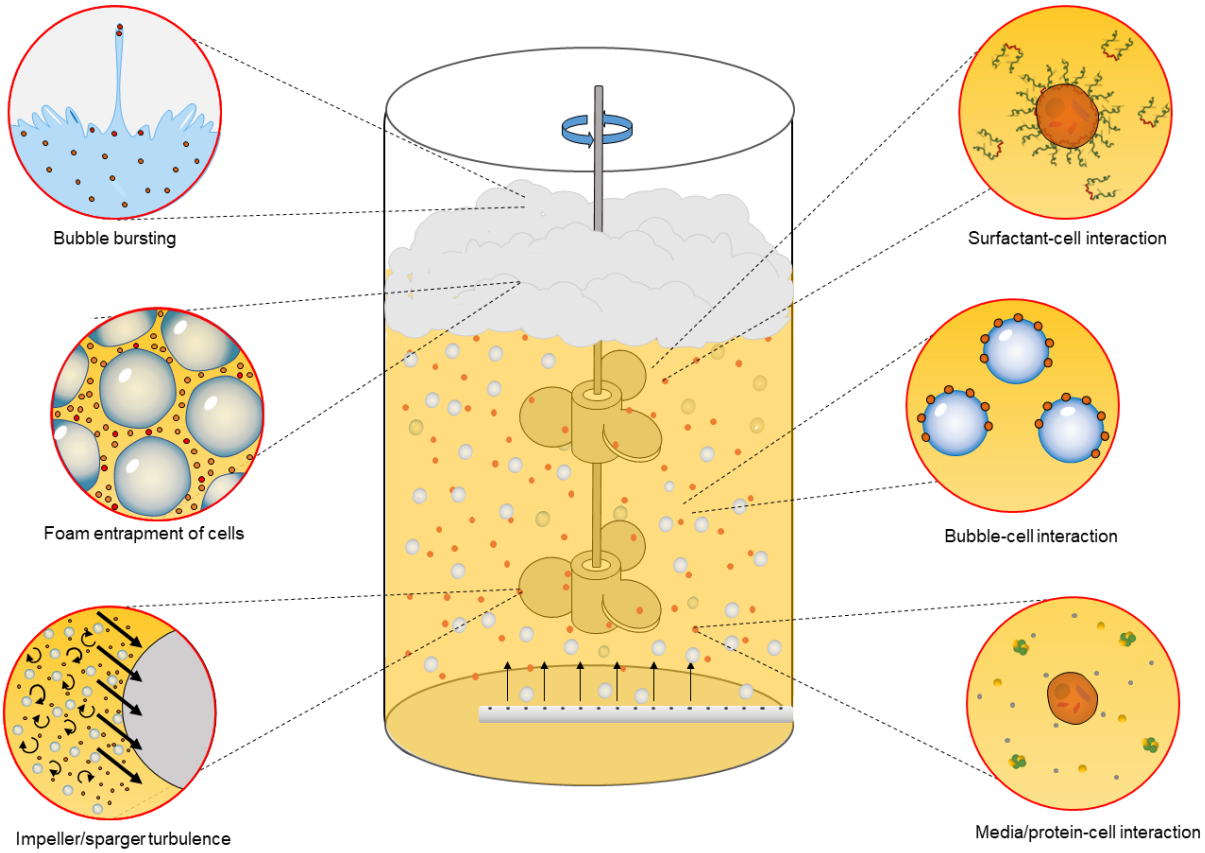

Figure 1.1: Summary of interfacial interactions in a fed-batch bioreactor process. Bubble bursting, foam entrapment, and turbulence from agitation and gas entrance velocity can lead to cell damage. The interfacial interactions between cells, bubbles, and surface active material in the bioreactor can be a processing challenge during protein production.

1.2 Interfacial interactions in animal cell bioreactors

Chinese Hamster Ovary (CHO) cells are the most widely used mammalian cell hosts for industrial production of recombinant protein therapeutics. Their ability to grow in suspension (as opposed to anchored to a surface) combined with their rapid reproduction rate makes them ideal host cells in the biopharmaceutical industry. With recent progress in metabolic engineering, protein titers as high as 10 g/L have been reported with cell densities greater than 2×10^7 cells/mL in a fed-batch process [5,6]. During bioreactor scale-up, however, several process engineering challenges have emerged as a result of the increased cell density and protein titer. Many of these problems can be ascribed to the interfacial interactions, as shown in

Figure 1.1. Hydrophobic cells on the order of 10-20 μm in diameter adsorb to rising gas bubbles, which are sparged into the system to maintain dissolved oxygen, an essential nutrient for cellular respiration. The cells subsequently become transported to the foam layer at the top of the bioreactor, where they can sustain damage from bubble bursting, or become nutrient-limited in the stagnant foam layer. Impeller agitation to keep the system well-mixed and high gas entrance velocity (GEV) also generate hydrodynamic stress on the cells. Changes in pH, temperature, cell density, and cell physiology add dynamic complexity to the system, while protein production and waste accumulation in the medium also significantly impact the interfacial activity during the course of the process.

Nonionic surfactants are routinely used in cell culture as shear protectants. These surfactants protect micron-sized cells from the mechanical damage caused by agitation and air bubbles as they burst and oscillate at the air-water interface. The typical surfactants used today are Poloxamer 188 (P188) or analoguous type surfactants from the Poloxamer family of triblock copolymers produced by BASF. Despite continued research efforts by industry and academia, the

mechanism of cell protection by surfactants is poorly understood. As a result, the type and concentration of Poloxamer surfactants used in bioreactor operation are largely determined on an empirical basis, with some Poloxamers being extremely effective protectants, while others offer no protection or are even toxic to cells. In addition, lot-to-lot variation of P188 has resulted in inconsistent performance in shear protection during commercial manufacturing [7–10]. While P188 has worked sufficiently for industrial purposes in past decades, fundamental knowledge of its role in surfactant protection of cells is needed to further intensify cell culture processes. Therefore, a major goal of this thesis is to expand our knowledge of surfactant interactions with gas, liquid, and cell interfaces.

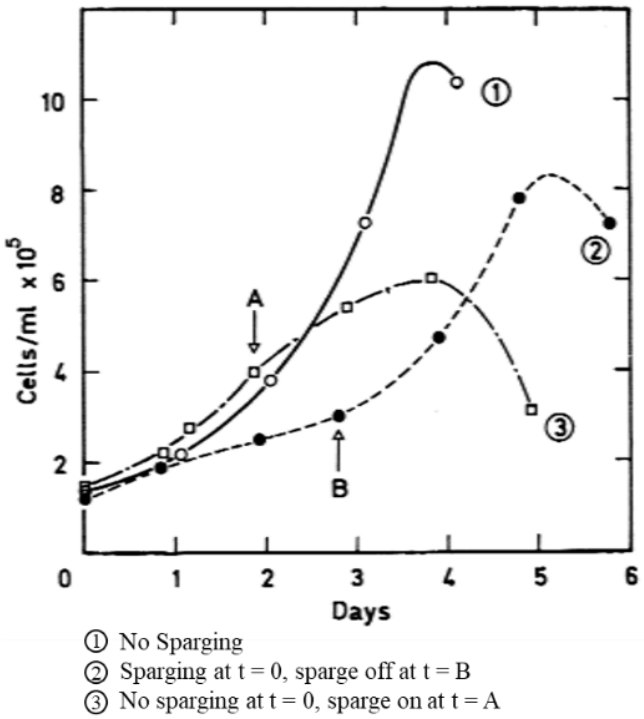

Figure 1.2: Example of cell damage during sparging adapted from Ref. [11]. Maximum cell growth is achieved in batch 1 with no sparging. In batch 2, the bioreactor begins with low cell growth as a result of initial sparging. At around day 3 (point B), the sparging is ceased and cell growth quickly increases. In batch 3, the cells start with high growth with no sparging. Around day 2 (point A), sparging is turned on, resulting in growth decline.

1.2.1 Aeration and agitation

Aeration is used to control the concentration of dissolved oxygen (DO) in the medium. Maintaining an optimum range of DO is one of the key process considerations in animal cell culture and in scale-up of such processes, as insufficient oxygen results in low cell growth and yield, while excess oxygen can result in cytotoxic hyperoxia [12]. Sparging of air or oxygen-enriched air is the most economical and scalable way to aerate the medium, and remains the most widely used method in industry today. Historically, gas sparging for DO control was discovered to damage cells during early scale-up attempts for suspension animal cell culture, as shown in **Figure 1.2** [11]. In this study, mouse LS cells were grown in 3-L culture with and without sparging. Cell growth was significantly hindered whenever air bubbles were introduced into the system. This problem was not encountered during development of previous biofermentation processes with microbial or plant cells [13]. As shown in **Figure 1.3**, the relative fragility of mammalian cells may be attributed to their lack of a rigid cell wall.

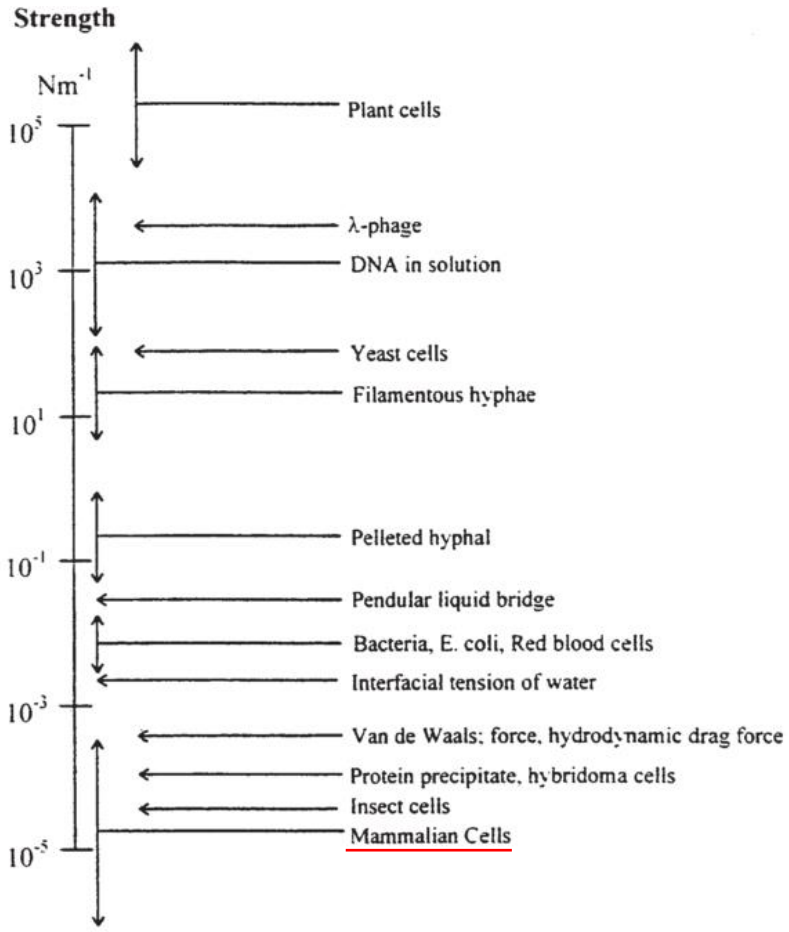

Figure 1.3: Estimated characteristic strength of several biological particles [14]. The strength of mammalian cells is lowest, indicating their fragility relative to other cell types.

In the presence of gas bubbles, animal cells sustain cell damage during the violent breakdown of foam collapse [15]. Gas bubbles at a free interface are inherently unstable, and require addition of surface-active agents (surfactant, protein, particles, etc.) which adsorb to the interfacial boundary, to add long-term stability to the liquid film. Eventually, the gas bubble becomes unstable due to drainage of fluid or diffusion of gas. During breakdown of a bubble, the liquid film surrounding the gas phase thins until the interface can no longer be sustained. Subsequently, the film breaks, and surface tension causes the edges of the film to rapidly recede down the side of the cavity, colliding at the bottom and producing upward and downward traveling

jets [16]. Cells attached to the breaking film or in the vicinity of the jet can sustain fatal damage. This sequence of events is shown below in **Figure 1.4.**

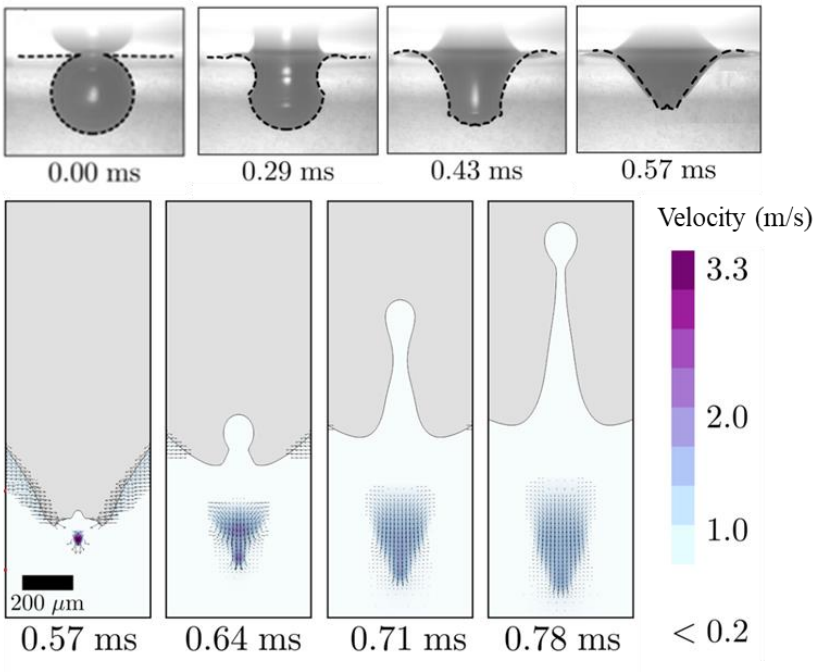

Figure 1.4: Sequence of events during bubble collapse. During initial film breakage (0 – 0.57 ms), the film recedes to a point. From 0.57 ms to 0.78 ms, the liquid forms an upward and downward jet with high velocity. In this image, only the velocity field for the downward jet is shown [17].

Several attempts have been made to quantify the hydrodynamic forces associated with bubble bursting by calculating the maximum energy dissipation rate (EDR) using computational modeling [15,17,18]. EDR is a scalar value representing the rate of work done on a fluid volume by the surrounding liquid, and is commonly used as a measure to relate hydrodynamic flow stresses to cell damage [19–22]. In **Figure 1.5**, literature values of EDR thresholds (EDRs at which adverse effects on the cell are observed) of various mammalian cells are compared to the calculated EDRs of common bioreactor hydrodynamic flows. Lethal cell responses have been recorded for CHO cells in suspension from 10^5 to 10^8 W/m^3. Other mammalian cells of industrial relevance including

HeLa, PER.C6, and Hybridoma cells also experience adverse effects between EDR of $10^6 – 10^8$ W/m^3. Additionally, the EDR threshold for CHO cells has been shown to decrease as much as 2 orders of magnitude when the culture is subjected to chronic hydrodynamic stresses [23]. To put these figures into perspective, the EDRs of several relevant hydrodynamic events have also been quantified in **Figure 1.5**. Interestingly, the highest calculated energy dissipation rates come from bubble bursting and pumping the cells through restricted orifices. This is consistent with the observations from other researchers, who have noted that agitation related hydrodynamics do not typically damage cells under standard bioreactor operating conditions [24,25].

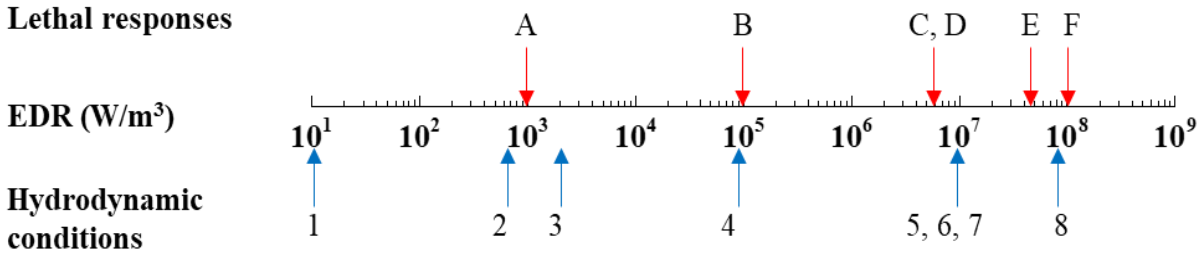

Lethal Cell Response

Symbol	EDR [W/m^3]	Cell Type	Cultivation mode	Reference
A	10^3	CHO-K1	Anchored	[26]
B	10^5	CHO-K1	Suspended	[27]
C	$6*10^6$	PER.C6	Suspended	[28]
D	$6*10^6$	CHO (GS)	Suspended	[22]
E	$5*10^7$	HELA S3	Suspended	[29]
F	10^8	CHO-K1	Suspended	[28]

Hydrodynamic Conditions

Symbol	EDR	Process	Description	Reference
1	10^1	Agitation	Average EDR in animal cell bioreactor	[2,30]
2	$8*10^2$	Agitation	Average EDR in 10L vessel	[31]
3	$2*10^3$	Agitation	Average EDR in 22000L fermentor	[32]
4	10^5	Agitation	Maximum EDR in 10L vessel	[31]
5	10^5	Agitation	Maximum EDR in 22000L vessel	[32]
6	10^5	Bubble burst	Air in water, D = 6.32 mm	[15]
7	10^7	Filtration	Cells pumped through membrane	[33]
8	10^8	Bubble burst	Air in water, D = 1.7 mm	[15]

Figure 1.5: Summary of reported energy dissipation rates (EDRs) where cell damage has been observed, along with EDRs of relevant hydrodynamic environments. Adapted from [34].

Recently, Walls et al. (2017) demonstrated in a numerical study that the maximum EDR (EDR_{max}) from bubble bursting depends strongly upon the computational model's mesh size, showing that increased mesh resolution resulted in unbounded EDR_{max} (**Figure 1.6**), while the volume affected by EDR_{max} decreased with increasing mesh resolution. All of their calculated EDR_{max} values exceeded the expected threshold for lethal cell response (10^6-10^8 W/m^3). The authors conclude that the EDR_{max} is not an accurate way to assess or predict cell damage [17]. Nevertheless, the stresses associated with sparging remain the primary source of cell damage in bioreactors. Bubble bursting damage is compounded by cell-bubble attachment, which concentrates the cells at the top of the bioreactor. Cells tend to adsorb at the surface of rising bubbles due to thermodynamic and hydrophobic interactions, similar to in a mineral flotation process [35–37]. The adsorption tendency can be quantified by measuring the induction time, which is the contact time between cell and bubble surface necessary for adsorption to occur [38,39].

As mentioned previously, impeller agitation is typically not a major source of damage in animal cell culture [25]. However, the impeller design and agitation rate greatly affects mass transfer rate by effecting the gas holdup (bubble residence time) and bubble coalescence in the bioreactor. Increasing agitation rate decreases the required gas flow rate, which can be an efficient strategy to decrease foaming or cell damage [40–42]. During scale-up, however, one must consider the process transfer to manufacturing scale. A common criterion to determine the agitation rate when transferring from 5-L to larger scales is to maintain a constant power-to-volume ratio (P/V) of the impeller. High agitation rates in the small scale are exacerbated during scale-up to 15000 L bioreactor, and can result in high turbulence and cell damage [40]. In addition, a minimum sparge rate should also be maintained to prevent CO_2 accumulation in the medium, which will be

discussed further in the following section. Therefore, a balance must be kept between agitation rate and gas flow rate.

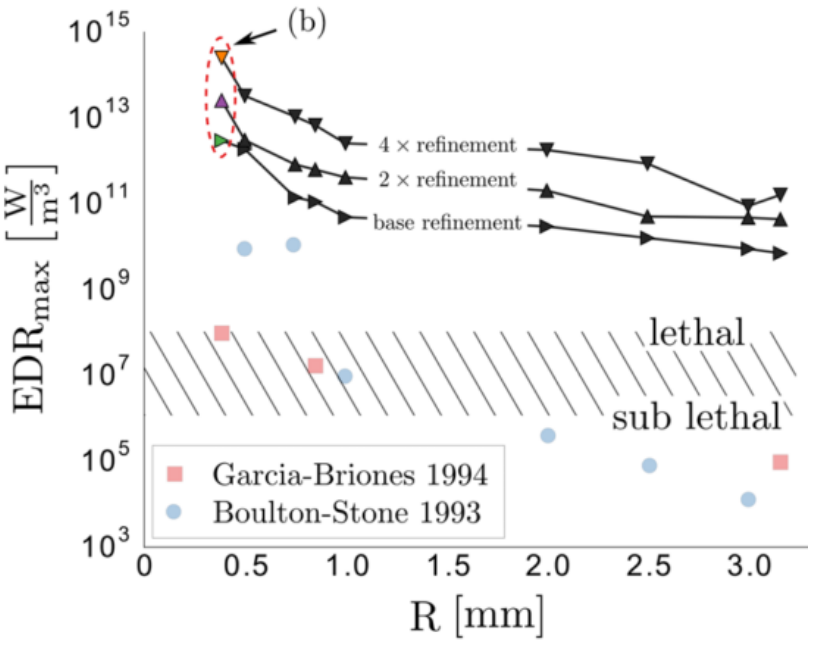

Figure 1.6: Summary of maximum EDRs calculated in several literature studies for bubbles of different sizes [17]. This figure illustrates that the EDR_{max} varies more than 2 orders of magnitude depending on the mesh refinement used in the simulation.

1.2.1.1 Basic mass transfer concepts in sparged bioreactors

The rate of mass transfer in the bioreactor is determined by the oxygen transfer rate (OTR):

$$OTR = k_L a(C_{O_2}^{*} - C_{O_2}) \quad \textbf{(Equation 1.1)}$$

where k_L and a are the mass transfer coefficient and surface area, respectively, and $C_{O_2}^{*}$ and C_{O_2} are the saturation oxygen concentration in the sparged gas and dissolved oxygen concentration in the medium, respectively. Simple inspection of **Equation 1.1** indicates that in order to maximize the OTR, one should increase the interfacial area, the mass transfer coefficient, and the driving force. Strategies to achieve this include increasing the vessel pressure to increase oxygen

solubility, using smaller bubble size for increased surface/volume gas ratio, and sparging pure oxygen. However, the aeration strategy must be balanced with CO_2 removal, as stripping of CO_2 (a byproduct of aerobic metabolism) is a crucial secondary function of sparging. Carbon dioxide accumulation can inhibit cell growth and protein production [43], change glycosylation profile of the product [44], and change the pH of the medium. Although sparging small bubbles and using pure O_2 both increase $(k_L a)_{O_2}$, they significantly reduce $(k_L a)_{CO_2}$ [45].

The type and design of the sparger affects not only the mass transfer rate, but also the magnitude of cell damage. Typically, drilled hole spargers (DHS) or sintered spargers (SS) are used in mammalian cell bioreactors, producing millimeter to micron-sized bubbles, respectively. The sparger can also be designed in the form of a straight pipe, ring, or concentric rings. Sintered spargers (also known as frit sparger or diffuser) have been associated with higher cell damage and foaming due to the small size of the bubbles, which have larger Laplace pressure. On the other hand, using drilled hole spargers with insufficient number of holes can result in high gas entrance velocity (GEV), which has been empirically shown to have negative impact on mammalian cell culture [46,47]. Therefore, proper sparger design is crucial during the scale-up process. One recent modeling study has shown that increased GEV does not correlate with high EDR. Instead, the authors hypothesized that the cell damage results from normal and shear stresses coupled with liquid phase turbulent velocity gradients, which they quantify with a parameter called the stress-induced turbulent energy production (STEP), a value generated from CFD models [48].

Bubble-free strategies for maintaining dissolved oxygen have been explored, including surface aeration and membrane aeration [49]. Surface aeration relies on high agitation rates and low aspect ratio of the vessel to maintain dissolved oxygen using air in the headspace, such as in a lab-scale shaker flask. In membrane aerated vessels, silicone tubing with high oxygen

permeability is arranged within the bioreactor to maximize the surface area, as shown in **Figure 1.7.** Although improved mass transfer efficiency can be achieved, membrane aeration is expensive to operate and design principles are limited, making it a niche application for particularly shear-sensitive cell lines [50].

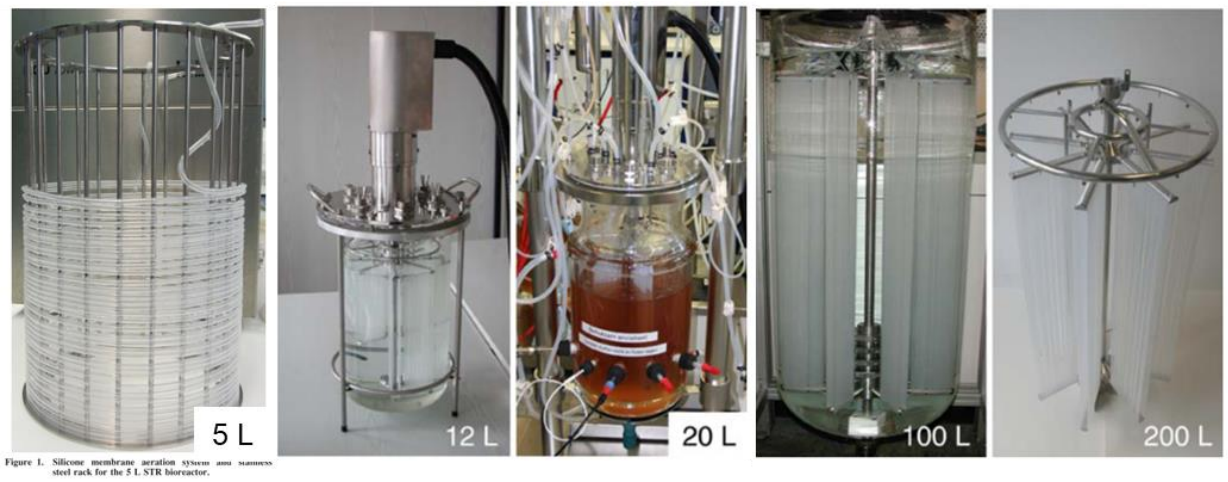

Figure 1.7: Examples of membrane aerated bioreactors at different scales [49,50]. Silicone tubing with high oxygen permeability is arranged to maximize mass transfer in the vessel. Air or oxygen-enriched air is flowed through the tubing during the process to maintain dissolved oxygen.

1.2.2 Foaming in bioreactors

Persistent foam in bioreactors results from the combination of gas bubbles and the presence of surface active molecules and/or particles in the medium. Generally, formation of a large foam head is undesirable, but a small foam head is of little concern and can be easily managed by addition of synthetic antifoam. However, in processes with particularly high cell debris or cell density, bioreactor foam can become extremely stable and resistant to antifoam due to Pickering stabilization of the thin films. In such systems, buildup of foam can clog vent filters, which can result in difficulties in maintaining vessel pressure or even contaminate the bioreactor [51]. Foam

production is typically autocatalytic, since cells can become trapped and lysed in foams, leading to additional foam stability. Therefore, understanding the factors contributing to foaming is important to limit their formation.

The composition of foam in bioreactors can range from “clean” foams stabilized by relatively small surfactant molecules, to “dirty” foams stabilized by cell debris, waste products, and large proteins in the foam films (**Figure 1.8**). Surfactant and molecularly stabilized foams are easily managed by addition of chemical antifoamers, whose fast-spreading oil droplets rapidly disrupt bubble films with Marangoni forces [52,53]. In cell culture, silica particle in silicone oil emulsions are the preferred antifoam due to physiological compatibility. The “dirty” foams, stabilized by proteins, cell debris, and particles, are much more difficult to manage due to their high film elasticity and ability to withstand perturbations [54,55]. These foams typically form at high cell density and protein titer, or when viability in the bioreactor has decreased, releasing large amounts of cell debris.

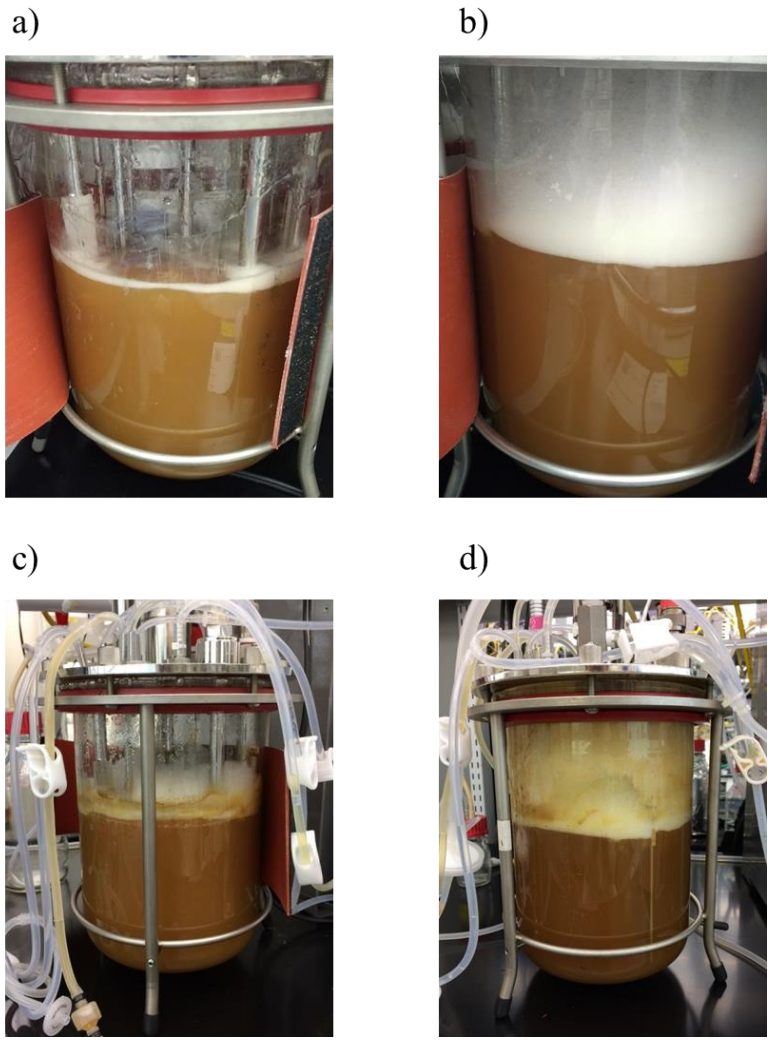

Figure 1.8: Examples of foam buildup in 5-L benchtop reactors in a CHO cell fed-batch process. In (a)-(b), the foams are relatively clean, indicating that the foam is stabilized by low-molecular species, including surfactant. In (c)-(d), the presence of cell debris, protein, and waste byproducts results in a stable foam which is difficult to suppress by antifoam addition.

Although addition of chemical antifoams is the simplest way to control foam, it also has significant drawbacks and side effects. Firstly, antifoam has been shown to decrease oxygen mass transfer rate [54]. When the silicone oil emulsifies into the bulk liquid, the oil droplets cause bubbles to coalesce as they rise through the medium, decreasing interfacial area. The quick-spreading oils also coat bubble surfaces, adding additional resistance to mass transfer [56]. The

decreased mass transfer necessitates additional sparging and foam formation in a positive feedback loop. Secondly, antifoam particles can become exhausted over time [52,57–59]. This leads to not only decreased antifoaming efficacy, but the particles also persist and can eventually contribute to foam stability. Lastly, chemical antifoam has also been shown to increase cell sensitivity in sparged cultures [60]. This would increase cell damage, which would in turn lead to higher foaming.

The mechanism of foam destruction by chemical antifoam begins with the oil phase entering the thin film of the bubble, as shown in **Figure 1.9**. The oil spreads through the aqueous film due to surface tension gradients, thinning the bubble film until the interface collapses. In practice, the energy barrier for the oil to enter the aqueous film is relatively high, hindering the rate of action. Solid nanoparticles, usually made of hydrophobically modified silica of jagged or irregular shape, are added to the antifoam formulation to decrease the energy barrier for oil to enter the thin film (**Figure 1.9C**). The nano-sized particles, which carry the oil phase, can easily pierce and enter the bubble film, releasing the oil to spread and destroy the foam [53]. However, once the particles become depleted of the oil phase, they become exhausted and do not contribute to foam destabilization. Exhausted particles can become reactivated by addition of the pure oil phase [61], but this principle has not yet been verified in cell culture processes.

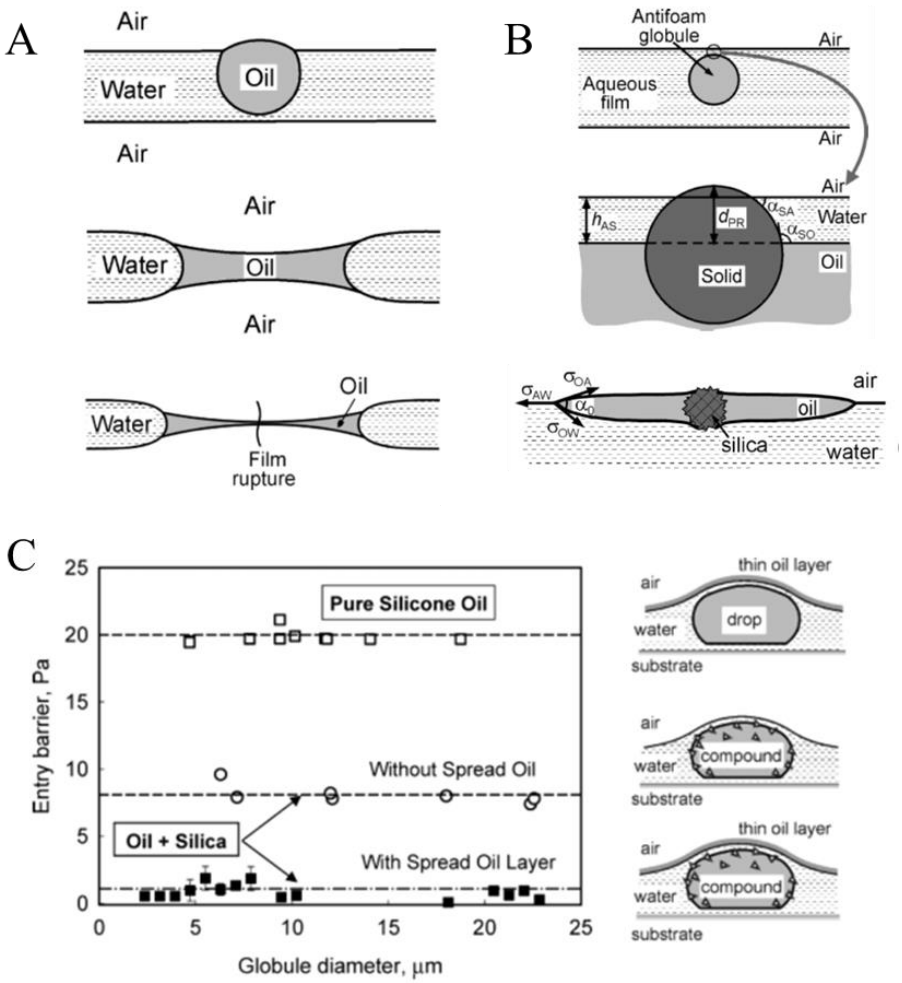

Figure 1.9: Mechanism of action of oil and particle-in-oil antifoams adapted from [52]. (A) The oil globule enters the thin film of the bubble, spreading and eventually causing film ripture. (B) Solid silica particles can enhance antifoam efficiency by carrying oil globules into the aqueous film. (C) The entry barrier (activation energy) of oil to enter the aqueous film is decreased by addition of silica particles. This synergy makes oil + silica antifoams much more effective than pure silicone oil antifoams.

1.3 Role of surfactants in shear protection of cells

The addition of surface active additives to the cell culture medium was found to mitigate sparging damage to both mammalian and insect cells [62,63]. The first additives used for this purpose were fetal bovine serum (FBS) and Poloxamer 188 (also known as Pluronic F-68) [11,64,65]. Because of the industry shift towards chemically defined media (CDM), Poloxamer

188 (P188) became the preferred choice, and is still the most widely used shear protectant in mammalian cell culture today. Besides Poloxamers, polymer additives such as methylcellulose, polyvinylpyrrolidone (PVP), polyethylene glycol (PEG), polyvinyl alcohol (PVA), and maltopyranosides have all been shown to decrease cell damage [66–69]. The structure of these molecules is shown in **Figure 1.10**. These compounds all have varying degrees of surface activity, with the ability to adsorb to both gas and cell interfaces. The mechanisms of surfactant-mediated protection of cells has been a topic of research for several decades. These studies have shown that the mechanisms can be broadly divided into two categories: (1) surfactant decreases adsorption of cells to bubbles, and (2) surfactant strengthens the plasma membrane to increase the cell's physical robustness.

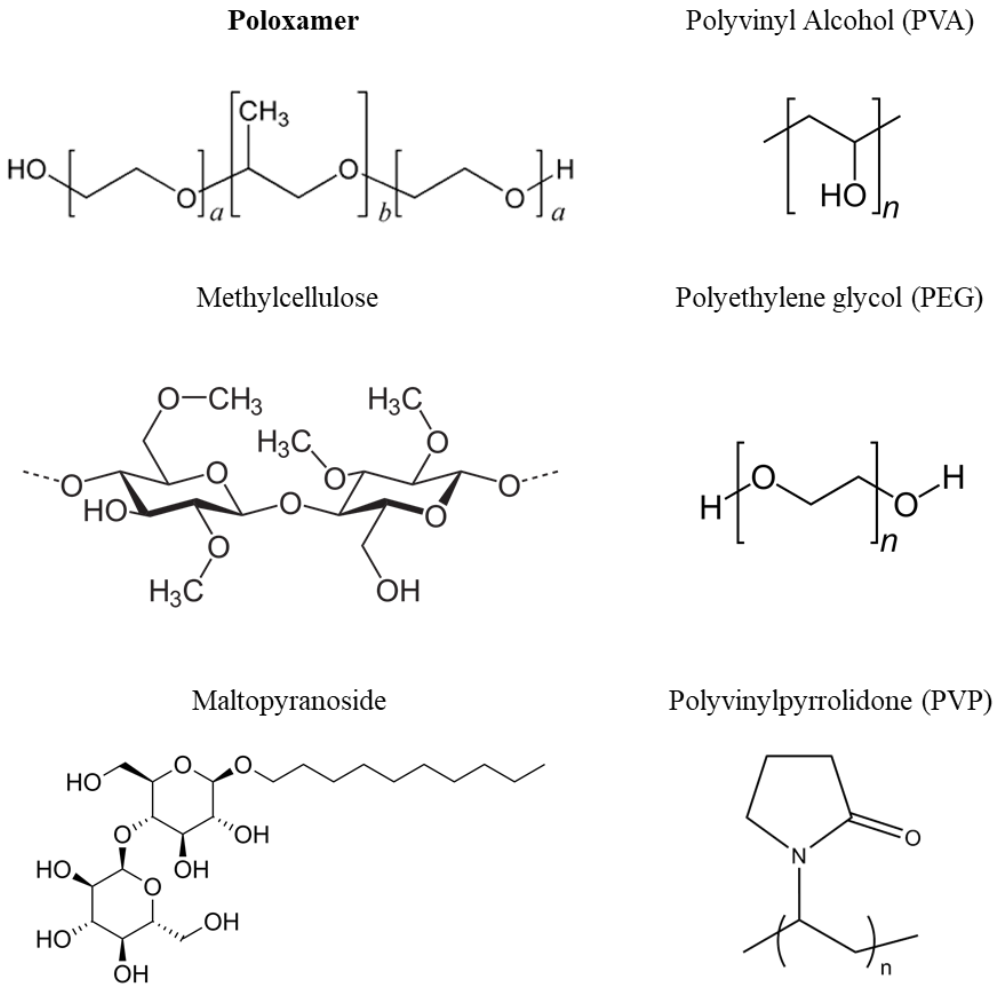

Figure 1.10: Chemical structure of several polymer molecules which have been shown to decrease shear damage in animal cell culture [39,69,70].

1.3.1 Effect of surfactant on cell-bubble attachment

The adsorption of cells to bubbles depends on the resulting free energy change when a new interface is formed, which is related to the interfacial tension of the three phases, shown in **Equation 1.2** [35]:

$$\Delta F_{adh} = \gamma_{bubble-cell} - (\gamma_{bubble-liquid} + \gamma_{cell-liquid}) \quad \textbf{(Equation 1.2)}$$

where ΔF_{adh} is the free energy change upon adhesion of cell to bubble, and $\gamma_{bubble-cell}$, $\gamma_{bubble-liquid}$, $\gamma_{cell-liquid}$ refer to the gas-cell, gas-liquid, and cell-liquid interfacial tensions, respectively. Addition of surfactant decreases $\gamma_{bubble-liquid}$, the liquid-vapor interfacial tension, increasing the free energy change of cell-bubble adhesion and making attachment less favorable. P188 also increases the induction time for cell-bubble adsorption [39], and reduces cell hydrophobicity, which may decrease hydrophobic interactions between cells and bubbles [71]. Therefore, the ability of surfactants to decrease cell-bubble attachment is believed to contribute strongly to the increased viability of cell culture in the presence of bubbles [39,72–74]. This phenomenon has been quantified using a variety of techniques. Ma et al. (2004) constructed a bubble column to collect the foam layer by bubbling air through a cell suspension [75], and found that addition of P188 decreased the number of cells adsorbed to each bubble by a factor of 3. Trinh et al. (1999) collected and observed the ejected droplet following bubble rupture, and found that P188 decreased both the cells adsorbed per bubble, and the number of cells killed per bubble [62]. Some researchers have also found that the rate of surfactant adsorption to the air interface, which can be quantified by the dynamic surface tension, also correlated with cell protection [69]. They explained that during bioreactor operation, the residence time of bubbles is short, and the surfactant should rapidly adsorb to the gas interface to prevent cell-bubble interactions. However, experimental studies have shown that surface tension and cell-bubble adsorption cannot fully explain the protective effects of surfactants. Some additives, including PEG and PVP, increased cell-bubble attachment compared to additive-free media, while still decreasing cell damage. Therefore, adsorption of surfactant to the cell interface likely contributes as a secondary mechanism of cell protection.

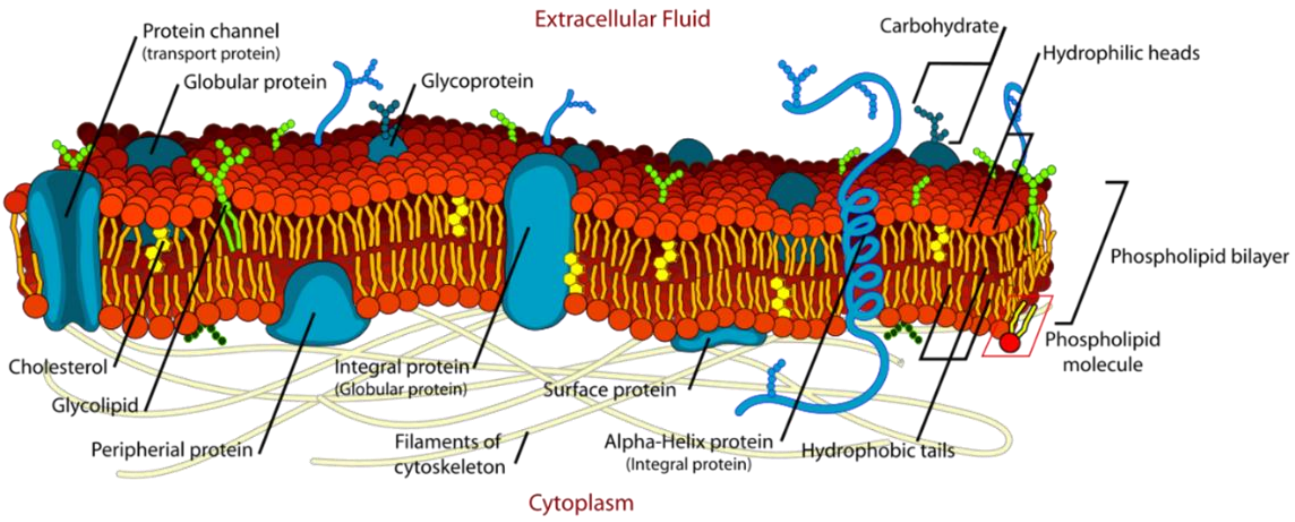

Figure 1.11: Schematic of the components in the cell's plasma membrane [76]. The phospholipid molecules self-assemble to form the bulk structure of the bilayer.

1.3.2 Effect of surfactant on cell interfaces

Surfactants have been shown to interact with cell membranes to change their mechanical stability. The mammalian cell plasma membrane is the cell's primary layer of defense against physical and chemical stresses, regulating chemical flux and separating internal organelles from the bulk environment. It is a self-assembled bilayer consisting of phospholipids, transmembrane proteins, cholesterol, and various glycolipids and glycoproteins (**Figure 1.11**). The lipid bilayer is a dynamic structure exhibiting lateral and rotational diffusion of the various components, as well as flip-flopping of the phospholipid molecules from the inner to outer layer or vice versa [77,78]. Adsorption of surfactant molecules increases or decreases the strength of the bilayer. Cell surfaces are negatively charged due to ionic concentration gradients regulated by the transmembrane proteins. In general, cationic and ionic surfactants tend to have cytotoxic or inhibitory effects on cell growth due to solubilization or strong electrostatic interactions with the membrane [69]. As a

result, the additives which have been thus far shown to efficiently protect cells are nonionic surfactants [66,79].

Table 1.1: Physical properties of several Poloxamer surfactants tested for cell protection with Sf-9 insect cells. The table is organized by increasing HLB, which correlates well with the surfactant's performance in protecting cells. Poloxamer 188, highlighted in bold, is the most widely used protectant in industry. Adapted from [80].

Poloxamer	Pluronic®	Avg MW (Da)	Wt% PPO	HLB	Effect on cell growth	Cell protection
401	L-121	4400	90	1	Lysis	N/A
181	L-61	2000	90	3	Lysis	N/A
403	P-123	5750	70	8	Lysis	N/A
333	P-103	4950	70	9	Lysis	N/A
334	P-104	5900	60	13	Inhibition	N/A
234	P-84	4200	60	14	Lysis	N/A
185	P-65	1900	50	15	Inhibition	N/A
335	P-105	6600	50	15	Inhibition	N/A
105	L-35	1900	50	19	None	Yes
407	F-127	12600	30	22	None	Yes
108	F-38	4700	20	27	None	Yes
338	F-108	14600	20	27	None	Yes
188	**F-68**	**8400**	**20**	**29**	**None**	**Yes**

Poloxamers are composed of two hydrophilic poly(ethylene oxide) (PEO) side groups attached to a hydrophobic poly(propylene oxide) center group (**Figure 1.10**). They are synthesized in a wide range of physical properties by varying the total molecule size (molecular weight), and the ratio of PPO to PEO (hydrophobicity). Poloxamers with high hydrophobicity, which can be characterized by low hydrophilic-lipophilic balance (HLB), tend to lyse the cell (**Table 1.1**). These

surfactants act as cell lysing agents by solubilizing or micellizing the phospholipid bilayer [81]. On the other hand, more hydrophilic Poloxamers (HLB > 15) are generally benign, and can be used in cell protection. A structure-performance study with Poloxamers of varying physical properties on *Spodoptera Frugiperda* Sf-9 insect cells found a strong correlation between HLB and cell protection, as shown in Table 1.1 [82]. However, this trend did not hold for Plurafacs with di-block PEO-PPO structure. Of the surfactants that did protect cells, no correlation between physical properties and efficacy was reported. Although Poloxamers with high HLB have better performance in biological applications, their interactions with the cell interface remains an ongoing topic of research.

Several Poloxamers have been shown to exhibit strong but benign interactions with cell membranes, making them useful in various biomedical applications. Beyond their use as cell protectants in bioreactors, Poloxamers have been used in drug delivery, medical imaging, and even as a treatment for vascular diseases [83–86]. Several studies have shown that Poloxamer 188 seals injured membranes, adsorbing to imperfections in the membrane structure similar to a "clotting" effect [87,88]. These interactions have been verified with computer simulations, as shown in **Figure 1.12**. P188 sealed membrane pores of model bilayers, while interaction with the more hydrophobic Poloxamer 235 resulted in significant distortion of the bilayer and low interaction between PEO chain and hydrophilic lipid headgroups [89]. P188 has also been experimentally shown to increase cell resistance to osmotic, electrical, and thermal stresses [90,91]. In studies with cell culture, Poloxamer 188 increases membrane bursting tension [92] and decreases cell membrane fluidity [93,94]. In addition, Poloxamer integration into cell membranes has been directly observed using a fluorescent derivative of P188 [95]. Although the effects on cell metabolism and protein production are unclear [96], these examples show that surfactant

adsorption to the membrane bilayer may play a significant role in increasing cell robustness, and will be major topic of discussion in this thesis.

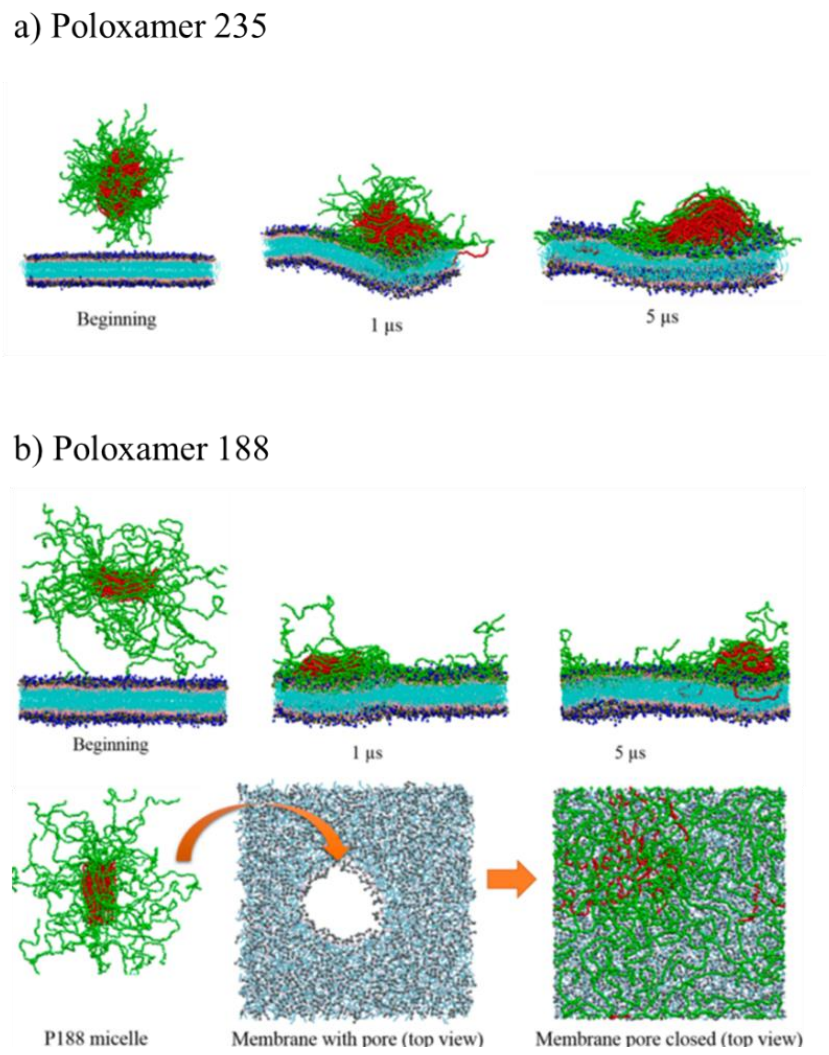

Figure 1.12: Computer simulation results illustrating Poloxamer micelle interaction with model lipid bilayer. PEO is shown in green and PPO is shown in red. (a) Spherical Poloxamer 235 micelle causes bending of the bilayer due to its high hydrophobicity. (b) Poloxamer 188, which forms a more cylindrical micelle, has strong interactions with the bilayer surface. The PEO groups spread out and cover the surface of the bilayer, sealing the pore. Adapted from [89].

1.4 Methods to quantify shear sensitivity of cell culture

Many different assays have been explored to quantify the shear sensitivity of cell culture. Generally, these assays stress the cells with defined hydrodynamic flows, and the resulting damage is quantified by measuring either the cell viability change (with Trypan blue dye exclusion), or lactase dehydrogenase (LDH) concentration [97]. The Trypan blue exclusion test determines cell viability based on cell membrane integrity, with stained cells considered nonviable and unstained cells considered viable. One limitation of this technique is that cells that are completely lysed while stressed are not counted. Also, cells with injured but recoverable membranes are considered nonviable. On the other hand, LDH is an intracellular enzyme released upon cell damage. This assay may be more reliable than Trypan blue because lysed cells and injured cells both release LDH, and is gaining popularity as automated instrumentation for metabolite analysis becomes widely available.

Examples of techniques which have been previously used to compare shear sensitivity of cell culture are shown in **Figure 1.13**. Each of these assays has advantages and limitations with respect to feasibility, accuracy, and practicality. For example, the rotary pump (**Figure 1.13b**) simulates a scenario in which the cells are being sheared during transportation, such as for cross-filtration or perfusion. However, this experimental setup is cumbersome and the associated EDRs and shear rates are difficult to quantify. On the other hand, shearing in a viscometer is highly controlled and simple to perform, but limited to laminar flows, which is not representative of bioreactor hydrodynamics [98,99]. Recirculation of cell suspension through a thin capillary or nozzle (**Figure 1.13a, d**) can also be used to investigate the effect of shear on cell growth and productivity, but requires long experiment time and expensive instrumentation. A large amount of literature has been published using the flow contraction microfluidic device, which was designed by the

Chalmers group [19,22,26,28,100–103]. This device has proven to be an insightful tool to compare EDR thresholds of CHO, dinoflagellate algae, HB-24 (mouse hybridoma), SF-9 (insect *Spodoptera frugiperda*), and MCF7 (human breast carcinoma) cells, and continues to be used in research.

More recently, the mechanism of Poloxamer action in cell protection has gained renewed interest due to widespread raw material variation of Poloxamer 188 within the biopharmaceutical industry. Several groups have observed that a high molecular weight (HMW) peak in the polymer's molecular weight distribution led to increased cell sensitivity, resulting in cell damage in manufacturing batches [7,9,104]. Although the HMW contaminant was identified and removed, the mechanism of disruption remains unclear. This recent problem illustrates that the problem of mitigating high shear sensitivity in bioreactor operation is still unsolved after more than 50 years. More broadly, improved understanding of the interfacial interactions between surfactants, bubbles, and cells, can further push mammalian cell culture process robustness and control, and will be the focus of this dissertation.

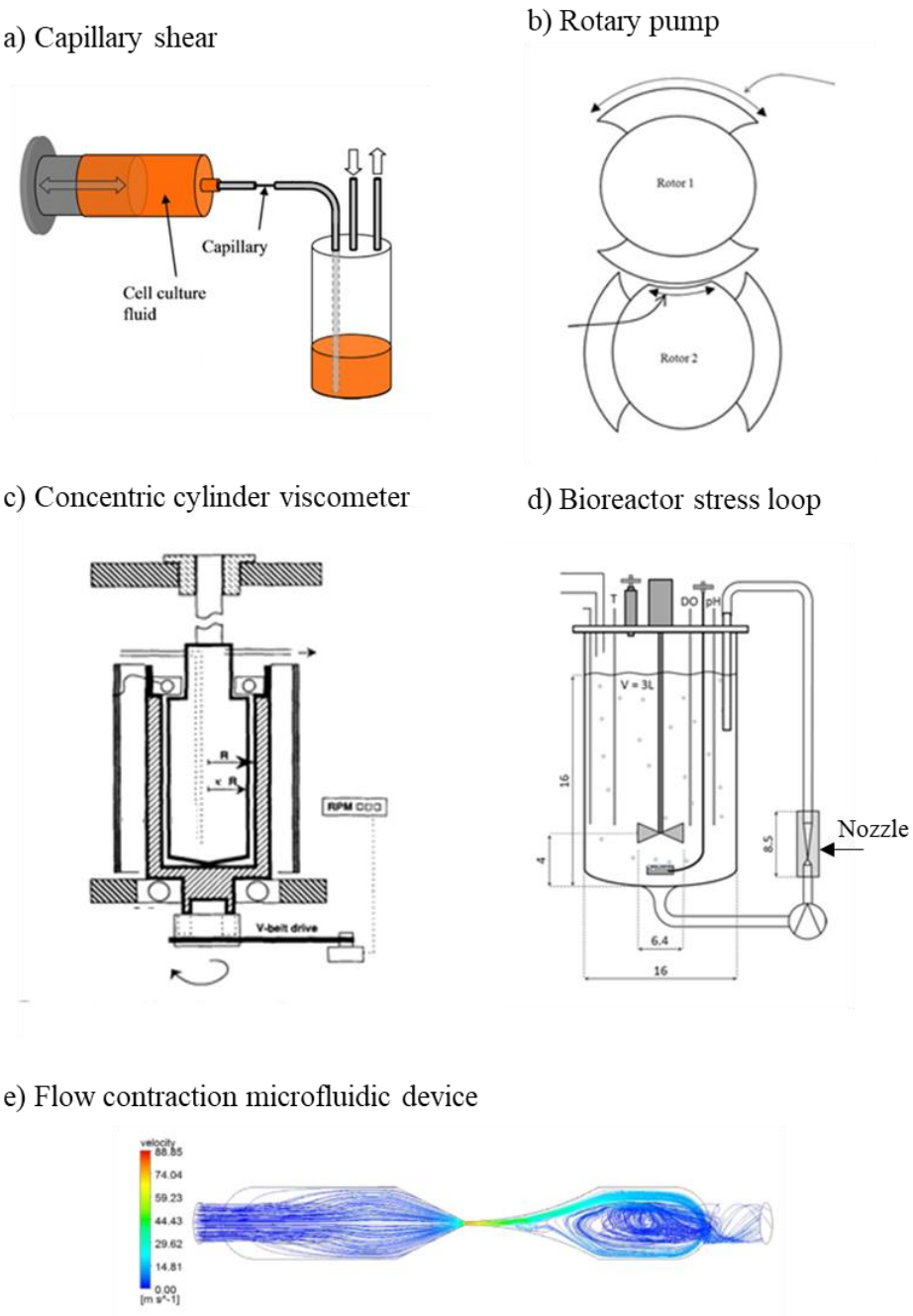

Figure 1.13: Examples of various assays used to measure the shear sensitivity of cell culture. (a) Cells are pumped through a thin capillary. Oscillating stresses are generated by operating the syringe pump in forward and reverse mode [105]. (b) Cells are sheared by pumping through a rotary positive displacement pump [106]. (c) Cells are sheared in a concentric cylinder viscometer [93]. (d) Cell culture is stressed during bioreactor operation by recirculating the suspension through an external loop with a narrow nozzle. (e) Cells are sheared in a narrow microfluidic channel with flow-focusing geometry. This device is nicknamed “cell torture chamber.” [28]

1.5 Layout of this dissertation

This dissertation will focus on understanding and applying fundamentals of surfactant-cell and surfactant-gas interactions to improve mammalian cell culture processes in bioreactors. Chapter 1 discusses the factors contributing to cell damage and foaming and provides a background of previous work in the field. Chapter 2 examines the surface properties of different Poloxamers on the gas-liquid interface. We investigate the air-water interfacial tension of Poloxamers 188 and 407, which have high and low protection of cells, respectively. We also report the measurements of the effects of these surfactants on cell-to-bubble attachment rates. Chapter 3 focuses on the effect of these two surfactants on the cell membrane interface. We use two methods, both based on fluorescent labeling of the cell membrane, to determine the cell membrane fluidity. We then measure the effects of P188 and P407 concentration on cell membrane fluidity in correlation with the culture's shear sensitivity. In chapter 4, we develop and characterize a novel method to quantify shear sensitivity of cells rapidly and efficiently. We use a concentric cylinder mixer to shear a small volume of cells, and correlate the resulting change in cell viability and LDH to the culture's mechanical stability. We also investigate the effect of surfactant on the colloidal properties of the cell suspension. In chapter 5, we apply the methods we developed to improve a commercial CHO cell process. Using the measured shear sensitivity, we determine the optimal concentration of P188 to minimize shear damage during scale-up and maximize cell viability during protein production. Finally, we summarize the impact of this work and examine future directions of this field.

1.6 References

[1] F.M. Wurm, Production of recombinant protein therapeutics in cultivated mammalian cells., Nat. Biotechnol. 22 (2004) 1393–1398. doi:10.1038/nbt1026.

[2] M. Al-rubeai, Animal Cell Culture, Springer, 2015. doi:10.1007/978-3-319-10320-4.

[3] J.A. DiMasi, H.G. Grabowski, R.W. Hansen, Innovation in the pharmaceutical industry: New estimates of R&D costs, J. Health Econ. 47 (2016) 20–33. doi:10.1016/j.jhealeco.2016.01.012.

[4] R. Otto, A. Santagostino, U. Schrader, Rapid growth in biopharma: Challenges and opportunities, in: From Sci. to Oper. Quest. Choices Strateg. Success Biopharma, 2014.

[5] W. Hu, C. Berdugo, J.J. Chalmers, The potential of hydrodynamic damage to animal cells of industrial relevance: current understanding., Cytotechnology. 63 (2011) 445–60. doi:10.1007/s10616-011-9368-3.

[6] Y.-M. Huang, W. Hu, E. Rustandi, K. Chang, H. Yusuf-Makagiansar, T. Ryll, Maximizing productivity of CHO cell-based fed-batch culture using chemically defined media conditions and typical manufacturing equipment, Biotechnol. Prog. 26 (2010) 1400–1410. doi:10.1002/btpr.436.

[7] H. Peng, K.M. Hall, B. Clayton, K. Wiltberger, W. Hu, E. Hughes, J. Kane, R. Ney, T. Ryll, Development of small scale cell culture models for screening poloxamer 188 lot-to-lot variation, Biotechnol. Prog. 30 (2014) 1411–1418. doi:10.1002/btpr.1967.

[8] T. Tharmalingam, C.T. Goudar, Evaluating the impact of high Pluronic F68 concentrations on antibody producing CHO cell lines, Biotechnol. Bioeng. 112 (2014) 832–7.

doi:10.1002/bit.25491.

[9] P.A. Apostolidis, A. Tseng, M.-E. Koziol, M.J. Betenbaugh, B. Chiang, Investigation of low viability in sparged bioreactor CHO cell cultures points to variability in the Pluronic F-68 shear protecting component of cell culture media, Biochem. Eng. J. 98 (2015) 10–17. doi:10.1016/j.bej.2015.01.013.

[10] D. Chang, R. Fox, E. Hicks, R. Ferguson, K. Chang, D. Osborne, W. Hu, O.D. Velev, Investigation of interfacial properties of pure and mixed poloxamers for surfactant-mediated shear protection of mammalian cells, Colloids Surfaces B Biointerfaces. 156 (2017) 358–365. doi:10.1016/j.colsurfb.2017.05.040.

[11] D.G. Kilburn, F.C. Webb, The Cultivation of Animal Cells at Controlled Dissolved Oxygen Partial Pressure, Biotechnol. Bioeng. X (1968) 801–814.

[12] M.A. Cacciuttolo, L. Trinh, J.A. Lumpkin, G. Rao, Hyperoxia Induces DNA Damage in Mammalian Cells, Free Radic. Biol. Med. 14 (1993) 267–276.

[13] N.C. Carpita, Tensile strength of cell walls of living cells., Plant Physiol. 79 (1985) 485–488. doi:10.1104/pp.79.2.485.

[14] K. Schugerl, H.-J. Henzler, G. Kretzmer, Influence of stress on cell growth and product formation, Springer Science & Business Media, Germany, 2000.

[15] J.R. Blake, J.M. Boulton-Stone, J.R. Blake, Gas bubbles bursting at a free surface, J. Fluid Mech. 254 (1993) 437–466.

[16] F. MacIntyre, Flow Patterns in Breaking Bubbles, J. Geophys. Res. 77 (1972) 5211–5228. doi:10.1029/JC077i027p05211.

[17] P.L.L. Walls, O. McRae, V. Natarajan, C. Johnson, C. Antoniou, J.C. Bird, Quantifying the potential for bursting bubbles to damage suspended cells, Sci. Rep. 7 (2017) 1–9. doi:10.1038/s41598-017-14531-5.

[18] M. a. Garcia-Briones, R.S. Brodkey, J.J. Chalmers, Computer simulations of the rupture of a gas bubble at a gas—liquid interface and its implications in animal cell damage, Chem. Eng. Sci. 49 (1994) 2301–2320. doi:10.1016/0009-2509(94)E0038-R.

[19] M. Mollet, R. Godoy-Silva, C. Berdugo, J.J. Chalmers, Computer simulations of the energy dissipation rate in a fluorescence-activated cell sorter: Implications to cells, Biotechnol. Bioeng. 100 (2008) 260–272. doi:10.1002/bit.21762.

[20] M. Mollet, N. Ma, Y. Zhao, R. Brodkey, R. Taticek, J.J. Chalmers, Bioprocess equipment: Characterization of energy dissipation rate and its potential to damage cells, Biotechnol. Prog. 20 (2004) 1437–1448. doi:10.1021/bp0498488.

[21] W. Hu, R. Gladue, J. Hansen, C. Wojnar, J.J. Chalmers, Growth inhibition of dinoflagellate algae in shake flasks: Not due to shear this time!, Biotechnol. Prog. 26 (2010) 79–87. doi:10.1002/btpr.301.

[22] R. Godoy-Silva, J.J. Chalmers, S.A. Casnocha, L.A. Bass, N. Ma, Physiological responses of CHO cells to repetitive hydrodynamic stress, Biotechnol. Bioeng. 103 (2009) 1103–1117. doi:10.1002/bit.22339.

[23] R. Godoy-Silva, M. Mollet, J.J. Chalmers, Evaluation of the effect of chronic hydrodynamical stresses on cultures of suspensed CHO-6E6 cells, Biotechnol. Bioeng. 102 (2009) 1119–1130. doi:10.1002/bit.22146.

[24] S.K.W. Oh, A.W. Nienow, M. Al-Rubeai, A.N. Emery, The effects of agitation intensity with and without continuous sparging on the growth and antibody production of hybridoma cells, J. Biotechnol. 12 (1989) 45–61. doi:10.1016/0168-1656(89)90128-4.

[25] K.T. Kunas, E.T. Papoutsakis, Damage mechanisms of suspended animal cells in agitated bioreactors with and without bubble entrainment., Biotechnol. Bioeng. 36 (1990) 476–83. doi:10.1002/bit.260360507.

[26] N. Gregoriades, J. Clay, N. Ma, K. Koelling, J.J. Chalmers, Cell damage of microcarrier cultures as a function of local energy dissipation created by a rapid extensional flow, Biotechnol. Bioeng. 69 (2000) 171–182. doi:10.1002/(SICI)1097-0290(20000720)69:2<171::AID-BIT6>3.0.CO;2-C.

[27] M. Mollet, R. Godoy-silva, C. Berdugo, J.J. Chalmers, Acute Hydrodynamic Forces and Apoptosis : A Complex Question, 98 (2007) 772–788. doi:10.1002/bit.

[28] N. Ma, K.W. Koelling, J.J. Chalmers, Fabrication and use of a transient contractional flow device to quantify the sensitivity of mammalian and insect cells to hydrodynamic forces, Biotechnol. Bioeng. 80 (2002) 428–437. doi:10.1002/bit.10387.

[29] D.C. Augenstein, A.J. Sinskey, D.I.C. Wang, Effect of shear on the death of two strains of mammalian tissue cells, Biotechnol. Bioeng. 13 (1971) 409–418. doi:10.1002/bit.260130308.

[30] J. Varley, J. Birch, Reactor design for large scale suspension animal cell culture, Cytotechnology. 29 (1999) 177–205. doi:10.1023/A:1008008021481.

[31] G. Zhou, S. Kresta, Distribution of Energy Between Convective and Turbulent-Flow for 3

Frequently Used Impellers, Chem. Eng. Res. Des. 74 (1996) 379–389.

[32] E. Ståhl Wernersson, C. Trägårdh, Scale-up of Rushton turbine-agitated tanks, Chem. Eng. Sci. 54 (1999) 4245–4256. doi:10.1016/S0009-2509(99)00127-X.

[33] B. Vickroy, K. Lorenz, W. Kelly, Modeling shear damage to suspended CHO cells during cross-flow filtration, Biotechnol. Prog. 23 (2007) 194–199. doi:10.1021/bp060183e.

[34] J.J. Chalmers, Mixing, aeration and cell damage, 30+ years later: What we learned, how it affected the cell culture industry and what we would like to know more about, Curr. Opin. Chem. Eng. 10 (2015) 94–102. doi:10.1016/j.coche.2015.09.005.

[35] D. Chattopadhyay, J.F. Rathman, J.J. Chalmers, Thermodynamic approach to explain cell adhesion to air-medium interfaces., Biotechnol. Bioeng. 48 (1995) 649–58. doi:10.1002/bit.260480613.

[36] F. Bavarian, L.S. Fan, J.J. Chalmers, Microscopic Visualization of Insect Cell-Bubble Interactions. I: Rising Bubbles, Air-Medium Interface, and the Foam Layer, Biotechnol. Prog. 7 (1991) 140–150. doi:10.1021/bp00008a009.

[37] J.J. Chalmers, F. Bavarian, Microscopic visualization of insect cell-bubble interactions. II: The bubble film and bubble rupture, Biotechnol. Prog. 7 (1991) 151–158. doi:10.1021/bp00008a010.

[38] Y. Ye, S.M. Khandrika, J.D. Miller, Induction-time measurements at a particle bed.pdf, Int. J. Heat Fluid Flow. 25 (1989) 221–240.

[39] J.D. Michaels, J.E. Nowak, A.K. Mallik, K.K. Koczo, D.T. Wasan, E.T. Papoutsakis, Analysis of cell-to-bubble attachment in sparged bioreactors in the presence of cell-

protecting additives., Biotechnol. Bioeng. 47 (1995) 407–19. doi:10.1002/bit.260470402.

[40] S. Xu, L. Hoshan, R. Jiang, B. Gupta, E. Brodean, K. O'Neill, T.C. Seamans, J. Bowers, H. Chen, A practical approach in bioreactor scale-up and process transfer using a combination of constant P/V and vvm as the criterion, Biotechnol. Prog. (2017) 1–6. doi:10.1002/btpr.2489.

[41] F. Garcia-Ochoa, E. Gomez, V.E. Santos, J.C. Merchuk, Oxygen uptake rate in microbial processes: An overview, Biochem. Eng. J. 49 (2010) 289–307. doi:10.1016/j.bej.2010.01.011.

[42] F. Garcia-Ochoa, E. Gomez, Bioreactor scale-up and oxygen transfer rate in microbial processes: An overview, Biotechnol. Adv. 27 (2009) 153–176. doi:10.1016/j.biotechadv.2008.10.006.

[43] S.S. Mostafa, X. Gu, Strategies for improved dCO2 removal in large-scale fed-batch cultures, Biotechnol. Prog. 19 (2003) 45–51. doi:10.1021/bp0256263.

[44] V.M. DeZengotita, A.E. Schmelzer, W.M. Miller, Characterization of hybridoma cell responses to elevated pCO2 and osmolality: Intracellular pH, cell size, apoptosis, and metabolism, Biotechnol. Bioeng. 77 (2002) 369–380. doi:10.1002/bit.10176.

[45] S. Xu, H. Chen, High-density mammalian cell cultures in stirred-tank bioreactor without external pH control, J. Biotechnol. 231 (2016) 149–159. doi:10.1016/j.jbiotec.2016.06.019.

[46] Y. Zhu, J. V. Cuenca, W. Zhou, A. Varma, NS0 cell damage by high gas velocity sparging in protein-free and cholesterol-free cultures, Biotechnol. Bioeng. 101 (2008) 751–760. doi:10.1002/bit.21950.

[47] J.D. Michaels, A.K. Mallik, E.T. Papoutsakis, Sparging and agitation-induced injury of cultured animal cells: Do cell- to-bubble interactions in the bulk liquid injure cells?, Biotechnol. Bioeng. 51 (1996) 399–409. doi:10.1002/(SICI)1097-0290(19960820)51:4<399::AID-BIT3>3.0.CO;2-D.

[48] Y. Liu, F. Li, W. Hu, K. Wiltberger, T. Ryll, Effects of bubble-liquid two-phase turbulent hydrodynamics on cell damage in sparged bioreactor, Biotechnol. Prog. 30 (2014) 48–58. doi:10.1002/btpr.1790.

[49] M.L. Velez-Suberbie, R.D.R. Tarrant, A.S. Tait, D.I.R. Spencer, D.G. Bracewell, Impact of aeration strategy on CHO cell performance during antibody production, Biotechnol. Prog. 29 (2013) 116–126. doi:10.1002/btpr.1647.

[50] B. Frahm, H. Brod, U. Langer, Improving bioreactor cultivation conditions for sensitive cell lines by dynamic membrane aeration., Cytotechnology. 59 (2009) 17–30. doi:10.1007/s10616-009-9189-9.

[51] F. Vardar-Sukan, Foaming: Consequences, prevention and destruction, Biotechnol. Adv. 16 (1998) 913–948. doi:10.1016/S0734-9750(98)00010-X.

[52] N.D. Denkov, Mechanisms of foam destruction by oil-based antifoams., Langmuir. 20 (2004) 9463–505. doi:10.1021/la049676o.

[53] N.D. Denkov, P. Cooper, J.Y. Martin, Mechanisms of action of mixed solid-liquid antifoams. 1. Dynamics of foam film rupture, Langmuir. 15 (1999) 8514–8529. doi:10.1021/la9902136.

[54] B. Junker, Foam and its mitigation in fermentation systems., Biotechnol. Prog. 23 (2007)

767–84. doi:10.1021/bp070032r.

[55] F. Delvigne, J. Lecomte, Foam Formation and Control in Bioreactors, Encycl. Ind. Biotechnol. (2010) 1–13. doi:10.1002/9780470054581.eib326.

[56] U.E. Viesturs, M.Z. Kristapsons, E.S. Levitans, Foam in Microbiological Processes, Microbes Eng. Asp. 21 (1982) 169–224.

[57] N.D. Denkov, K.G. Marinova, C. Christova, A. Hadjiiski, P. Cooper, Mechanisms of Action of Mixed Solid−Liquid Antifoams: 3. Exhaustion and Reactivation, Langmuir. 16 (2000) 2515–2528. doi:10.1021/la9910632.

[58] D.T.W. Gyorgy Racz, Kalman Koczo, Mechanisms of Antifoam Deactivation, J. Colloid Interface Sci. 181 (1996) 124–135.

[59] V. Bergeron, P. Cooper, C. Fischer, J. Giermanska-Kahn, D. Langevin, A. Pouchelon, Polydimethylsiloxane (PDMS)-based antifoams, Colloids Surfaces A Physicochem. Eng. Asp. 122 (1997) 103–120. doi:10.1016/S0927-7757(96)03774-0.

[60] L.A. Van Der Pol, D. Bonarius, G. Van De Wouw, J. Tramper, Effect of Silicone Antifoam on Shear Sensitivity of Hybridoma Cells in Sparged Cultures, Biotechnol. Prog. 9 (1993) 504–509. doi:10.1021/bp00023a009.

[61] K.G. Marinova, S. Tcholakova, M.D. Denkov, Nikolai D., Stoian Roussev, Model Studies on the Mechanism of Deactivation (Exhaustion) of Mixed Oil-Silica Antifoams, Langmuir. 19 (2003) 3084–3089.

[62] K. Trinh, M. Garcia-Briones, J.J. Chalmers, F. Hink, J.J. Chalmers, F. Hink, Quantification of damage to suspended insect cells as a result of bubble rupture., Biotechnol. Bioeng. 43

(1994) 37–45. doi:10.1002/bit.260430106.

[63] D.W. Murhammer, C.F. Goochee, Scaleup of Insect Cell Cultures: Protective Effects of Pluronic F-68, Nat. Biotechnol. 6 (1988) 1411–1418.

[64] H.E. Swim, R.F. Parker, Effect of Pluronic F68 on Growth of Fibroblasts in Suspension on Rotary Shaker, Exp. Biol. Med. 103 (1960) 252–254.

[65] R.C. Telling, A. Virus, Submerged Culture of Hamster Kidney Cells in a Stainless Steel Vessel, Biotechnol. Bioeng. 7 (1965) 417–434.

[66] D. Chattopadhyay, J.F. Rathman, J.J. Chalmers, The protective effect of specific medium additives with respect to bubble rupture, Biotechnol. Bioeng. 45 (1995) 473–480. doi:10.1002/bit.260450603.

[67] E.T. Papoutsakis, Media additives for protecting freely suspended animal cells against agitation and aeration damage, Trends Biotechnol. 9 (1991) 316–24. doi:10.1016/0167-7799(91)90102-N.

[68] J. Wu, Insights into protective effects of medium additives on animal cells under fluid stresses: the hydrophobic interactions., Cytotechnology. 22 (1996) 103–9. doi:10.1007/BF00353929.

[69] W. Hu, J.J. Rathman, J.J. Chalmers, An investigation of small-molecule surfactants to potentially replace pluronic F-68 for reducing bubble-associated cell damage, Biotechnol. Bioeng. 101 (2008) 119–27. doi:10.1002/bit.21872.

[70] J.D. Michaels, J.E. Nowak, A.K. Mallik, K. Koczo, D.T. Wasan, E.T. Papoutsakis, Interfacial properties of cell culture media with cell-protecting additives, Biotechnol.

Bioeng. 47 (1995) 420–430. doi:10.1002/bit.260470403.

[71] H. Ghebeh, J. Gillis, M. Butler, Measurement of hydrophobic interactions of mammalian cells grown in culture, J. Biotechnol. 95 (2002) 39–48. doi:10.1016/S0168-1656(01)00440-0.

[72] S.J. Meier, T.A. Hatton, D.I.C.C. Wang, Cell death from bursting bubbles: role of cell attachment to rising bubbles in sparged reactors, Biotechnol. Bioeng. 62 (1999) 468–478. doi:10.1002/(SICI)1097-0290(19990220)62:4<468::AID-BIT10>3.0.CO;2-N.

[73] T. Tharmalingam, H. Ghebeh, T. Wuerz, M. Butler, Pluronic enhances the robustness and reduces the cell attachment of mammalian cells, Mol. Biotechnol. 39 (2008) 167–177. doi:10.1007/s12033-008-9045-8.

[74] J.J. CHALMERS, Cells and bubbles in sparged bioreactors., Cytotechnology. 15 (1994) 311–20. doi:10.1007/BF00762406.

[75] N. Ma, J.J. Chalmers, J.G. Auniņs, W. Zhou, L. Xie, Quantitative studies of cell-bubble interactions and cell damage at different pluronic F-68 and cell concentrations, Biotechnol. Prog. 20 (2004) 1183–91. doi:10.1021/bp0342405.

[76] M. Ruiz, A detailed diagram of the cell membrane, (2007).

[77] S.J. Singer, G.L. Nicolson, The Fluid Mosaic Model of the Structure of Cell Membranes, Science (80-.). 175 (1972) 720–731.

[78] G. Vereb, J. Szollosi, J. Matko, P. Nagy, T. Farkas, L. Vigh, L. Matyus, T.A. Waldmann, S. Damjanovich, Dynamic, yet structured: The cell membrane three decades after the Singer-Nicolson model, Proc. Natl. Acad. Sci. 100 (2003) 8053–8058.

doi:10.1073/pnas.1332550100.

[79] S. Goldblum, Y.K. Bae, W.F. Hinkj, J. Chalmers, W.F. Hink, J. Chalmers, Protective Effect of Methylcellulose and Other Polymers on Insect Cells Subjected to Laminar Shear Stress, Biotechnol. Prog. 6 (1990) 383–390. doi:10.1021/bp00005a011.

[80] D.W. Murhammer, Pluronic polyols, cell protection, in: Encycl. Bioprocess Technol., 2002: pp. 3965–3968. doi:10.1002/9780470054581.

[81] M. le Maire, P. Champeil, J. V. Møller, Interaction of membrane proteins and lipids with solubilizing detergents, Biochim. Biophys. Acta - Biomembr. 1508 (2000) 86–111. doi:10.1016/S0304-4157(00)00010-1.

[82] D.W. Murhammer, C.F. Goochee, Structural features of nonionic polyglycol polymer molecules responsible for the protective effect in sparged animal cell bioreactors, Biotechnol. Prog. 6 (1990) 142–148. doi:10.1021/bp00002a008.

[83] S.M. Moghimi, A.C. Hunter, Poloxamers and poloxamines in nanoparticle engineering and experimental medicine, Trends Biotechnol. 18 (2000) 2958–2964.

[84] S. Yasuda, D. Townsend, D.E. Michele, E.G. Favre, S.M. Day, J.M. Metzger, Dystrophic heart failure blocked by membrane sealant poloxamer, Nature. 436 (2005) 1025–1029. doi:10.1038/nature03844.

[85] L.E. Nita, A. Chiriac, M. Bercea, B.A. Wolf, Synergistic behavior of poly(aspartic acid) and Pluronic F127 in aqueous solution as studied by viscometry and dynamic light scattering, Colloids Surfaces B Biointerfaces. 103 (2013) 544–549. doi:10.1016/j.colsurfb.2012.10.054.

[86] S. Stolnik, N.C. Felumb, C.R. Heald, M.C. Garnett, L. Illum, S.S. Davis, Adsorption behaviour and conformation of selected poly(ethylene oxide) copolymers on the surface of a model colloidal drug carrier, Colloids Surfaces A Physicochem. Eng. Asp. 122 (1997) 151–159. doi:10.1016/S0927-7757(96)03826-5.

[87] S.A. Maskarinec, K.Y.C. Lee, Comparative Study of Poloxamer Insertion into Lipid Monolayers, Langmuir. 19 (2003) 1809–1815. doi:10.1021/la026175z.

[88] W. Zhang, G. Wang, E. See, J.P. Shaw, B.C. Baguley, J. Liu, S. Amirapu, Z. Wu, Post-insertion of poloxamer 188 strengthened liposomal membrane and reduced drug irritancy and in vivo precipitation, superior to PEGylation, J. Control. Release. 203 (2015) 161–169. doi:http://dx.doi.org/10.1016/j.jconrel.2015.02.026.

[89] U. Adhikari, A. Goliaei, L. Tsereteli, M.L. Berkowitz, Properties of poloxamer molecules and poloxamer micelles dissolved in water and next to lipid bilayers: results from computer simulations, J. Phys. Chem. B. 120 (2016) 5823–5830. doi:10.1021/acs.jpcb.5b11448.

[90] V. Sharma, K. Stebe, J.C. Murphy, L. Tung, Poloxamer 188 decreases susceptibility of artificial lipid membranes to electroporation., Biophys. J. 71 (1996) 3229–41. doi:10.1016/S0006-3495(96)79516-4.

[91] J.-Y.Y. Wang, J. Chin, J.D. Marks, K.Y.C. Lee, Effects of PEO-PPO-PEO triblock copolymers on phospholipid membrane integrity under osmotic stress, Langmuir. 26 (2010) 12953–12961. doi:10.1021/la101841a.

[92] Z. Zhang, M. Al-Rubeai, C.R. Thomas, Effect of Pluronic F-68 on the mechanical properties of mammalian cells, Enzyme Microb. Technol. 14 (1992) 980–983. doi:10.1016/0141-0229(92)90081-X.

[93] O.T. Ramírez, R. Mutharasan, The role of the plasma membrane fluidity on the shear sensitivity of hybridomas grown under hydrodynamic stress., Biotechnol. Bioeng. 36 (1990) 911–920. doi:10.1002/bit.260360906.

[94] O.T. Ramirez, R. Mutharasan, Effect of serum on the plasma membrane fluidity of hybridomas: an insight into its shear protective mechanism, Biotechnol. Prog. 8 (1992) 40–50.

[95] A. Gigout, M.D. Buschmann, M. Jolicoeur, The fate of Pluronic F-68 in chondrocytes and CHO cells., Biotechnol. Bioeng. 100 (2008) 975–87. doi:10.1002/bit.21840.

[96] M.-F.M.-F. Clincke, E. Guedon, F.T. Yen, V. Ogier, O. Roitel, J.-L. Goergen, Effect of Surfactant Pluronic F-68 on CHO Cell Growth , Metabolism , Production , and Glycosylation of Human Recombinant IFN- c in Mild Operating Conditions, Biotechnol. Prog. 27 (2010) 181–90. doi:10.1002/btpr.503.

[97] K. Braasch, M. Nikolic-Jaric, T. Cabel, E. Salimi, A. Bhide, V. Jung, D.J. Thomson, G.E. Bridges, M. Butler, D.J. Thomson, M. Butler, The changing dielectric properties of CHO cells can be used to determine early apoptotic events in a bioprocess, Biotechnol. Bioeng. 110 (2013) 2902–2914. doi:10.1002/bit.24976.

[98] I. Abu-Reesh, F. Kargi, Biological responses of hybridoma cells to defined hydrodynamic shear stress, J. Biotechnol. 9 (1989) 167–178. doi:10.1016/0168-1656(89)90106-5.

[99] J.F. Petersen, L. V. McIntire, E.T. Papoutsakis, Shear sensitivity of cultured hybridoma cells (CRL-8018) depends on mode of growth, culture age and metabolite concentration, J. Biotechnol. 7 (1988) 229–246. doi:10.1016/0168-1656(88)90054-5.

[100] R.M. Shenkman, R. Godoy-Silva, K.K. Papas, J.J. Chalmers, Effects of energy dissipation rate on islets of langerhans: Implications for isolation and transplantation, Biotechnol. Bioeng. 103 (2009) 413–423. doi:10.1002/bit.22241.

[101] J.J. Gallardo-Rodríguez, L. López-Rosales, A. Sánchez-Mirón, F. García-Camacho, E. Molina-Grima, J.J. Chalmers, New insights into shear-sensitivity in dinoflagellate microalgae, Bioresour. Technol. 200 (2016) 699–705. doi:10.1016/j.biortech.2015.10.105.

[102] W. Hu, R. Gladue, J. Hansen, C. Wojnar, J.J. Chalmers, The sensitivity of the dinoflagellate Crypthecodinium cohnii to transient hydrodynamic forces and cell-bubble interactions, Biotechnol. Prog. 23 (2007) 1355–1362. doi:10.1021/bp070306a.

[103] M. Mollet, R. Godoy-silva, C. Berdugo, J.J. Chalmers, Computer Simulations of the Energy Dissipation Rate in a Fluorescence-Activated Cell Sorter : Implications to Cells, 100 (2008) 260–272. doi:10.1002/bit.21762.

[104] H. Peng, A. Ali, M. Lanan, E. Hughes, K. Wiltberger, B. Guan, S. Prajapati, W. Hu, Mechanism investigation for Poloxamer 188 raw material variation in cell culture, Biotechnol. Prog. 32 (2016) 767–775. doi:10.1002/btpr.2268.

[105] B. Neunstoecklin, M. Stettler, T. Solacroup, H. Broly, M. Morbidelli, M. Soos, Determination of the maximum operating range of hydrodynamic stress in mammalian cell culture, J. Biotechnol. 194 (2015) 100–109. doi:10.1016/j.jbiotec.2014.12.003.

[106] H. Kamaraju, K. Wetzel, W.J. Kelly, Modeling shear-induced CHO cell damage in a rotary positive displacement pump, Biotechnol. Prog. 26 (2010) 1606–1615.

Chapter 2 – Investigation of interfacial properties of pure and mixed Poloxamers for surfactant-mediated shear protection of mammalian cells

2.1 Introduction

Poloxamer 188 (P188) has widely been used as a shear protective additive in cell culture production of therapeutic proteins. [1–3]. Although protein production is primarily controlled via biological pathways, bioreactor process optimization can be achieved through improved understanding and control of colloidal interactions between cells, gas bubbles and surfactants. The relevant interfacial events in a sparged bioreactor are illustrated in **Figure 2.1**. As air bubbles rise through the cell culture mixture, the hydrophobic cells adsorb to the air interface, resulting in a high concentration of cells near the air-water interface [4–7]. Cells can be trapped in liquid films and plateau borders between the bubbles of the foam layer, where they can perish from starvation of essential nutrients [8]. Several researchers have suggested that air bubbles bursting at the medium interface are the primary origin of physical cell damage [6,8–13]. Shear stresses generated by impeller agitation do not damage cells at typical agitation levels [14,15]. Instead, small air bubbles burst and dissipate a large amount of energy [16], leading to damage of cells in the liquid film surrounding the bubbles [7,17,18]. Shear protective additives such as P188 decrease physical damage to suspensions of animal cell cultures by physical and biochemical means [19]. Several mechanisms of cell protection by surfactants have been demonstrated, including decreasing cell-to-bubble attachment rate by reducing adsorption of cells to bubbles [4,5,7,20–23], increasing membrane strength through adsorption to the membrane [20,24], and decreasing membrane fluidity [25,26]. The mechanism of shear protection predominantly occurs at the gas bubble interface and the membrane interface, suggesting that a fundamental understanding of the interactions between poloxamers and gas, liquid, and cell membrane interfaces are important for

cell protection.

Poloxamers are nonionic triblock copolymer surfactants with a central hydrophobic poly(propylene oxide) (PPO) chain linked to two hydrophilic poly(ethylene oxide) (PEO) side chains, denoted PEO_x-PPO_y-PEO_x, where x and y are the number of respective oligomer units. Poloxamers can be synthesized with a range of molecular weights and hydrophobicities by varying the PPO/PEO ratio. As a result, over thirty poloxamers are commercially available within the 1500-15000 Da range with a large range of hydrophilic-lipophilic balance (HLB) values [27]. Studies on the structure-shear protective relationship show that poloxamers with high HLB have stronger shear protective effect on cells, while highly hydrophobic poloxamers tend to solubilize and lyse cell membranes [28]. Micellization behavior of poloxamers has been extensively studied by dye solubilization, light-scattering, and surface tension, but inherent polydispersity and batch-to-batch variation have caused large variability in published data [29].

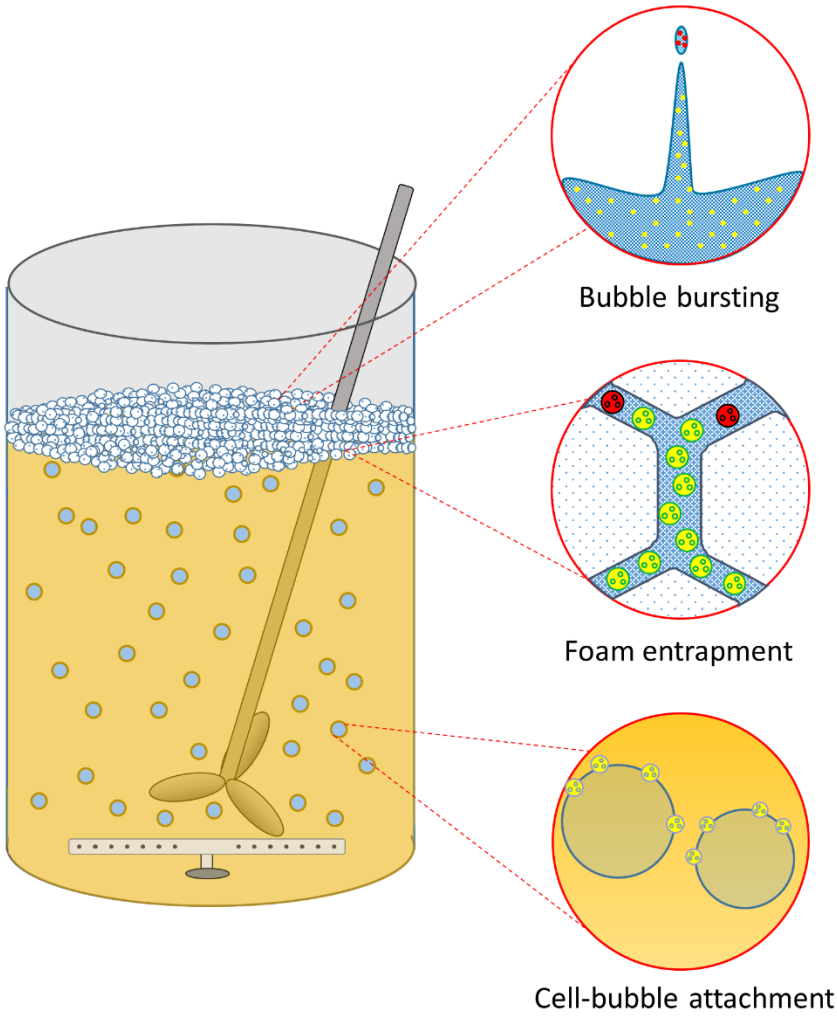

Figure 2.1: Schematic of a well-mixed and gas-sparged bioreactor,including the interfacial events that contribute to cell damage. Cells in suspension attach to rising air bubbles and become concentrated in the foam, where they can become trapped in the foam layer or damaged by bursting bubbles.

Recent studies have shown that the lot-to-lot variation of P188 also has a strong impact on its shear protective capabilities in cell culture [30–33]. Researchers have determined that a high molecular weight impurity in several P188 lots was responsible for negatively impacting culture

viabilities in sparged bioreactors. These impurities could be removed by foam fractionation, suggesting that they are also surface active. The batch-to-batch variability of poloxamers impacts their surface properties, thereby affecting the interactions between bubbles and cells.

The aim of this work is to investigate the mechanism by which P188 lot-to-lot variation, Poloxamer 407 (P407), and a mixed P188/P407 system lead to varying levels of shear-protection of cells. P407 has the same PEO-PPO-PEO structure as P188, but with higher average molecular weight and hydrophobicity. P407 was selected to investigate because it provides lower shear protection in a sparged environment compared to P188 [32]. The mixed P188/P407 system pairs a shear protective surfactant (P188) with a high molecular weight surface active impurity (P407). Foam stability and the equilibrium surface tension (γ-logC) isotherms of these surfactant systems were correlated to their shear protection for Chinese Hamster Ovary (CHO) cells. Additionally, we quantified the cell-to-bubble attachment rates in P188 and P407 solutions to determine the relative importance of the gas-bubble interface in surfactant-mediated shear protection of cells. The results from this investigation may elucidate the mechanism of how surfactants protect cells in a sparged bioreactor in order to maintain higher cell viability in harsh culture environments.

2.2 Materials and methods

2.2.1 Chemicals and materials

P188 and P407 were provided by BASF Corporation (Florham Park, NJ) and used as received. Six separate lots of P188 were prescreened using the baffled shake flask assay described below. Lots P188-A and P188-B were selected as representative lots providing high and low protection to cells, respectively. Physical properties of P188 and P407 are shown in **Table 2.1**, as

reported by BASF. Poloxamer stock solutions were prepared by dissolving solid flakes in purified MilliQ water (Millipore, Billerica, MA) to 10% w/v and diluting to the desired surfactant concentration. Poloxamer stock solutions for cell culture were sterilized by filtration before use (0.22 µm, Millipore, Billerica, MA). All other chemical reagents were obtained from Sigma Aldrich Co. (St. Louis, MO) and used as received.

Table 2.1: Physical properties of Poloxamers used in this study.

Surfactant	**Average MW**	**PEO_x-PPO_y-PEO_x**	**HLB**	**%PEO**
P188	8400	80-27-80	29	81.8
P407	12600	101-56-101	22	73.2

2.2.2 Cell culture maintenance and baffled shake flask (BSF) assay

A proprietary monoclonal antibody producing CHO cell line incorporating chemically defined media were provided by Biogen (RTP, NC) and used for all cell culture experiments. Cells were cultured at 36ºC and 5% CO_2 with a constant agitation rate of 125 rpm in unbaffled shake flasks (Corning, Corning, NY). Viable cell density (VCD) and cell viability were measured using trypan blue dye exclusion either manually in a hemocytometer (Cole-Parmer, Varnon Hills, IL) observed with an Olympus BX-61 optical microscope (Center Valley, PA), or with ViCell XR automated cell counter (Beckman Coulter, Brea, CA). Unstained cells were considered viable, while stained cells were considered nonviable.

A baffled shake flask assay was used to compare the relative shear protection provided by poloxamer solutions on cells [30,32]. Briefly, cells harvested in exponential growth phase were centrifuged at 300g for 5 min. After discarding the supernatant, the cell pellet was gently

resuspended into an unbaffled shake flask to a VCD of 10^6 cells/mL in media supplemented with desired surfactant concentration. After one hour of agitation at 200 rpm and 25 mm orbital diameter, the viability and VCD were measured by ViCell XR. A portion of the cell suspension was then transferred to a baffled shake flask (Corning, Corning, NY). After one hour of incubation at the same agitation rate, the change in VCD and viability were calculated.

2.2.3 Foam preparation and characterization

Foam samples were prepared by vigorous shaking at room temperature of 250 mL glass cylinders containing 0.1% surfactant solution in purified water. The total volume and liquid level volume were recorded over one hour. Foam volume was defined as the difference between total volume and liquid volume. The foam stability was calculated by the following equation:

$$\text{Stability}(\%) = \left(\frac{V_f^{foam}}{V_i^{foam}}\right)100$$

where V_f^{foam} and V_i^{foam} are the final and initial foam volumes, respectively.

2.2.4 Surface tension isotherm (γ-logC) characterization

Equilibrium surface tension was characterized using a platinum Wilhelmy plate on an Attension Sigma 703D tensiometer (Biolin Scientific, Paramus, NJ) equipped with circulating water bath at 36ºC (Fisher Scientific, Waltham, MA). Aqueous surfactant solutions were prepared by dilution of stock solutions with purified water at least 24 h before measurement. Each solution was equilibrated for 10 min at 36ºC before measurement. The Wilhelmy plate was rinsed in purified water and ethanol then ablated with a propane blowtorch after each measurement. The surface tension of purified water was measured between each experiment to ensure all surfaces and glassware were clean. All measurements were performed in triplicate.

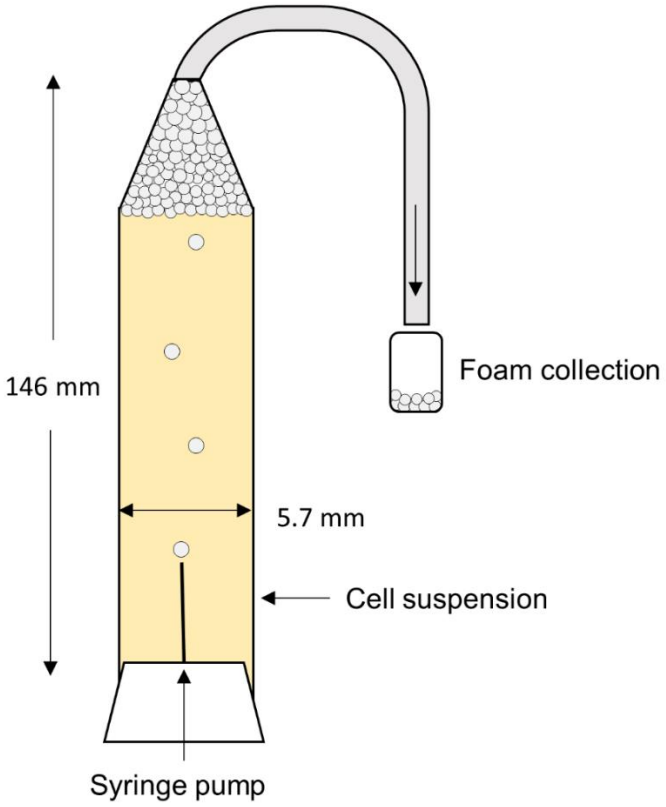

Figure 2.2: Schematic of foam collection column used to quantify the rate of cell-to-bubble attachment. Single bubbles rise through a glass column filled with a cell suspension. The bubbles are pushed through a tube and collected in a glass vial, where the foam is broken down and analyzed.

2.2.5 Quantifaction of cell-bubble attachment

To quantify the frequency of cell-bubble attachment in different surfactant mediums, we constructed a foam collection column based on a previously described apparatus by Ma et al. [7] (**Figure 2.2**). A 5.75 in. glass Pasteur pipette (Fisher Scientific, Waltham, MA) with tapered end pointed up was filled with 10^6 cells/mL CHO cells in 0.15 M phosphate-buffered saline (PBS) supplemented with desired surfactant concentration. The bottom of the glass column was sealed

with a 30-gauge needle (Becton Dickinson, Franklin Lakes, NJ). Air was pumped through the needle using a syringe pump (NE-4000, New Era Pump Systems Inc., Farmingdale, NY), resulting in single bubbles of uniform size rising through the glass column. After a brief equilibration time, the foam, consisting of bubbles and their surrounding liquid films, was collected for 3 minutes at the top of the column then weighed and analyzed with hemocytometer. The normalized cell concentration in the foam relative to bulk cell concentration was calculated as the enrichment factor (EF), as defined by the following equation:

$$\mathrm{EF} = \frac{\mathrm{TCD_{foam}}}{\mathrm{TCD_{bulk}}}$$

where TCD_{foam} and TCD_{bulk} are the total cell densities in the foam and bulk, respectively.

2.3 Results and discussion

2.3.1 Evaluation of surfactant-mediated shear protection

The baffled shake flask (BSF) assay was previously developed as a benchtop assay to address P188 lot-to-lot variability by ensuring consistent cell protection. Baffled shake flasks induce physical damage to fragile CHO cells by promoting turbulent flow and entrainment of air bubbles when agitated at high rates [30]. We used the BSF assay to compare the shear protective capacity of four poloxamer systems on CHO cells in chemical defined media: P188-A, P188-B, P407, and a mixed P188-A/P407 system in a 99:1 mass ratio. The results of the BSF assay are shown in **Figure 2.3**. To separate shear damage from potential toxic impact from surfactants, BSF assay results were compared to identical experiments with unbaffled shake flasks. The unbaffled shake flask results from show small VCD and viability changes, indicating that all surfactants are nontoxic and no cell damage occurs in a low-shear environment. We observed no stable foam layer

after agitation with unbaffled flasks.

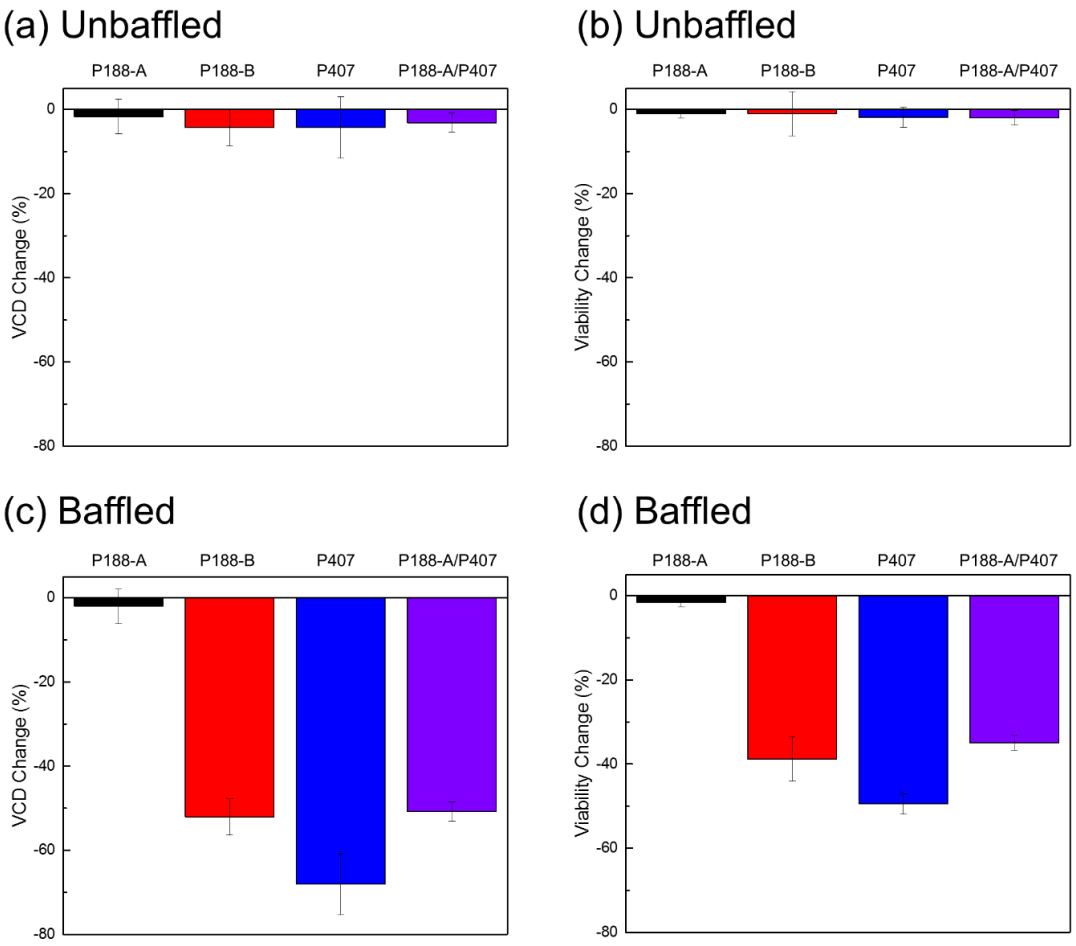

Figure 2.3: (a) VCD and (b) viability change in unbaffled shake flasks, compared to (c) VCD and (d) viability change in baffled shake flasks for 0.05% P188-A, P188-B, P407, and P188-A/P407 mixture (n = 3, mean ± SD). These data show that all surfactant systems are nontoxic to cells, but in the turbulent environment of baffled shake flasks, only P188-A provides high shear protection

The baffled shake flask results are reported in **Figure 2.3(c)-(d)**. P188-A demonstrated minimal impact to culture viable cell density (VCD) and viability, indicating a high level of

protection. Culture incorporating P188-B, P407, and P188-A/P407 demonstrated negative changes in both VCD and viability. These surfactants failed to protect the cells in this turbulent environment. In all BSF tests, a stable foam layer was observed following agitation, indicating entrainment of air from turbulent mixing.

The disparity in shear protection due to lot to lot variability of P188 has been observed by multiple researchers [30–32]. Specifically, Poloxamers prepared by base-catalyzed polymerization often have inhomogeneous molecular weight distributions [34]. Previous studies have shown that high molecular-weight species present in some P188 lots have a negative impact on cell viability in high-shear sparging environments. P407, a high-molecular weight Poloxamer with higher hydrophobicity than P188, provides inferior shear protection. Additionally, culture with the P188-A/P407 mixture led to cell death, consistent with prior studies [32]. These results suggest that P407 acts as a surface-active contaminant, disrupting the protection provided by P188 even when it is present in miniscule amounts.

2.3.2 Detection of surface active contaminants using foam stability and surface tension

In order to understand the mechanism of negative impact of hydrophobic contaminants on the shear protection of cells, we characterized the foam properties and equilibrium surface tension of the gas-liquid interface. It has been previously reported that the presence of impurities affects surfactant foaming properties [35]. The foam stability of 0.1% P188-A, P188-B, P407, and P188-A/P407 solutions is reported in **Figure 2.4.** P407 produced a much more stable foam than all other systems due to its higher molecular weight and hydrophobicity. These physical characteristics increase the ability of such surfactants to adsorb to and sterically stabilize foam films [36]. P188-B and P188-A/P407 both produced more stable foams than P188-A, consistent with observations made in previous studies [32]. This suggests that the highly surface active components in P188-B

and P188-A/P407 are responsible for their increased foam stability.

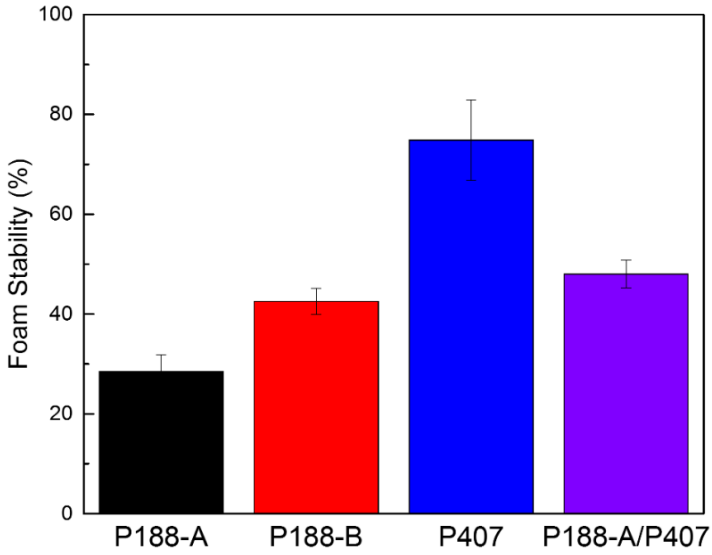

Figure 2.4: Foam stability of 0.1% P188-A, P188-B, P407, and P188-A/P407 systems after 60 minutes (n = 3, mean ± SD). P188-A/P407 has higher foam stability compared to P188-A, indicating that high molecular weight moieties stabilize the foam. The increased foam stability of P188-B compared to P188-A suggests that a high molecular weight impurity may be present in the system.

The surface tension isotherms at 36°C of the four surfactant systems are shown in **Figure 2.5**. At low concentrations (10^{-5} to 10^{-4}%), the surface tension decreases steeply with increasing concentration, corresponding to poloxamer adsorption to the interface. In this regime, the slope is related to the area of hydrophobic head group according to the Gibbs isotherm, given in the following equations:

$$\Gamma = \sum_{i=1}^{n} \Gamma_i$$

$$\Gamma = -\sum_{i=1}^{n} \frac{1}{\mathrm{RT}} \frac{d\gamma_i}{d \ln C_i}$$

$$A_i = (\Gamma_i N)^{-1}$$

where Γ and Γ_i are the total and individual surface excesses, respectively, R is the molar gas constant, T is the temperature, γ_i and C_i are component surface tensions and concentrations, respectively, A_i is the area of individual components, and N is Avogadro's number. Despite the polydispersity of Poloxamers, we can treat each Poloxamer as one component [34]. For P188-A/P407 mixture, the resulting interface can be considered an ideal mixture due to the homologous composition of poloxamers [37]. Therefore, the steeper the slope, the smaller the average head group size of the adsorbed molecules. P407 has higher surface activity and larger head group size than P188 in this regime, indicated by its lower surface tension and shallower slope in **Figure 2.5**. Moreover, both P188-A/P407 and P188-B have higher surface activity and larger head group size than P188-A in this regime. For the P188-A/P407 mixture, the larger and more hydrophobic P407 molecules preferentially adsorb at the air-water interface despite being the minority species. The surface activity of P188-B system is similar to P188-A/P407 in this regime, further suggesting that P188-B contains a high molecular weight surface active impurity.

When the concentration increases from 10^{-4} to 10^{-1}%, surfactant continues to adsorb to the interface and decrease the surface tension, but with a shallower slope than in the low concentration regime. The molecules are believed to undergo a structural transition at the interface, forming a more compact monolayer by switching from a horizontal configuration to a brush-like configuration with PPO anchored at the interface [29,34,38]. The surface tension of P407 system continues to decrease in this regime until it reaches a minimum of 38.0 mN/M at a critical micelle concentration (CMC) of 0.05%. We observe that the surface tensions of P188-B and P188-A/P407 mixtures become indistinguishable from that of P188-A in this concentration regime. This may indicate that the impurity has been micellized by P188, or that a configuration change at the

interface has diminished their contribution to the surface pressure. Industrially relevant concentrations for bioreactor use are typically in this regime, which may be why previous studies on poloxamer raw material variation have not reported a significant difference in equilibrium surface tension [30]. However, some researchers have reported differences in dynamic surface tension using the maximum bubble pressure method in this concentration regime between protective P188 lots and non-protective lots [31], which may indicate that the impurities are present in the bulk liquid.

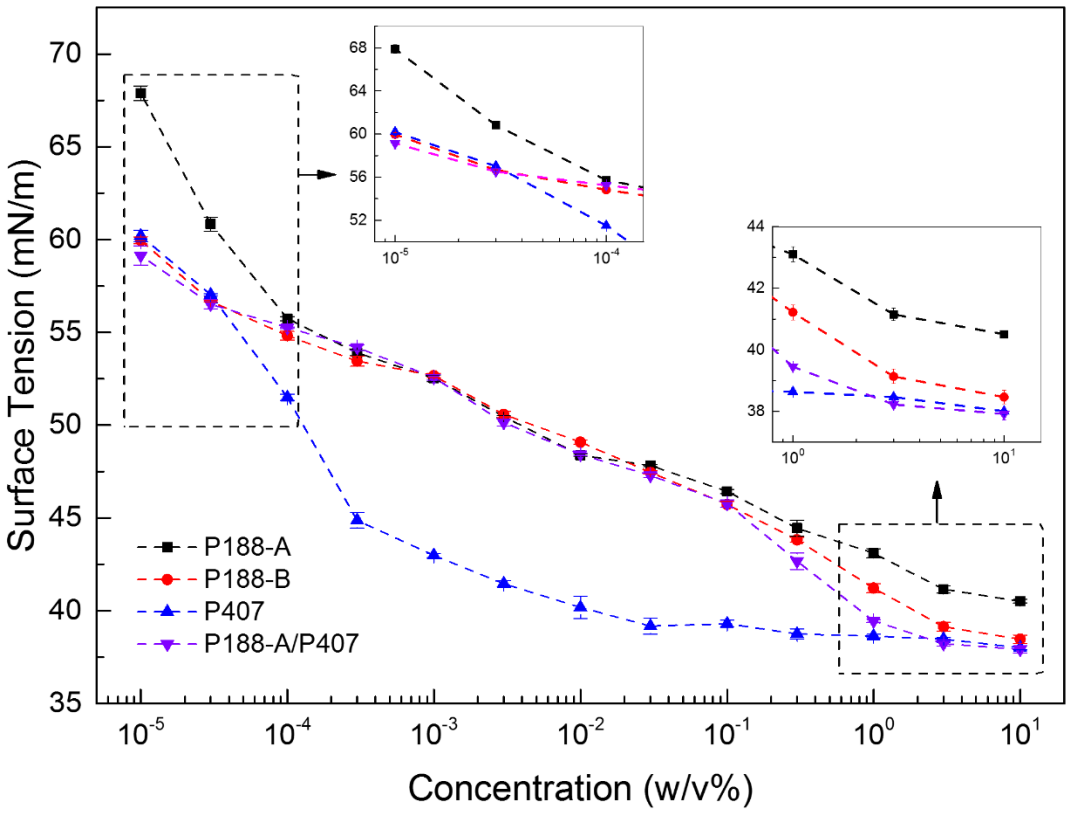

Figure 2.5: Equilibrium surface tension measurements of P188-A, P188-B, P407, and P188-A/P407 mixture at 36°C (n ≥ 3, mean ± SD). P188-B, P407, and P188-A/P407 all show higher surface activity than P188-A in the low and high concentration regimes. The similarities in the surface activity of P188-B and P188-A/P407 suggest that P188-B contains a surface active impurity.

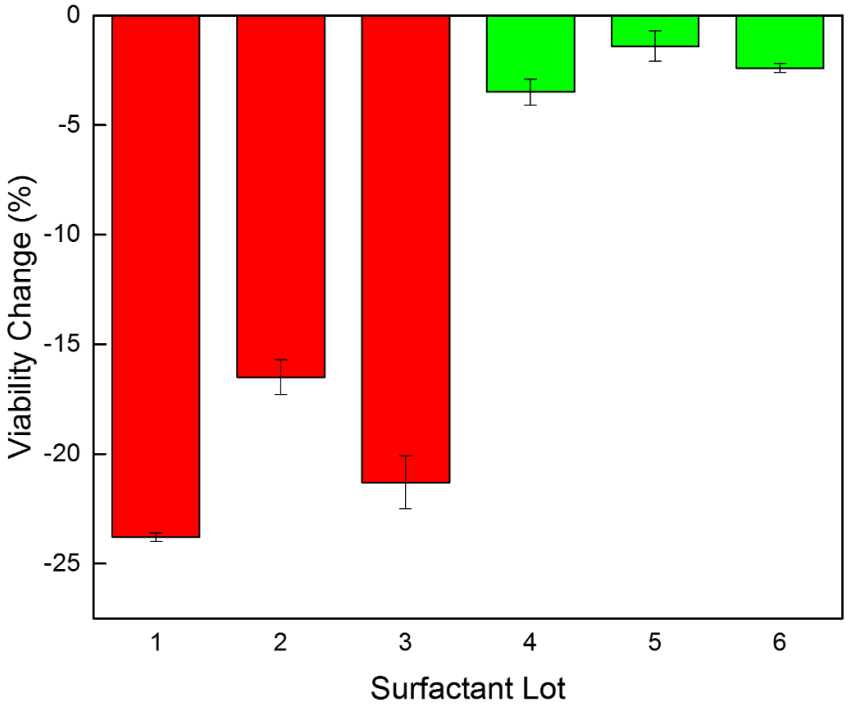

Figure 2.6: BSF assay results of cells in six different lots of P188 at 0.1% w/v. Cells with P188 lots 1-3 decreased in viability by more than 10%, indicating poor protection of cells, while Lots 4-6 offered high protection (n = 3, mean ± SD).

In the high concentration range above 1%, the surface tensions of P188-A, P188-B, and P188-A/P407 mixture diverge, with P188-B and P188-A/P407 exhibiting higher surface activity than P188-A. Mixed surfactant systems or impure surfactants often exhibit a negative peak or break in the γ-logC curve near the CMC region [39,40], which has been previously reported to be 3-5% at 37°C [41,42]. A break in the surface tension isotherm was observed for both P188-A/P407 and P188-B around 1%. This phenomenon is attributed to the presence of a more surface active species (such as P407), which can adsorb to the air-water interface and further decrease the surface tension beyond the pure system. For P188-A, the surface tension at 10% was 40.5 mN/m, while

the surface tensions of P188-B, P188A/P407, and P407 systems reached about 38.0 mN/m. We hypothesized that P188 lots which contain surface active impurities, and therefore impart poor shear protection in cell culture, could be detected by measuring the interfacial tension at 10% concentration. Six lots of P188 were first characterized in the BSF assay and categorized as poor protectants if cell viability decreased by more than 10% (data shown in **Figure 2.6**). The equilibrium surface tension of the six P188 lots in 10% solution is shown in **Figure 2.7**. We found a strong correlation between shear protection and equilibrium surface tension measured at this concentration. P188 solutions with less than 38.0 mN/m provided poor protection, while those higher than 40.0 mN/m provided high shear protection to cells. These results suggest that detection of surface active impurities in P188 lots achieved through equilibrium surface tension measurements may be used as a simple, cell-free, assay to screen for quality of shear protection of surfactant lots.

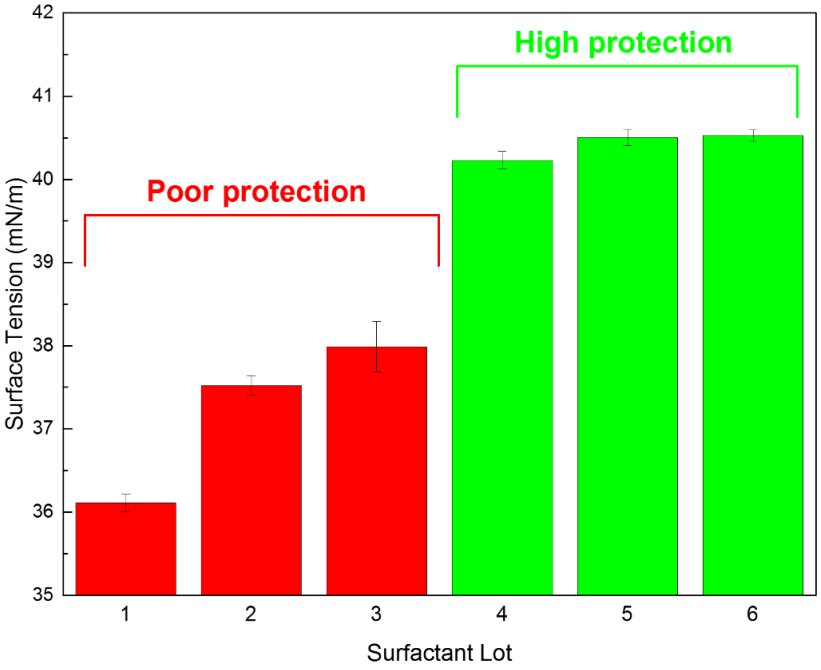

Figure 2.7: Equilibrium surface tension measurements of six different batches of P188 at 10% w/v and 36ºC. Lots 1-3 provided poor protection of cells, while Lots 4-6 offered high protection (n = 5, mean ± SD). The decreased surface tension in all poorly protective batches suggests the presence of surface active impurities.

2.3.3 Quantification of cell-bubble attachment with P188 and P407

Surface active impurities in P188 may disrupt shear protection to cells, but their mechanism of action remains unclear. Surfactants in bioreactors have been shown to decrease cell-to-bubble attachment, which limits the number of cells transported to and subsequently damaged in the foam layer [7,8,17,20,21]. As means of detecting the role of the interfacial effects on a larger scale, we characterized the effect of P188 and P407 on the adhesion of cells to rising air bubbles. During cell-bubble attachment, cells come into physical contact with bubbles, and a new interface between the membrane and gas bubble may form. Thermodynamically, the free energy change associated with the formation of a cell-vapor interface can be generally described by the equation [43]

$$\Delta F_{adh} = \gamma_{cell-vapor} - (\gamma_{liquid-vapor} + \gamma_{cell-liquid})$$

where $\gamma_{cell-vapor}, \gamma_{liquid-vapor},$ and $\gamma_{cell-liquid}$ are the interfacial tensions between the cell-vapor, liquid-vapor and cell-liquid phases, respectively. A decrease in liquid-vapor interfacial tension from surfactants increases the free energy change of cell-bubble adhesion, making attachment less favorable. Poloxamer has also been shown to reduce cell hydrophobicity [44], which may also decrease hydrophobic interactions between cells and bubbles.

In our foam collection experiment, we quantified cell-bubble attachment by collecting the foam layer produced by bubbling uniform air bubbles through a cell suspension. The enrichment factors for P188 and P407 at 0.01% and 0.05% surfactant concentration are plotted in **Figure 2.8(a).** As P188 concentration increases from 0.01 to 0.05%, EF decreases from 1.2 to 0.5. These EF values agree with those reported in literature [7]. For P407, a similar trend was observed. Interestingly, the EF was not significantly different between P188 and P407 despite the higher surface activity of P407. This result indicates that the cell-bubble attachment rate is not negatively impacted by P407, despite its poor cell protective properties. Consequently, this result also suggests that the cell-bubble attachment is not directly correlated with cell protection. Both P188 and P407 decrease the cell-bubble attachment rate by decreasing the interfacial tension, but P188 clearly shows a superior cell protective capacity. From this, we hypothesize that cell-bubble attachment may contribute to surfactant-mediated shear protection of cells in bioreactors, but is not the dominant mechanism. Instead, adsorption of surfactant to the membrane interface appears to play a greater role in shear protection.

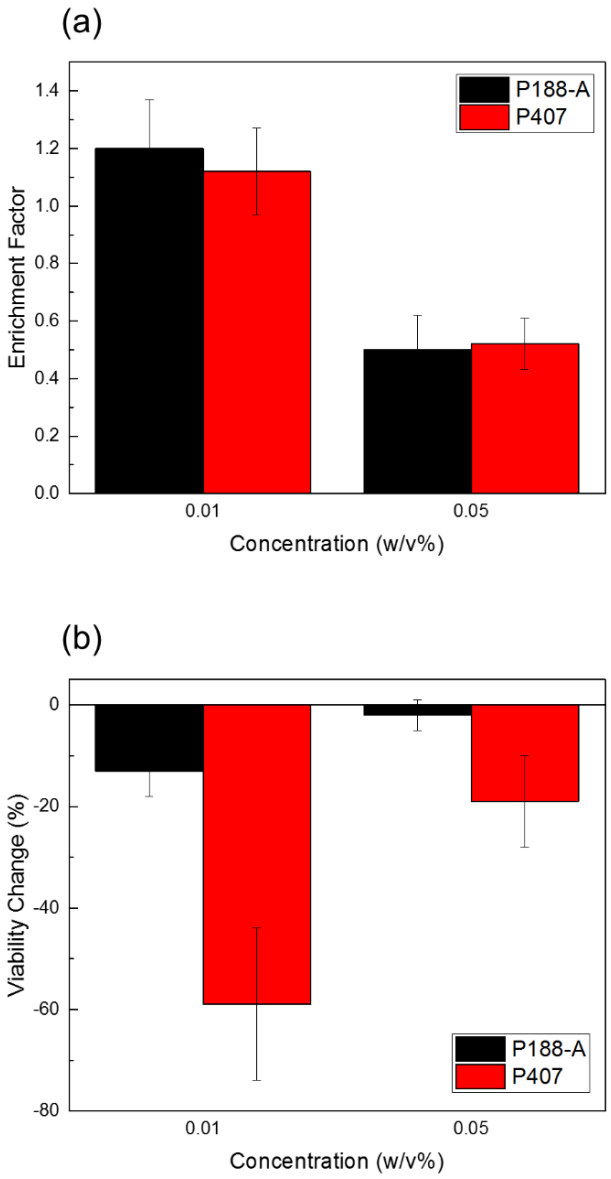

Figure 2.8: (a) Ratio of cells concentrated in the foam relative to the bulk for P188-A and P407. (b) Viability change of the cells in the foam following foam collapse for P188-A and P407 (n = 3, mean ± SD). The data show that P407 does not impact cell-to-bubble attachment rate, but provides poor protection to cells upon foam breakdown.

The interaction between poloxamers and model lipid monolayers and bilayers has recently been discussed by several groups in the perspective of wound healing and cell repair [45–47]. P188 has been demonstrated to have various therapeutic effects on damaged cells, functioning as a membrane "sealant" for cells with compromised membranes [48]. In **Figure 2.8(b)**, we show that cells collected from the collapsed foam of P188 show almost no viability drop, compared to a 20% viability drop with P407. During breakdown of the foam, cells in close proximity to bursting films experience large energy dissipation rates, which can disrupt cell membrane integrity and induce lethal cell response [17]. The high survival rate of cells in collapsed P188 foam compared to P407 foam suggests that P188 primarily protects cells by strengthening of the cell membrane. It should be noted that an increase in surfactant concentration increased shear protection with both surfactants, consistent with other studies [30,49]. P407 may offer some protection, but is not as effective as P188. We hypothesize that more surface active species such as P407 preferentially adsorb to the cell membrane, as shown schematically in **Figure 2.9.** Once adsorbed, these high molecular weight surfactants prevent the bulk species from adsorbing to the cells and protecting them. Under a high shear environment, these highly adsorbent surface-active species render the cell more fragile and susceptible to damage, resulting in low cell viability.

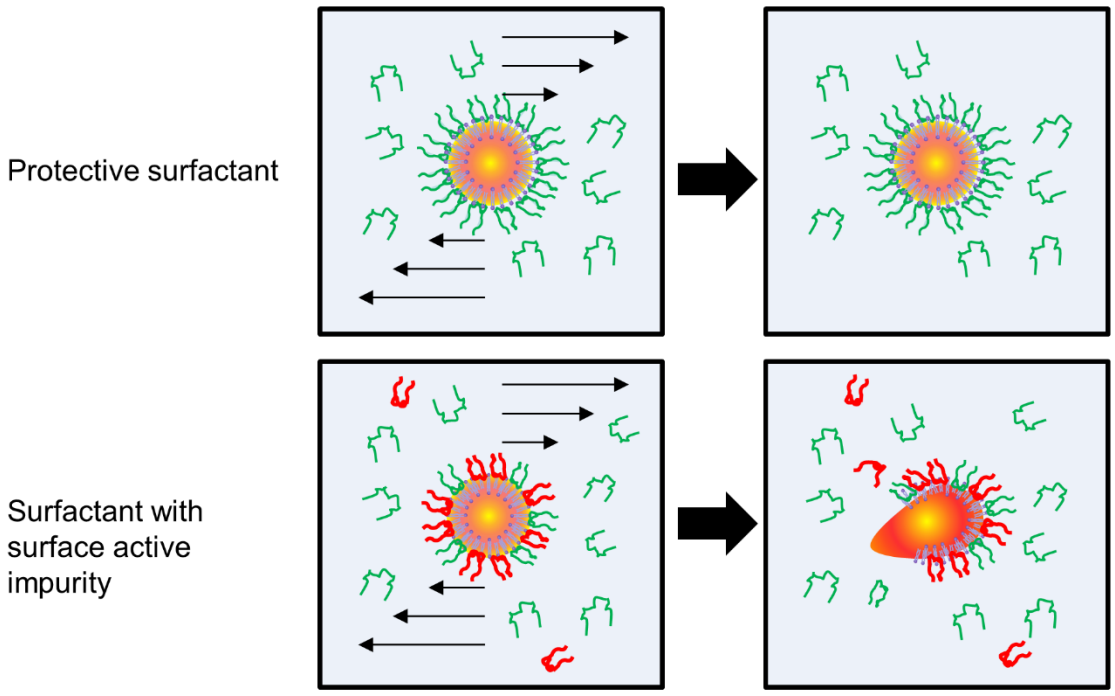

Figure 2.9: Schematic of the proposed mechanism of cell protection disruption by surface active impurities (red). The bulk species (green), protect cells from shear when adsorbed to the membrane interface. Surface active impurities preferentially adsorb to the membrane interface and render the cell more susceptible to physical damage.

2.4 Conclusion

As the biotechnology industry pushes towards higher product titers through increased cell density and process intensification, the bioreactor environment will only become harsher through increased oxygen demand and aeration rates. A fundamental understanding of surfactant-mediated cell protection is necessary in order to minimize shear related damage in the manufacturing environment. At present, the mechanism of surfactant-mediated shear protection of cells is believed to originate from adsorption of surfactant molecules both at the bubble and at the cell membrane interface. In this investigation, we explored the effect of single and mixed poloxamers

of varying cell protection on the gas-liquid interface. P407 imparts low cell protection compared to P188, but has higher surface activity, as determined by foam stability and equilibrium surface tension measurements. When the two surfactants are mixed, the more surface active P407 preferentially adsorbs to the interface. Therefore, cells are fragile in the presence of a P188/P407 mixture, even when P407 is the minority species. The presence of surface active impurities similar to P407 can occur during the industrial synthesis of P188 batches, which may lead to high cell damage during production of therapeutic proteins. We have shown that equilibrium surface tension can be used to detect these impurities, demonstrating the potential use of this simple technique in screening for lot to lot variability of P188 batches.

Finally, we have shown that despite having different interfacial properties, P188 and P407 do not significantly differ in their effect on cell-bubble attachment. Instead, cells in the presence of P407 sustained higher damage during bubble rupture and the subsequent foam breakdown. These results suggest that poloxamer-mediated cell protection is not primarily dependent on adsorption of surfactant to the gas liquid interface, but may instead depend on the adsorption of surfactants to the membrane interface, strengthening and increasing cell robustness. Incorporation of these findings may enable a new fundamental approach to optimize surfactant selection and further improve shear protective properties of new surfactants.

Acknowledgements

We gratefully acknowledge financial support from Biogen (RTP, NC). The authors would also like to thank Joe Lavoie for his help with the surface tensiometer, and Eric Peng for insightful discussions.

2.5 References

[1] D.G. Kilburn, F.C. Webb, The Cultivation of Animal Cells at Controlled Dissolved Oxygen Partial Pressure, Biotechnol. Bioeng. X (1968) 801–814.

[2] H.E. Swim, R.F. Parker, Effect of Pluronic F68 on Growth of Fibroblasts in Suspension on Rotary Shaker, Exp. Biol. Med. 103 (1960) 252–254.

[3] D.W. Murhammer, C.F. Goochee, Scaleup of Insect Cell Cultures: Protective Effects of Pluronic F-68, Nat. Biotechnol. 6 (1988) 1411–1418.

[4] S.J. Meier, T.A. Hatton, D.I.C. Wang, Cell death from bursting bubbles: role of cell attachment to rising bubbles in sparged reactors, Biotechnol. Bioeng. 62 (1999) 468–478.

[5] J.D. Michaels, J.E. Nowak, A.K. Mallik, K.K. Koczo, D.T. Wasan, E.T. Papoutsakis, Analysis of cell-to-bubble attachment in sparged bioreactors in the presence of cell-protecting additives, Biotechnol. Bioeng. 47 (1995) 407–419. doi:10.1002/bit.260470402.

[6] A. Handa-Corrigan, A.N. Emery, R.E. Spier, Effect of gas-liquid interfaces on the growth of suspended mammalian cells: mechanisms of cell damage by bubbles, Enzyme Microb. Technol. 11 (1989) 230–235. doi:http://dx.doi.org/10.1016/0141-0229(89)90097-5.

[7] N. Ma, J.J. Chalmers, J.G. Auniņs, W. Zhou, L. Xie, Quantitative studies of cell-bubble interactions and cell damage at different pluronic F-68 and cell concentrations, Biotechnol. Prog. 20 (2004) 1183–91. doi:10.1021/bp0342405.

[8] F. Bavarian, L.S. Fan, J.J. Chalmers, Microscopic Visualization of Insect Cell-Bubble Interactions. I: Rising Bubbles, Air-Medium Interface, and the Foam Layer, Biotechnol. Prog. 7 (1991) 140–150. doi:10.1021/bp00008a009.

[9] Y. Chisti, Animal-cell damage in sparged bioreactors, Trends Biotechnol. 18 (2000) 420–432. doi:10.1016/S0167-7799(00)01474-8.

[10] E.T. Papoutsakis, Fluid-mechanical damage of animal cells in bioreactors, Trends Biotechnol. 9 (1991) 427–437.

[11] M. Garcia-Briones, J.J. Chalmers, Cell-bubble interactions, Ann. N. Y. Acad. Sci. 665 (1992) 219–229.

[12] J.J. Chalmers, F. Bavarian, Microscopic visualization of insect cell-bubble interactions. II: The bubble film and bubble rupture, Biotechnol. Prog. 7 (1991) 151–158. doi:10.1021/bp00008a010.

[13] S. Zhang, A. Handa-Corrigan, R.E. Spier, Foaming and media surfactant effects on the cultivation of animal cells in stirred and sparged bioreactors, J. Biotechnol. 25 (1992) 289–306.

[14] K.T. Kunas, E.T. Papoutsakis, Damage mechanisms of suspended animal cells in agitated bioreactors with and without bubble entrainment., Biotechnol. Bioeng. 36 (1990) 476–83. doi:10.1002/bit.260360507.

[15] R.S. Cherry, E.T. Papoutsakis, Physical mechanisms of cell damage in microcarrier cell culture bioreactors, Biotechnol. Bioeng. 32 (1988) 1001–1014. doi:10.1002/bit.260320808.

[16] J.M. Boulton-Stone, J.R. Blake, Gas bubbles bursting at a free surface, J. Fluid Mech. 254 (1993) 437–466.

[17] K. Trinh, M. Garcia-Briones, F. Hink, J.J. Chalmers, F. Hink, Quantification of damage to suspended insect cells as a result of bubble rupture, Biotechnol. Bioeng. 43 (1994) 37–45.

doi:10.1002/bit.260430106.

[18] M.A. Garcia-Briones, R.S. Brodkey, J.J. Chalmers, Computer simulations of the rupture of a gas bubble at a gas-liquid interface and its implications in animal cell damage, Chem. Eng. Sci. 49 (1994) 2301–2320. doi:10.1016/0009-2509(94)E0038-R.

[19] W. Hu, C. Berdugo, J.J. Chalmers, The potential of hydrodynamic damage to animal cells of industrial relevance: current understanding, Cytotechnology. 63 (2011) 445–460. doi:10.1007/s10616-011-9368-3.

[20] T. Tharmalingam, H. Ghebeh, T. Wuerz, M. Butler, Pluronic enhances the robustness and reduces the cell attachment of mammalian cells, Mol. Biotechnol. 39 (2008) 167–177. doi:10.1007/s12033-008-9045-8.

[21] W. Hu, J.J. Rathman, J.J. Chalmers, An investigation of small-molecule surfactants to potentially replace pluronic F-68 for reducing bubble-associated cell damage, Biotechnol. Bioeng. 101 (2008) 119–127. doi:10.1002/bit.21872.

[22] D. Chattopadhyay, J.F. Rathman, J.J. Chalmers, The protective effect of specific medium additives with respect to bubble rupture, Biotechnol. Bioeng. 45 (1995) 473–480. doi:10.1002/bit.260450603.

[23] J.D. Michaels, J.E. Nowak, A.K. Mallik, K. Koczo, D.T. Wasan, E.T. Papoutsakis, Interfacial Properties of Cell Culture Media with Cell-Protecting Additives, Biotechnol. Bioeng. 47 (1995) 420–430.

[24] Z. Zhang, M. Al-Rubeai, C.R. Thomas, Effect of Pluronic F-68 on the mechanical properties of mammalian cells, Enzyme Microb. Technol. 14 (1992) 980–983.

[25] O.T. Ramírez, R. Mutharasan, The role of the plasma membrane fluidity on the shear sensitivity of hybridomas grown under hydrodynamic stress, Biotechnol. Bioeng. 36 (1990) 911–920. doi:10.1002/bit.260360906.

[26] O.T. Ramirez, R. Mutharasan, Effect of serum on the plasma membrane fluidity of hybridomas: an insight into its shear protective mechanism, Biotechnol. Prog. 8 (1992) 40–50.

[27] V.M. Nace, Nonionic Surfactants: Polyoxyalkylene Block Copolymers, CRC Press, 1996.

[28] D.W. Murhammer, C.F. Goochee, Structural features of nonionic polyglycol polymer molecules responsible for the protective effect in sparged animal cell bioreactors, Biotechnol. Prog. 6 (1990) 142–148. doi:10.1021/bp00002a008.

[29] P. Alexandridis, V. Athanassiou, S. Fukuda, T.A. Hatton, Surface Activity of Poly(ethylene oxide)-block-Poly(propylene oxide)-block-Poly(ethylene oxide) Copolymers, Langmuir. 10 (1994) 2604–2612.

[30] H. Peng, K.M. Hall, B. Clayton, K. Wiltberger, W. Hu, E. Hughes, et al., Development of small scale cell culture models for screening poloxamer 188 lot-to-lot variation, Biotechnol. Prog. 30 (2014) 1411–1418. doi:10.1002/btpr.1967.

[31] P.A. Apostolidis, A. Tseng, M.-E. Koziol, M.J. Betenbaugh, B. Chiang, Investigation of low viability in sparged bioreactor CHO cell cultures points to variability in the Pluronic F-68 shear protecting component of cell culture media, Biochem. Eng. J. 98 (2015) 10–17. doi:10.1016/j.bej.2015.01.013.

[32] H. Peng, A. Ali, M. Lanan, E. Hughes, K. Wiltberger, B. Guan, et al., Mechanism

investigation for Poloxamer 188 raw material variation in cell culture, Biotechnol. Prog. 32 (2016) 767–775. doi:10.1002/btpr.2268.

[33] B. Guan, A. Ali, H. Peng, W. Hu, L.R. Markely, S. Estes, et al., Characterization of poloxamers by reversed-phase liquid chromatography, Anal. Methods. 8 (2016) 2812–2819. doi:10.1039/C5AY03311J.

[34] P. Alexandridis, T.A. Hatton, Poly(ethylene oxide)-poly(propylene oxide)-poly(ethylene oxide) block copolymer surfactants in aqueous solution and at interfaces: thermodynamics, structure, dynamics, and modeling, Colloids Surfaces A Physicochem. Eng. Asp. 96 (1995) 1–46.

[35] C. Stubenrauch, K. Khristov, Foams and foam films stabilized by CTAB: Influence of the chain length and of impurities, J. Colloid Interface Sci. 286 (2005) 710–718. doi:10.1016/j.jcis.2005.01.107.

[36] B.R. Blomqvist, S. Folke, P.M. Claesson, The Stabilization of Aqueous PEO-PPO-PEO Triblock Copolymer Foam, J. Dispers. Sci. Technol. 27 (2006) 469–479. doi:10.1080/01932690500374201.

[37] K. Ogino, M. Abe, Mixed Surfactant Systems, CRC Press, 1992.

[38] M.G. Muñoz, F. Monroy, F. Ortega, R.G. Rubio, D. Langevin, Monolayers of symmetric triblock copolymers at the air-water interface. 1. Equilibrium properties, Langmuir. 16 (2000) 1083–1093. doi:10.1021/la990142a.

[39] S.-Y. Lin, Y.-Y. Lin, E.-M. Chen, C.-T. Hsu, C.-C. Kwan, A Study of the Equilibrium Surface Tension and the Critical Micelle Concentration of Mixed Surfactant Solutions,

Langmuir. 15 (1999) 4370–4376. doi:10.1021/la981149f.

[40] G.D. Miles, L. Shedlovsky, Minima in surface tension-concentration curves of solutions of sodium alcohol sulfates, J. Phys. Chem. 48 (1944) 57–62.

[41] S.M. Moghimi, A.C. Hunter, C.M. Dadswell, S. Savay, C.R. Alving, J. Szebeni, Causative factors behind poloxamer 188 (Pluronic F68, Flocor)-induced complement activation in human sera. A protective role against poloxamer-mediated complement activation by elevated serum lipoprotein levels, Biochim. Biophys. Acta. 1689 (2004) 103–13. doi:10.1016/j.bbadis.2004.02.005.

[42] G. Serbest, J. Horwitz, K. Barbee, The effect of poloxamer-188 on neuronal cell recovery from mechanical injury, J. Neurotrauma. 22 (2005) 119–32. doi:10.1089/neu.2005.22.119.

[43] D. Chattopadhyay, J.F. Rathman, J.J. Chalmers, Thermodynamic approach to explain cell adhesion to air-medium interfaces., Biotechnol. Bioeng. 48 (1995) 649–58. doi:10.1002/bit.260480613.

[44] H. Ghebeh, J. Gillis, M. Butler, Measurement of hydrophobic interactions of mammalian cells grown in culture, J. Biotechnol. 95 (2002) 39–48. doi:10.1016/S0168-1656(01)00440-0.

[45] S.A. Maskarinec, J. Hannig, R.C. Lee, K.Y.C. Lee, Direct observation of poloxamer 188 insertion into lipid monolayers, Biophys. J. 82 (2002) 1453–1459. doi:10.1016/S0006-3495(02)75499-4.

[46] M.A. Firestone, S.S. Wolf, Amanda C., A.C. Wolf, S. Seifert, Small-Angle X-ray Scattering Study of the Interaction of Poly (ethylene oxide)-b-Poly (propylene oxide)-b-Poly (ethylene

oxide) Triblock Copolymers with Lipid Bilayers, Biomacromolecules. 4 (2003) 1539–1549. doi:10.1021/bm034134r.

[47] L.C. Chang, Y.-Y. Chang, C.-S. Gau, Interfacial properties of Pluronics and the interactions between Pluronics and cholesterol/DPPC mixed monolayers, J. Colloid Interface Sci. 322 (2008) 263–273. doi:10.1016/j.jcis.2008.02.051.

[48] S. Yasuda, D. Townsend, D.E. Michele, E.G. Favre, S.M. Day, J.M. Metzger, Dystrophic heart failure blocked by membrane sealant poloxamer, Nature. 436 (2005) 1025–1029. doi:10.1038/nature03844.

[49] T. Tharmalingam, C.T. Goudar, Evaluating the impact of high Pluronic F68 concentrations on antibody producing CHO cell lines, Biotechnol. Bioeng. 112 (2014) 832–837. doi:10.1002/bit.25491.

Chapter 3 Analysis of Poloxamer-mediated modulation of membrane fluidity to enhance shear protection of CHO cells in commercial bioreactors

3.1 Introduction

Although protein production in cell-based biotechnology is primarily controlled via biological pathways, interfacial interactions of surface-active components (proteins, surfactants, antifoam, waste byproducts) with cell and bubble surfaces can also have significant impact on bioreactor performance. As process improvements push cell densities towards 10^8 cells/mL to reach greater than 10 g/L titer, high mass-transfer requirements make these interactions increasingly important [1]. Hydrophobic cells in suspension tend to adsorb to rising bubbles and concentrate at the top of the bioreactor, where they can be damaged by bursting bubbles in the foam layer, or trapped in the foam layer (**Figure 3.1**). The extent of damage is determined by the cell's physiology (intrinsic property), the hydrodynamic shear environment in the bioreactor, and chemical additives in the media (extrinsic properties). The effects of bioreactor hydrodynamics and aeration on cell damage have been well summarized in a number of recent reviews [2,3], but less is known about the effect of additives on cell physiology in the context of shear protection.

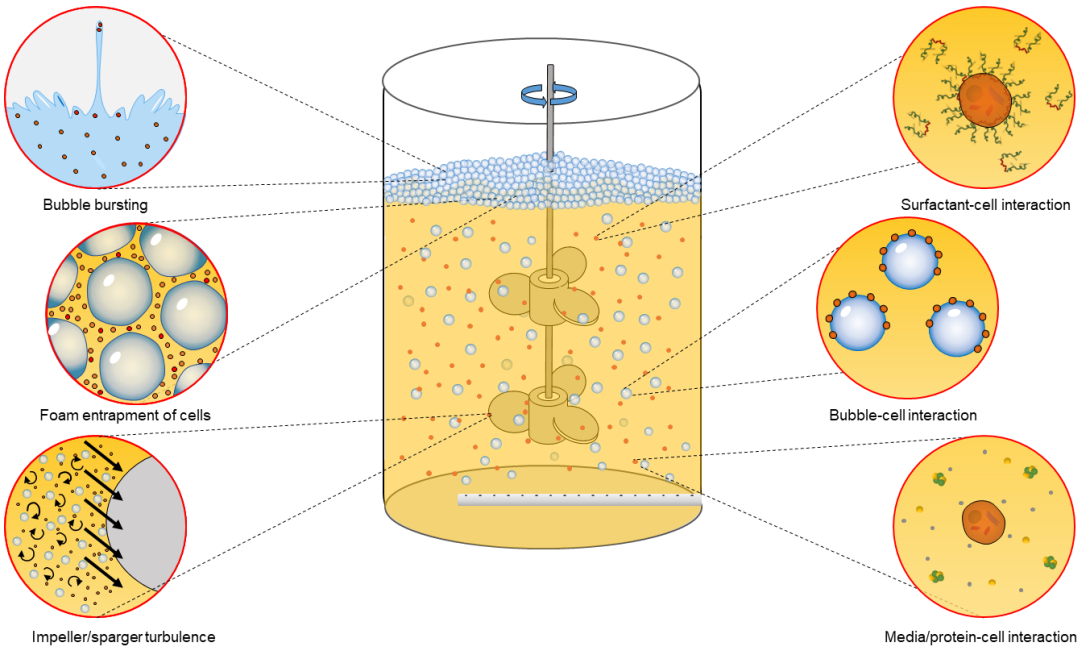

Figure 3.1*:* Schematic of relevant interfacial interactions during bioreactor operation. Bubble bursting, foam entrapment, and turbulence from agitation or sparging can all contribute to cell damage. The complex interactions between cells, bubbles, surfactants, and media components determine the cell's sensitivity and response to shear and are the focus of this report.

The addition of surface-active compounds to cell culture media was empirically discovered to mitigate shear damage more than 50 years ago [4,5]. The Poloxamer class of surfactants remains the most widely used shear protectant in industry today, but several types of polymers have been shown to be effective for this purpose, including polyvinyl alcohol (PVA), polyvinylpyrrolidone (PVP), methylcellulose, dextran, and polyethylene glycol (PEG) [6,7]. Extensive literature exists on the various sources of physical damage in animal cell bioreactors, with the major contributors being bubble bursting at the air-water interface [8–10] and energy dissipation from high gas entrance velocity [11,12]. However, detailed analysis of surfactant interactions with cells remains an ongoing topic of research. The need for alternative and improved shear protective additives necessitates a more complete understanding of these interactions [13].

Previous studies suggest that in order to be an effective shear protectant, the additive must (1) inhibit cell-bubble attachment, and (2) strengthen the mechanical stability of the cells [14–16]. The first mechanism precludes cells from becoming concentrated near the foam layer, where incessant bubble bursting from foam breakdown damages cells [17]. This also implies that protective additives should be amphiphilic in nature to make cell-gas adhesion thermodynamically unfavorable [18]. The second mechanism allows cells to withstand increasing levels of physical stress, which suggests that surfactant-cell interactions, governed by the additive's physical and chemical properties, play an important role in cell protection efficiency. Therefore, the combination of interfacial and physicochemical properties determine the additive's ability to prevent cell damage [17,19]. Poloxamers, and more specifically, Poloxamer 188, are the most widely used shear protectants because of their proficiency in both the above mechanisms. In addition to decreasing cell-bubble attachment, Poloxamer 188 has been found to increase membrane bursting tension and decrease cell membrane fluidity [15,20,21]. It has also been used as a cell membrane sealant for therapeutic applications [22,23].

Poloxamers are a class of nonionic triblock copolymers consisting of a hydrophobic poly(propylene oxide) (PPO) center group anchoring two hydrophilic poly(ethylene oxide) (PEO) tails. Generally, Poloxamers with low hydrophilic-lipophilic balance (HLB) tend to lyse or inhibit cell growth due to their strong emulsifying power, while more hydrophilic Poloxamers can protect cells from sparging damage [24]. Poloxamer efficiency in cell protection is related to the molecule's structure, which can be characterized by two parameters: average molecular weight (MW), and %PEO. In addition, the polydispersity of these polymers greatly affects their performance. Recently, renewed interest in the mechanism of Poloxamer protection of cell culture has arisen due to raw material variation in P188, which has resulted in multiple cases of low cell

viability and titer on the manufacturing scale [25,26]. The poorly performing lots of P188 were found to contain a high molecular weight (HMW) peak in their MW distributions. This HMW impurity was not cytotoxic, but decreased the cell protective abilities of P188. Therefore, cell culture prepared with these poor P188 lots sustained cell damage when subjected to the high-shear environment in manufacturing scale. Additionally, the HMW impurity was found to be highly surface-active, preferentially adsorbing to the air/water interface. While problematic for industry, the raw material variation presents an opportunity to elucidate the mechanism of cell protection. The adverse effect of the HMW moiety could be modeled by adding a small amount of Poloxamer 407 (P407), which has higher MW, hydrophobicity, and surface activity than P188 [27]. Previous experiments have shown that P407 decreases P188's cell protection without affecting the cell-bubble attachment rate [28]. Hence, the HMW impurities are believed to affect the cell interface.

The cell membrane fluidity is correlated to the molecular mobility of the lipid bilayer [29]. This mobility can be measured by tracking the lateral and rotational motion of molecular fluorescent probes that localize within the plasma membrane [30,31]. Ramirez and Mutharasan (1990) were the first to correlate rotational membrane fluidity and shear sensitivity in hybridoma cells, using steady-state fluorescent anisotropy to show that temperature, cholesterol, alcohol, serum, and P188 all affected both rotational membrane fluidity and cell sensitivity. More recently, P188 was discovered to have membrane resealing properties, repairing cell membrane damage by adsorption and insertion into damaged areas [23,32]. To understand the intricate mechanisms involved in surfactant-cell interactions and design robust means of their control for cell protection, we investigated the effect of Poloxamers of varying protective capacity on membrane physiology of CHO cells.

In this work, we characterized the effects of two chemically similar Poloxamers (P188 and P407) on both CHO cell membrane fluidity and shear sensitivity. These surfactants have similar tendency to decrease cell-bubble attachment but vary in cell protection efficiency. By isolating their effect on membrane fluidity, we can provide physiological basis for what makes P188 a superior cell protectant. In order to achieve these goals, first, we designed, tested and used a new cell sensitivity assay based on turbulent concentric shearing to rapidly (within 5 minutes) characterize the culture's robustness as a function of cell line and surfactant composition. Then, we characterized the cell suspension's membrane fluidity, which we determined using two separate techniques: fluorescence anisotropy and pyrene excimer fluorescence. These techniques use fluorescent probes to measure both rotational and lateral membrane fluidity, providing a more comprehensive analysis of the surfactant's effect on membrane properties. By combining the results from the above three methods, we correlate shear sensitivity to membrane fluidity for different CHO cell lines and surfactant compositions. The findings of this investigation show how membrane properties are significantly impacted by surfactants in the process of shear protection in animal cell culture.

3.2 Materials and methods

3.2.1 Surfactants and chemicals

P188 and P407 were provided by BASF Corporation and used as received. The physical properties of P188 and P407, as described by the manufacturer, are shown in Table I. Different lots of P188 provide different levels of shear protection. A P188 lot which provided low shear protection, as determined previously, was labeled "Bad P188" [28]. Experiments with each type of surfactant (P188, P407, and Bad P188) were performed using the same respective lots to ensure consistency. Poloxamer stock solutions were prepared by dissolving solid flakes in purified MilliQ

water (Millipore, Billerica, MA) to 100 g/L and sterilizing by filtration before use (0.22 µm, Millipore). Antifoam Q7 (Dow Corning) was diluted to 15% stock solution prior to use. 0.15 M phosphate buffer saline (PBS) solution was prepared by dissolving PBS tablets (Sigma-Aldrich) in water according to supplier's instructions, then filtered before use. Trimethylammonium diphenylhexatriene (TMA-DPH) for fluorescence anisotropy measurements was obtained from Thermo Fisher Scientific and dissolved in spectrophotometric grade dimethylformamide (Sigma-Aldrich) to make a 2.7 mM stock solution.

Table 3.1: Physical properties of Poloxamers used in this study.

Surfactant	**Average MW**	**PEO_x-PPO_y-PEO_x**	**HLB**	**%PEO**
P188	8400	80-27-80	29	81.8
P407	12600	101-56-101	22	73.2

3.2.2 Cell culture and maintenance

Experiments were performed using two recombinant CHO cell lines of DG44 lineage (CHO-A and CHO-B) secreting monoclonal antibodies. Cells were cultured at 36-37^{o}C and 5% CO_2 with a constant agitation rate of 125 rpm in 1L unbaffled shake flasks (Corning, Corning, NY). Flasks were passaged every 3-4 days in Biogen's proprietary chemically defined media and kept in exponential growth phase for all experiments. Media was prepared without P188, then supplemented with P188 stock solution to 2 g/L during passage to ensure the same P188 lot was used. Viable cell density (VCD) and cell viability were measured using trypan blue dye exclusion with ViCell XR automated cell counter (Beckman Coulter, Brea, CA). Unstained cells were considered viable, while stained cells were considered nonviable.

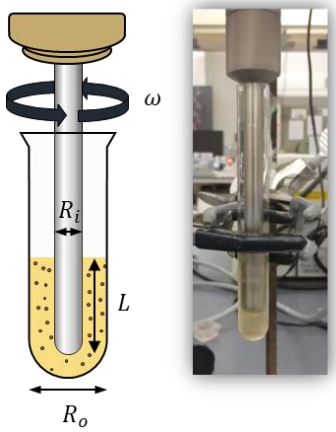

Figure 3.2: Schematic and photo of our concentric cylinder mixer (CCM) assay to measure cell shear sensitivity. The culture is sheared in the mixer for 5 minutes at 6000 rpm, and the resulting VCD change is measured using trypan blue exclusion to determine the cell sensitivity.

3.2.3 Scale-down model of cell sensitivy using concentric shearing

A concentric cylinder mixer (CCM) was used to measure cell culture shear sensitivity. A ServoDyne electronic mixer (Cole-Parmer, Vernon Hills, IL) equipped with a stainless-steel shaft with radius $R_i = 4.75$ mm was used to shear the cell suspension (see **Figure 3.2**). To prepare cell suspension, cells in exponential growth phase were centrifuged at 400*g* for 5 min. After discarding the supernatant, the cell pellet was gently resuspended to a VCD of 10^6 cells/mL in media supplemented with desired surfactant composition. Then, 5 mL of cell suspension was transferred to a glass test tube with radius $R_o = 6.25$ mm and centered with the steel shaft to form a gap distance $R_o - R_i$ of 1.5 mm with solid-liquid contact length L of 5.5 cm as shown in **Figure 3.2**. Antifoam stock solution was added to the suspension to final concentration of 150 ppm to prevent foam formation (which would change contact length L) during shearing. Cells were sheared in the CCM for 5 minutes at 6000 rpm, then analyzed by trypan blue exclusion. We calculate the normalized change in VCD as a measure of cell damage, given in Equation 1. VCD_i and VCD_f refer to the viable cell density before and after shearing, respectively.

$$\text{Normalized } \Delta\text{VCD} = \left(\frac{VCD_f - VCD_i}{VCD_i} \right) \cdot 100\% \quad \text{(Eq 1)}$$

The baffled shake flask (BSF) assay was used to validate the data obtained in the CCM. Cell suspension, prepared as above, was transferred to a 1L unbaffled shake flask (Corning, Corning, NY). After one hour of agitation at 200 rpm and 25 mm orbital diameter, the viability and VCD were measured and set as VCD_i. A portion of the cell suspension was then transferred to a baffled shake flask. After one hour of agitation at the same agitation conditions, the change in VCD and viability of the culture in the BSF assay were calculated by Equation 1.

3.2.4 Fluorescence anisotropy measurements for rotational membrane fluidity

3.2.4.1 Sample preparation for anisotropy experiments

Cell samples were washed twice with PBS, then resuspended to 10^6 cells/mL with desired surfactant concentration in PBS. TMA-DPH stock solution was then added to reach a final concentration of 2 μM. The suspension was equilibrated in shake flasks for at least 10 minutes prior to anisotropy measurements, then transferred to a 10 mm pathlength quartz cuvette for anisotropy measurement. Samples were stirred continuously throughout the duration of the experiment using a Starna Spinette (Starna Cells) electronic cell stirrer to prevent settling of the cells. At the end of anisotropy experiments, samples were analyzed by trypan blue to confirm that viability did not decrease during measurement.

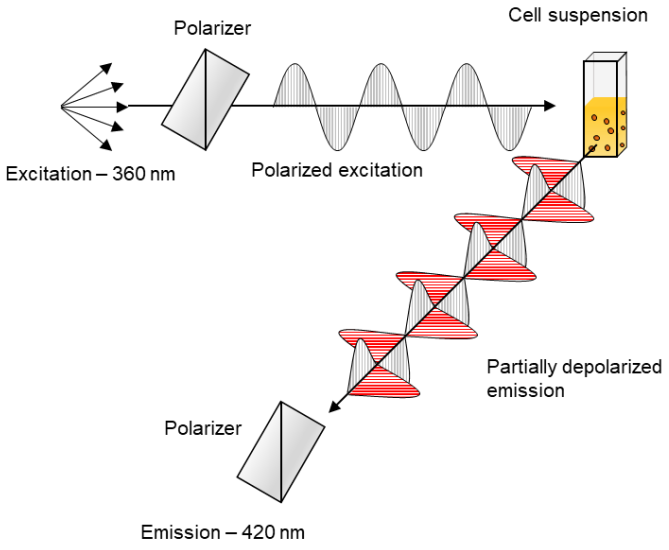

Figure 3.3*:* Schematic of the optical setup for fluorescence anisotropy measurements. Polarized light at 360 nm excites the cell suspension labeled with fluorophore. The resulting emission is partially depolarized depending on cell's membrane fluidity. The emission is detected at 420 nm with emission polarizer oriented parallel and perpendicular to excitation polarization.

3.2.4.2 Measurement of time-resolved fluorescence anisotropy

Time-resolved fluorescence anisotropy decays were measured by a time correlated single photon counting (TCSPC) detection system (LifeSpec II, Edinburgh Instruments, UK). In this system, polarized 360 nm excitation source was generated using the second-harmonic (HarmoniXX, A.P.E. 4 MHz, ~1 nJ/pulse) of a widely tunable mode-locked femtosecond Ti-Sapphire laser tuned to 720 nm (Chameleon Ultra II, Coherent, Santa Clara, CA). Emission was collected at 420 ($\Delta\lambda$ = 4 nm) with a rotary Glan-Thompson polarizing lens in the emission path and 395 nm long pass filter to block any scattered excitation light. The instrument response function (IRF) was measured using scattered excitation light from a 10 mm pathlength optical cell containing water and determined to be ~150 ps.

The setup for anisotropy measurements is schematically depicted in **Figure 3.3**. Cell suspension labeled with TMA-DPH was excited with polarized light, and emission was detected

with the emission polarizer oriented parallel ($I_{\parallel}$) and perpendicular ($I_{\perp}$) to excitation light. Then, anisotropy decay function $r(t)$ was calculated using Equation (2):

$$r(t) = \frac{I_{\parallel}(t) - GI_{\perp}(t)}{I_{\parallel}(t) + 2GI_{\perp}(t)} \quad \text{(Eq 2)}$$

$I_{\parallel}(t)$ and $I_{\perp}(t)$ are the parallel and perpendicular emission intensities with respect to the excitation light, and G is the G-factor, which corrects for any polarization-dependent bias in instrument response. The G-factor was measured using the tail fitting method [33] with a solution of Coumarin 450 in methanol (OD = 0.13 at λ_{ex}= 360 nm). The calculated anisotropy function $r(t)$ then was fit to an exponential decay given in Equation 3:

$$r(t) = (r_0 - r_\infty)e^{-t/\theta} + r_\infty \quad \text{(Eq 3)}$$

where r_0 is the time-zero anisotropy, r_∞ is the limiting anisotropy (also known as residual anisotropy or long-time anisotropy), and θ is the rotational correlation time. The limiting anisotropy r_∞ is correlated with the orientational order of the membrane, and we report this value in our data [34,35].

3.2.5 Pyrene decanoic acid (PDA) fluorescence measurements for lateral membrane fluidity

3.2.5.1 Sample preparation for PDA fluorescence experiments

Membrane fluidity kit containing pyrene decanoic acid (PDA) in ethanol was purchased from Abcam (Cambridge, MA) as a 100 µM stock solution and used as received. Cell suspensions were prepared according to the supplier's recommendations. 10^5 cells/mL in media with desired surfactant composition was incubated with 2.5 µM PDA for 20 minutes. The solution was then

washed multiple times to remove residual PDA, resuspended with surfactant in PBS, and transferred to a 96-well plate for analysis.

3.2.5.2 Measurement of PDA intensity ratio

PDA fluorescence was quantified on a fluorescent plate reader (Synergy 2, BioTek, Winooski, VT). Pyrene excimers have been previously used as fluorescent probes in lateral membrane fluidity experiments [36,37]. Samples were excited at 350 nm, and the emission was collected at 400 and 470 nm for detection of monomer and dimer, respectively. Emission intensities were normalized with PBS containing only surfactant, then the intensity of monomer (C_m) to dimer (C_d) ratio was calculated according to Eq 4:

$$\text{Intensity Ratio (monomer/dimer)} = \frac{C_m}{C_d} \quad \text{(Eq 4)}$$

3.3 Results

3.3.1 Rapid characterization of CHO cell sensitivity using concentric cylinder mixer (CCM)

Initial data to evaluate the performance of the concentric cylinder mixer (CCM) as a scale-down assay is presented in **Figure 3.4**. Scale-down models for cell shear sensitivity are used to understand the effect of media composition or cell line dependence on cell robustness prior to scale-up. In **Figure 3.4**A, we plot data where CHO-A cells at 10^6 cells/mL in media of various surfactant systems were subjected to both the CCM and BSF assays, and the normalized VCD change was calculated to determine the shear sensitivity of the culture (large VCD decrease → high sensitivity). All surfactants were added at a constant concentration of 2.0 g/L. The CCM was operated at 6000 rpm for 5 minutes, while the BSF was run at 200 rpm for 1 hour. At the tested conditions, both assays showed similar trends and magnitudes of VCD change. The P188 system showed high protection of the cell culture, with approximately 10% VCD decrease. Both the bad

lot of P188 and the P188/P407 mixed system (1.98 g/L P188 and 0.02 g/L P407) exhibited large decreases in VCD (>30%), indicating inadequate shear protection. Two observations were made from this data. First, the agreement between the two methods validates the CCM's use as a scale-down model. Second, it is notable that the CCM could reproduce the BSF results rapidly and efficiently, using only 5 mL of solution in 5 minutes. Because of its high throughput capability, the new CCM assay was used to quantify cell sensitivity in subsequent experiments.

The dependence of cell sensitivity on surfactant type and concentration using the CCM is shown in **Figure 3.4**B. The data show a strong dose-dependent relationship between surfactant concentration and shear protection in all systems. A steep increase in cell protection efficiency was observed between 0 and 1 g/L for P188, with only minor increases above 2 g/L. This is consistent with the concentration range used in industry [38]. The cell protection of the bad lot of P188 and P188/P407 system was low compared to P188, but similar in magnitude. Therefore, we used the P188/P407 mixture in subsequent experiments to model the performance of P188 with HMW impurity. Note that a dose-dependent relationship is observed for all surfactant systems, indicating the absence of cytotoxic effects.

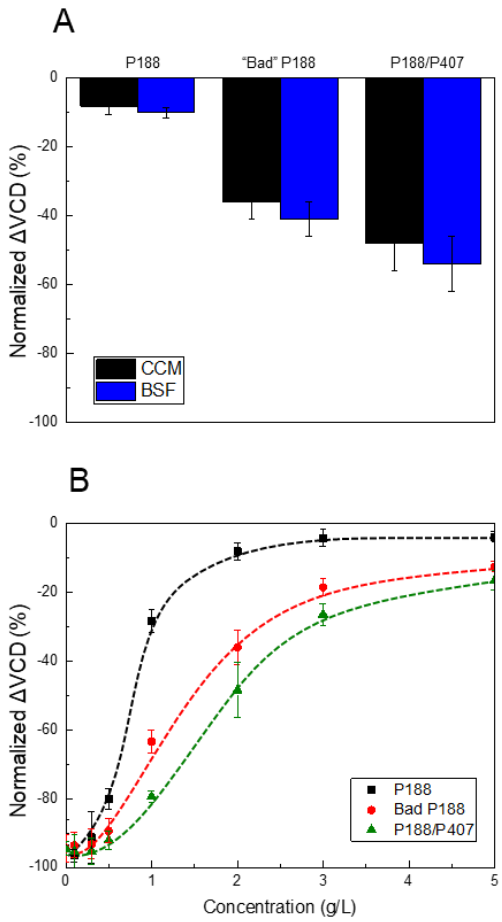

Figure 3.4: (A) Comparison of cell sensitivity with CCM (6000 rpm. 5 minutes) and BSF (200 rpm, 1 hour) assays in 2 g/L P188, 2 g/L bad lot of P188, and 2 g/L of 99% P188 1% P407 mixture (i.e. 1.98 g/L P188, 0.02 g/L P407). Results of cell sensitivity agree between CCM and BSF assays for all surfactant systems. (B) Concentration dependence of shear sensitivity with CCM with P188, bad lot of P188, and P188/P407. Bad P188 and P188/P407 system show similarly low cell protection compared to P188.

3.3.2 Effect of surfactant on rotational and lateral membrane fluidity

3.3.2.1 Rotational membrane fluidity

Surfactants adsorb to both gas-liquid and cell-liquid interfaces. To investigate the effect of surfactant on CHO cell lipid bilayers, we probed the membrane fluidity using two complementary methods. In the first method, we quantify the limiting anisotropy r_∞ of the fluorescent probe TMA-

DPH as a molecular measure of rotational membrane fluidity. TMA-DPH embedded in the cell membrane [39] is initially excited by vertically polarized light. As the fluorophore rotates within the bilayer, the emitted photon becomes partially depolarized. The magnitude of r_∞ is governed by the fluorophore's degree (angle) of rotation, which is related to the structural order of the membrane. A highly fluid membrane results in a high depolarization and low r_∞, while in a less fluid (i.e. ordered) membrane, the molecule has restricted rotation and the emission is less depolarized, resulting in relatively higher r_∞ (Equations 2 and 3). In our anisotropy experiments, we investigated the effects of surfactant composition and CHO cell line on limiting fluorescence anisotropy in correlation with shear sensitivity. **Figure 3.5**A shows a strong relationship between limiting anisotropy and cell sensitivity for CHO-A in three surfactant systems: 1.0 g/L P188, 1.0 g/L P407, and a surfactant-free system. The anisotropy of the cell suspension in P407 and without surfactant is significantly lower than cells with P188, indicating higher rotational fluidity. CHO-A cell line was then compared with CHO-B cell line, both suspended in 1.0 g/L P188. The cell line with higher shear resistance (CHO-B) also displayed higher anisotropy, indicating a more ordered membrane. Both CHO-A and CHO-B are derived from CHO DG44, but have slightly different shear sensitivities as determined by CCM. The concentration dependence of P188 on anisotropy for CHO-A showed a steep increase between 0 and 1 g/L, followed by a gradual plateau up to 10 g/L. These trends were again strongly correlated with the shear sensitivity of the culture.

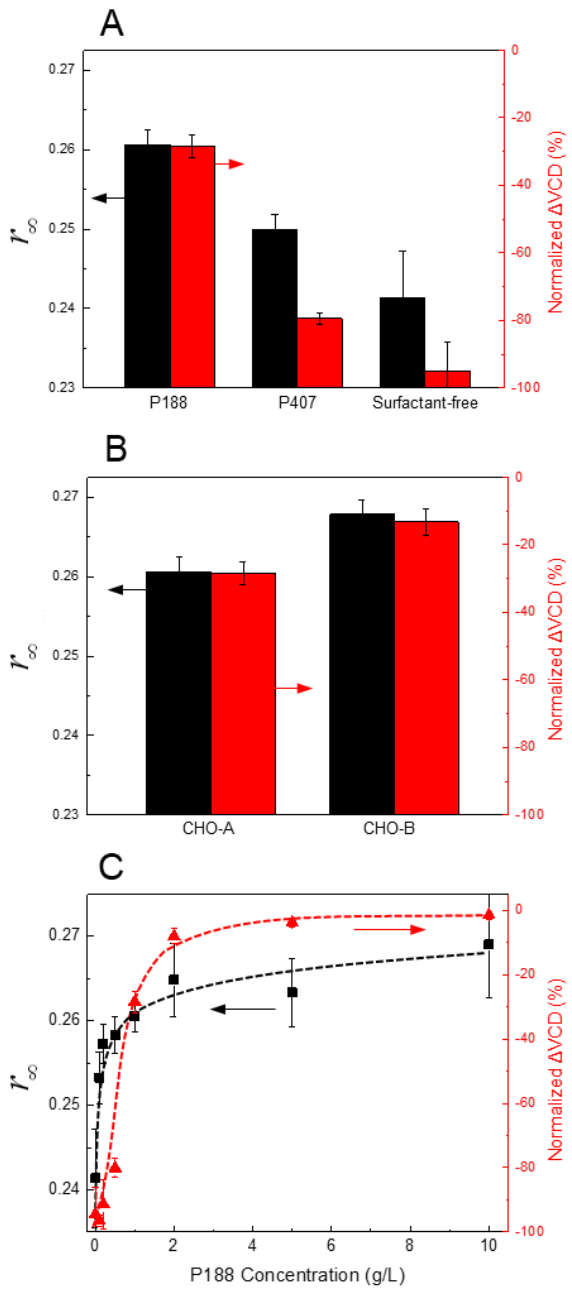

Figure 3.5: Effect of surfactant composition and CHO cell line type on limiting fluorescence anisotropy (r_∞) and shear resistance of the culture. r_∞ is a measure of rotational membrane order. (A) r_∞ and shear resistance of CHO-A cells in 1.0 g/L P188, 1.0 g/L P407, and without surfactant. Cells with higher r_∞ correlate with higher shear resistance. (B) Cell line dependence of r_∞ and shear resistance. CHO-B shows higher r_∞ and higher shear resistance. (C) Effect of P188 concentration on r_∞ and shear resistance for CHO-A, showing strong correlation of shear resistance and r_∞ with P188 concentration.

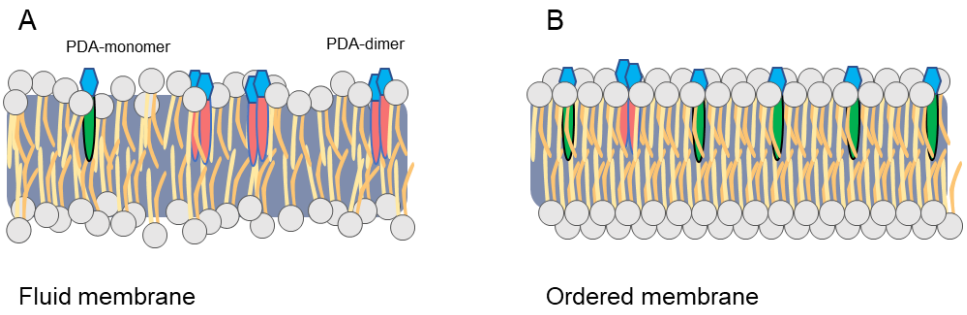

Figure 3.6: Schematic of lateral membrane fluidity measurement using PDA fluorescence. (A) A fluid membrane allows for high lateral mobility of PDA molecules, resulting in high dimer formation within the lipid bilayer. (B) In a more ordered membrane, lateral diffusion is restricted, resulting in relatively lower dimer formation. The ratio of PDA monomer intensity to PDA dimer intensity is related to the lateral membrane order.

3.3.2.2 *Lateral membrane fluidity*

To further investigate the observed dependence of membrane fluidity on surfactant type and concentration, we used pyrene excimer fluorescence to probe the lateral membrane fluidity. In this assay, schematically illustrated in **Figure 3.6**, the cell membrane is labeled with pyrene decanoic acid (PDA). PDA localizes in the cell membrane, and diffuses laterally within the bilayer [37,40]. As PDA molecules translate throughout the membrane, they can form dimers, resulting in a redshift of emission wavelength. In a lipid bilayer with low fluidity and high order, the motion of PDA is restricted, resulting in decreased dimer formation, while a fluid membrane allows for higher lateral diffusion and dimer fluorescence. Therefore, the ratio of monomer to dimer intensity (Eqn. 4) is directly correlated to the lateral lipid order and inversely correlated to the lateral membrane fluidity [31,41]. **Figure 3.7** shows the dependence of the monomer/dimer intensity ratio on P188 concentration. We observed an increase in PDA intensity ratio with increasing surfactant concentration, similar to the anisotropy trends in **Figure 3.5**C. Interestingly, the intensity ratio continues to increase up to 10 g/L instead of the previous plateau at 1-2 g/L observed with

anisotropy measurements. This may indicate that lateral order continues to increase with increasing surfactant concentration. Note that the plateau in normalized VCD change using CCM does not necessarily indicate a maximum in cell shear resistance, but rather that the level of applied shear is insufficient to induce lethal cell response.

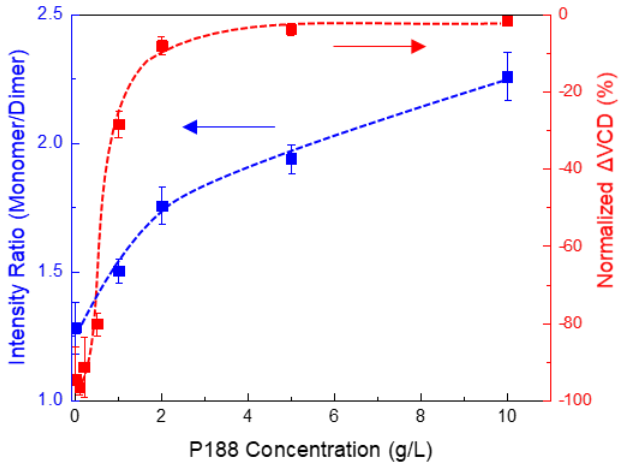

Figure 3.7: Effect of P188 concentration on both PDA intensity ratio and VCD change after shearing for CHO-A cells. The intensity ratio is a measure of lateral membrane order. At higher P188 concentrations, the membrane becomes more ordered and more shear resistant.

Finally, the effects of HMW impurity (P407) on membrane fluidity and shear sensitivity were investigated. While keeping a constant total surfactant concentration of 2.0 g/L, we varied the surfactant mixture composition from pure P188 to pure P407 and measured the resulting cell PDA intensity ratio and cell sensitivity with CCM. **Figure 3.8** shows that both the intensity ratio and shear resistance significantly decreased with only 5% P407 (i.e. 1.9 g/L P188, 0.1 g/L P407). Interestingly, neither intensity ratio nor shear sensitivity significantly decreased upon further increase of P407 ratio. This indicates that a small amount of HMW surfactant is sufficient to

saturate the cell interface, effectively decreasing the membrane mechanical stability in response to shear.

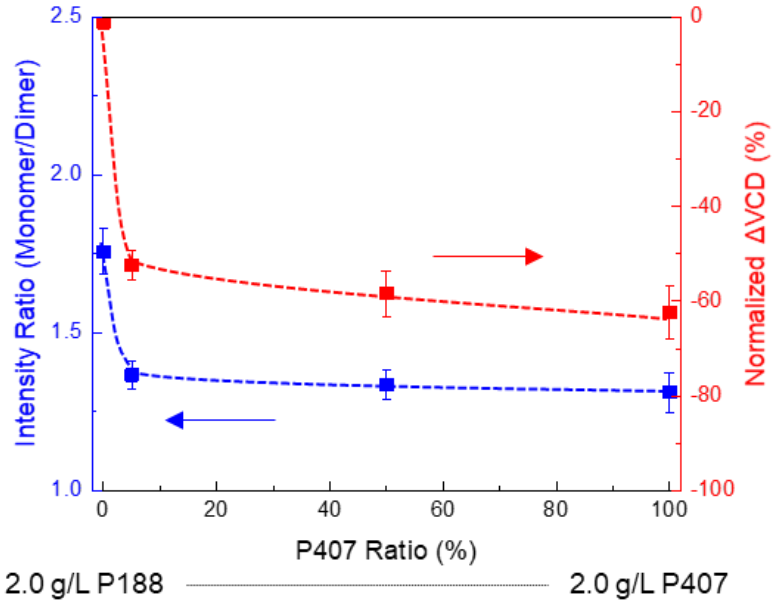

Figure 3.8: Effect of mixed surfactant composition at 2 g/L on PDA intensity ratio and VCD change after shearing for CHO-A cells. The addition of 5% (0.1 g/L) P407 results in rapid and large increase in membrane fluidity and shear sensitivity, indicating that it preferentially adsorbs to the cell interface.

3.4 Discussion

This investigation revealed the effects of two Poloxamers (P188 and P407) on CHO cell membrane properties and shear sensitivity. Both of these surfactants are relevant to industrial CHO cell culture – P188 is the most commonly used media additive for shear protection, while P407 is an example of a HMW impurity in P188 lot-to-lot variation which can lead to cell damage. By determining how P407 disrupts P188 shear protection, we can further understand the fundamentals of surfactant-mediated shear protection. The two proposed mechanisms for the protective effect of P188 in agitated cell cultures are (1) reduction of cell-bubble adhesion and (2) increase in cell

membrane strength. Several authors have observed that even in a bubble-free environment, P188 still confers substantial protective effects against shear [16,42]. Our investigation shows that CHO cell shear sensitivity is strongly correlated with the culture's membrane fluidity, independent of cell-bubble adhesion. This trend was consistent across intrinsic (cell line dependence) and extrinsic (surfactant dependence) properties.

Characterization of a cell culture's shear sensitivity has been accomplished in various assays including microfluidic flow contraction device [43,44], thin capillary channels [42], rheometry/viscometry [21,45], rotary pump [46], 2L bioreactors [47], and baffled shake flasks (BSF) [25]. All of these techniques have advantages and limitations in speed, accuracy, and feasibility. Quantitative assays can generate exact shear or energy dissipation rates, but require either laminar flow, or precise control of the hydrodynamic microflows in order to generate reliable data for computational fluid dynamics (CFD) models. In contrast, semi-quantitative approaches such as the BSF and CCM assay can be used to investigate relative trends in shear sensitivity, but lack the quantitative data to compare with other techniques. In this study, we used turbulent concentric mixing in the CCM assay to stress 5 mL of cell suspension. By coupling this assay with automated ViCell XR cell counting device (which uses ~1 mL), rapid characterization of shear sensitivity trends was achieved in as little as 5 minutes. It is important to point out that although bubble bursting is primarily responsible for damage on the bioreactor scale, the aforementioned assays do not specifically consider the cell-bubble attachment rate or bubble bursting energy, but instead focus on the cell's response to hydrodynamic flows. Quantification of cell-bubble attachment has been previously achieved using a bubble flotation column [13,14]. However, such a device has shown that P188 and P407 do not have different cell-bubble attachment rates, despite their disparity in shear protection [28]. In addition, certain polymeric additives like

polyvinylpyrrolidone (PVP) increase cell-bubble attachment while still granting shear protection [48]. From these observations, we believe that inhibiting cell-bubble interaction contributes to, but is not a prerequisite for, surfactant-mediated shear protection of cell culture.

CCM data showed that P188 and P188/P407 mixture both had a dose-dependent relationship on shear protection. The only difference between the two systems is the presence of 1% P407 (no cytotoxic affect), which led to significantly lower cell protection (**Figure 3.4**B). Therefore, P407's high interfacial activity allows it to preferentially adsorb to the cell-liquid interface, effectively sensitizing the cells. Interaction between surfactants and cells can affect a variety of physiological parameters. P188 has been shown to have positive effects on cell growth and substrate utilization even in the absence of shear, which may be a result of improved nutrient transport across the membrane [49]. Although Poloxamer surfactants can internalize and accumulate within CHO cells [50], cell protection is generally attributed to physisorption with cell membranes. The time scale of P188 uptake occurs on the order of hours to days, while the positive and negative effects of P188 and P407, respectively, occur instantaneously upon addition to the suspension or resuspension in new media.

We clearly demonstrated using fluorescence anisotropy and PDA excimer fluorescence ratio that cell membrane fluidity decreases in a dose-dependent fashion with increasing surfactant concentration. To our knowledge, this concentration dependent relationship on membrane physiology has not been shown previously. Between 0-1 g/L, which is the range of the P188's critical micelle concentration (CMC), the cells display an increase in limiting anisotropy signal corresponding to decreased rotational membrane fluidity (**Figure 3.5**C). In this P188 concentration regime, the culture also experiences the greatest gains in cell robustness. This may be attributed to strong surfactant unimer adsorption and embedding within the membrane-liquid interface, similar

to the Gibbs adsorption model. As P188 concentration increases above 2 g/L, the anisotropy plateaus, which indicates TMA-DPH has reached its limit in rotational freedom. At this point, the membrane is saturated with unimers and TMA-DPH rotation is at a minimum. Interestingly, the PDA intensity ratio also increased with P188 concentration, but did not level off at the same plateau (**Figure 3.7**). This method probes lateral diffusion of PDA fluorophores, which reflects the translational mobility in the phospholipid bilayer. PDA intensity ratio increased in the 2-10 g/L P188 range, indicating that PDA lateral mobility continued to decrease. This may be attributed to micellar interaction with the membrane. Simulation studies have shown that P188 micelles strongly interact with lipid bilayers to seal membrane pores on the surface, which would increase membrane order [51]. Above 2 g/L P188, formation of excess micelles and their subsequent adsorption to the membrane would restrict lateral PDA motion without affecting the rotational motion, as the micelle's hydrophilic corona is unlikely to penetrate far into the bilayer. Additionally, this would explain why increased shear resistance has been observed for CHO cell lines beyond 2 g/L [38].

Another finding of this study is that a small amount of high molecular weight (HMW) surfactant (P407) significantly increased membrane fluidity. Industrial researchers have observed that such an impurity in P188 MW distribution negatively affects shear protection during bioreactor operation, but its impact on cell physiology has been a mystery up to this point. Upon adding 5% P407 to the cell suspension (**Figure 3.8**), we observed a clear decrease in PDA monomer/dimer intensity ratio, indicating that the P407 "fluidizes" the membrane as it sensitizes the cells. This provides insight into the physical phenomena which mediate cell resistance and cell sensitivity. P188 and P407 both provide cell protection compared to the surfactant-free system, as evidenced by **Figure 3.5**A; however, the latter is less effective. The cell membrane takes on the

properties of the more surface-active component, which is P407. This results in a more fluid membrane and shear-sensitive culture compared to with P188. We illustrate this principle schematically in **Figure 3.9**. Without surfactants, CHO cell lipid bilayer is extremely fragile and highly fluid, leading to membrane destruction and cell lysis under shear stress. Adding P407 results in a relatively stronger membrane as the copolymer strongly adsorbs to the bilayer and decreases the apparent membrane fluidity. Finally, the addition of P188 results in a membrane with the lowest apparent membrane fluidity. This membrane has the highest shear resistance and membrane order of the three systems. P407's larger molecular size results in lower adsorption density, while its higher hydrophobicity may enhance partitioning of the molecule into the fatty acid bilayer. We speculate that the combination of these phenomena results in P407 being less effective than P188 at both decreasing membrane fluidity and protecting cells from shear. To further develop a structure-performance relationship, future studies should investigate the effects of a diverse set of Poloxamers (or other class of surfactants) on membrane physiology and shear sensitivity.

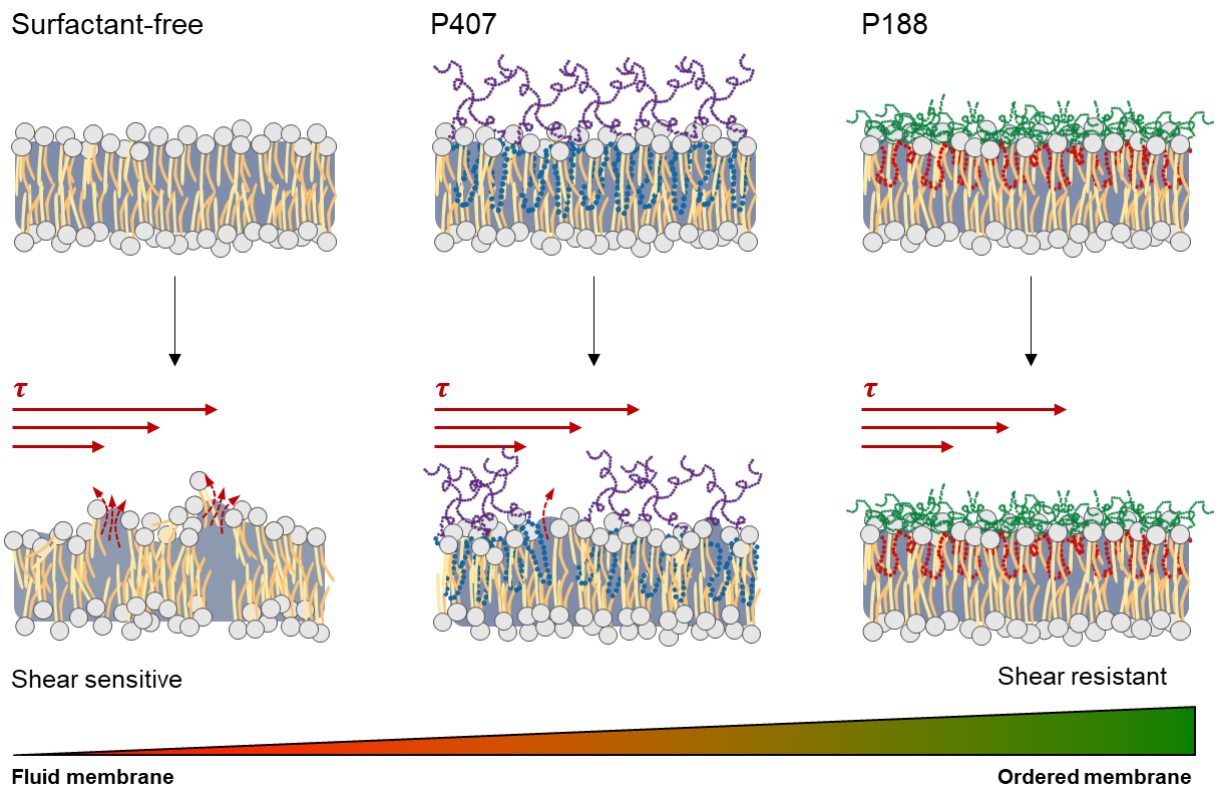

Figure 3.9: Schematic depiction of cell membrane protection with various surfactant systems. Without surfactant, the lipid bilayer is relatively fluid, fragile and sensitive to shear. Addition of P407 and P188 to the system increases the shear resistance of the cell suspension in correlation with the lipid membrane order.

While the results of this study highlight the importance of membrane fluidity in shear sensitivity, cell membranes are complex structures and cannot be characterized by just one parameter. The plasma membrane is a viscoelastic fluid, which has dynamic responses to shear, compression, and bending [29]. Some of these responses may be important to cell shear sensitivity and are not reflected by the motion of fluorescent probes. In addition, low levels of shear can have other non-lethal effects on cell culture [45,52]. Nevertheless, we have shown that membrane fluidity is strongly correlated to CHO cell shear sensitivity and that the surfactant's physical and interfacial properties determine the resulting shear protection. Our findings provide a more

fundamental basis of surfactant-cell interactions for shear protection of cell culture, and pave the way for discovery of improved additives.

3.5 Conclusion

Shear protectants are vital to large-scale mammalian cell culture, and recent biotechnology problems originating in raw material variation have shown that the fundamental understanding of these complex systems is still incomplete. In this study, we successfully demonstrated that increased shear resistance is correlated with decreased membrane fluidity across CHO cell lines, surfactant types, and surfactant concentrations. We first characterized the shear sensitivity of cell culture in a new type of rapid concentric cylinder mixer (CCM) assay. On this basis, we determined the membrane fluidity using both fluorescence anisotropy and pyrene excimer fluorescence. Higher cell protection correlated with the surfactant's ability to decrease cell membrane fluidity, and the CHO cell line with higher shear resistance also had lower membrane fluidity. We then showed that mixing P188 with a small amount of P407, which acts as a HMW contaminant, significantly increased the cell culture's membrane fluidity and shear sensitivity. This suggests that shear damage from P188 raw material variation was caused by higher cell membrane fluidity. Our results provide a physical explanation for the observed dose-dependent relationship between surfactant concentration and shear protection. Surfactant unimer and micellar interaction with the lipid bilayer imparts higher apparent membrane order, resulting in increased shear resistance of the culture.

As cell line and processes are pushed to generate even higher yields, improvement to shear protective compounds may be required [2]. Our findings above contribute to the understanding of surfactant-mediated cell protection and enable a path forward to identify potential shear protectants, and robust cell lines. While previous screening efforts have focused on cell-bubble

interactions, we have demonstrated that the cell membrane interface also plays a crucial role in cell protection and should not be neglected. Adoption of use of the CCM assay, along with the other methods used in this study, can be combined with established techniques to characterize surface activity to predict the effectiveness of potential new shear protectants based on their physical and interfacial properties.

Acknowledgements

We gratefully acknowledge financial support from Biogen (RTP, NC). We thank Ethan Hicks, Rachel Ferguson, Marshall Bowden and Alex Vaca for their contributions to this work, and Weiwei Hu, An Zhang, and Haofan Peng for their advice and guidance.

3.6 References

[1] W. Hu, C. Berdugo, J.J. Chalmers, The potential of hydrodynamic damage to animal cells of industrial relevance: current understanding., Cytotechnology. 63 (2011) 445–60. doi:10.1007/s10616-011-9368-3.

[2] J.J. Chalmers, Mixing, aeration and cell damage, 30+ years later: What we learned, how it affected the cell culture industry and what we would like to know more about, Curr. Opin. Chem. Eng. 10 (2015) 94–102. doi:10.1016/j.coche.2015.09.005.

[3] J.J. Chalmers, N. Ma, Hydrodynamic Damage to Animal Cells, in: M. Al-Rubeai (Ed.), Anim. Cell Cult., Springer International Publishing, Cham, 2015: pp. 169–183. doi:10.1007/978-3-319-10320-4_6.

[4] H.E. Swim, R.F. Parker, Effect of Pluronic F68 on Growth of Fibroblasts in Suspension on Rotary Shaker, Exp. Biol. Med. 103 (1960) 252–254.

[5] D.G. Kilburn, F.C. Webb, The Cultivation of Animal Cells at Controlled Dissolved Oxygen Partial Pressure, Biotechnol. Bioeng. X (1968) 801–814.

[6] S. Goldblum, Y.K. Bae, W.F. Hinkj, J. Chalmers, W.F. Hink, J. Chalmers, Protective Effect of Methylcellulose and Other Polymers on Insect Cells Subjected to Laminar Shear Stress, Biotechnol. Prog. 6 (1990) 383–390. doi:10.1021/bp00005a011.

[7] E.T. Papoutsakis, Media additives for protecting freely suspended animal cells against agitation and aeration damage, Trends Biotechnol. 9 (1991) 316–24. doi:10.1016/0167-7799(91)90102-N.

[8] K. Trinh, M. Garcia-Briones, J.J. Chalmers, F. Hink, J.J. Chalmers, F. Hink,

Quantification of damage to suspended insect cells as a result of bubble rupture., Biotechnol. Bioeng. 43 (1994) 37–45. doi:10.1002/bit.260430106.

[9] J.D. Michaels, A.K. Mallik, E.T. Papoutsakis, Sparging and agitation-induced injury of cultured animal cells: Do cell- to-bubble interactions in the bulk liquid injure cells?, Biotechnol. Bioeng. 51 (1996) 399–409. doi:10.1002/(SICI)1097-0290(19960820)51:4<399::AID-BIT3>3.0.CO;2-D.

[10] S.J. Meier, T.A. Hatton, D.I.C.C. Wang, Cell death from bursting bubbles: role of cell attachment to rising bubbles in sparged reactors, Biotechnol. Bioeng. 62 (1999) 468–478. doi:10.1002/(SICI)1097-0290(19990220)62:4<468::AID-BIT10>3.0.CO;2-N.

[11] Y. Zhu, J. V. Cuenca, W. Zhou, A. Varma, NS0 cell damage by high gas velocity sparging in protein-free and cholesterol-free cultures, Biotechnol. Bioeng. 101 (2008) 751–760. doi:10.1002/bit.21950.

[12] Y. Liu, F. Li, W. Hu, K. Wiltberger, T. Ryll, Effects of bubble-liquid two-phase turbulent hydrodynamics on cell damage in sparged bioreactor, Biotechnol. Prog. 30 (2014) 48–58. doi:10.1002/btpr.1790.

[13] N. Ma, J.J. Chalmers, J.G. Auniņs, W. Zhou, L. Xie, Quantitative studies of cell-bubble interactions and cell damage at different pluronic F-68 and cell concentrations, Biotechnol. Prog. 20 (2004) 1183–91. doi:10.1021/bp0342405.

[14] W. Hu, J.J. Rathman, J.J. Chalmers, An investigation of small-molecule surfactants to potentially replace pluronic F-68 for reducing bubble-associated cell damage, Biotechnol. Bioeng. 101 (2008) 119–27. doi:10.1002/bit.21872.

[15] Z. Zhang, M. Al-Rubeai, C.R. Thomas, Effect of Pluronic F-68 on the mechanical properties of mammalian cells, Enzyme Microb. Technol. 14 (1992) 980–983. doi:10.1016/0141-0229(92)90081-X.

[16] T. Tharmalingam, H. Ghebeh, T. Wuerz, M. Butler, Pluronic enhances the robustness and reduces the cell attachment of mammalian cells, Mol. Biotechnol. 39 (2008) 167–177. doi:10.1007/s12033-008-9045-8.

[17] J.D. Michaels, J.E. Nowak, A.K. Mallik, K. Koczo, D.T. Wasan, E.T. Papoutsakis, Interfacial properties of cell culture media with cell-protecting additives, Biotechnol. Bioeng. 47 (1995) 420–430. doi:10.1002/bit.260470403.

[18] D. Chattopadhyay, J.F. Rathman, J.J. Chalmers, Thermodynamic approach to explain cell adhesion to air-medium interfaces., Biotechnol. Bioeng. 48 (1995) 649–58. doi:10.1002/bit.260480613.

[19] D.W. Murhammer, Pluronic polyols, cell protection, in: Encycl. Bioprocess Technol., 2002: pp. 3965–3968. doi:10.1002/9780470054581.

[20] O.T. Ramirez, R. Mutharasan, Effect of serum on the plasma membrane fluidity of hybridomas: an insight into its shear protective mechanism, Biotechnol. Prog. 8 (1992) 40–50.

[21] O.T. Ramírez, R. Mutharasan, The role of the plasma membrane fluidity on the shear sensitivity of hybridomas grown under hydrodynamic stress., Biotechnol. Bioeng. 36 (1990) 911–920. doi:10.1002/bit.260360906.

[22] S. Yasuda, D. Townsend, D.E. Michele, E.G. Favre, S.M. Day, J.M. Metzger, Dystrophic

heart failure blocked by membrane sealant poloxamer, Nature. 436 (2005) 1025–1029. doi:10.1038/nature03844.

[23] E.W. Mina, C. Lasagna-Reeves, C.G. Glabe, R. Kayed, Poloxamer 188 Copolymer Membrane Sealant Rescues Toxicity of Amyloid Oligomers In Vitro, J. Mol. Biol. 391 (2009) 577–585. doi:10.1016/j.jmb.2009.06.024.

[24] D.W. Murhammer, C.F. Goochee, Structural features of nonionic polyglycol polymer molecules responsible for the protective effect in sparged animal cell bioreactors, Biotechnol. Prog. 6 (1990) 142–148. doi:10.1021/bp00002a008.

[25] H. Peng, K.M. Hall, B. Clayton, K. Wiltberger, W. Hu, E. Hughes, et al., Development of small scale cell culture models for screening poloxamer 188 lot-to-lot variation, Biotechnol. Prog. 30 (2014) 1411–1418. doi:10.1002/btpr.1967.

[26] P.A. Apostolidis, A. Tseng, M.-E. Koziol, M.J. Betenbaugh, B. Chiang, Investigation of low viability in sparged bioreactor CHO cell cultures points to variability in the Pluronic F-68 shear protecting component of cell culture media, Biochem. Eng. J. 98 (2015) 10–17. doi:10.1016/j.bej.2015.01.013.

[27] H. Peng, A. Ali, M. Lanan, E. Hughes, K. Wiltberger, B. Guan, et al., Mechanism investigation for Poloxamer 188 raw material variation in cell culture, Biotechnol. Prog. 32 (2016) 767–775. doi:10.1002/btpr.2268.

[28] D. Chang, R. Fox, E. Hicks, R. Ferguson, K. Chang, D. Osborne, et al., Investigation of interfacial properties of pure and mixed poloxamers for surfactant-mediated shear protection of mammalian cells, Colloids Surfaces B Biointerfaces. 156 (2017) 358–365.

doi:10.1016/j.colsurfb.2017.05.040.

[29] G. Espinosa, I. Lopez-Montero, F. Monroy, D. Langevin, Shear rheology of lipid monolayers and insights on membrane fluidity, Proc. Natl. Acad. Sci. 108 (2011) 6008–6013. doi:10.1073/pnas.1018572108.

[30] L. Best, E. John, F. Jähnig, Order and fluidity of lipid membranes as determined by fluorescence anisotropy decay, Eur. Biophys. J. 15 (1987) 87–102. doi:10.1007/BF00257502.

[31] J.A. Dix, A.S. Verkman, Pyrene excimer mapping in cultured fibroblasts by ratio imaging and time-resolved microscopy, Biochemistry. 29 (1990) 1949–1953. doi:10.1021/bi00459a041.

[32] W. Zhang, G. Wang, E. See, J.P. Shaw, B.C. Baguley, J. Liu, et al., Post-insertion of poloxamer 188 strengthened liposomal membrane and reduced drug irritancy and in vivo precipitation, superior to PEGylation, J. Control. Release. 203 (2015) 161–169. doi:http://dx.doi.org/10.1016/j.jconrel.2015.02.026.

[33] J.R. Lakowicz, Principles of Fluorescence Spectroscopy, 3rd ed., Springer Science & Business Media, New York, New York, 2006. doi:10.1007/978-0-387-46312-4.

[34] F. Jähnig, Structural order of lipids and proteins in membranes: evaluation of fluorescence anisotropy data., Proc. Natl. Acad. Sci. 76 (1979) 6361–6365. doi:10.1073/pnas.76.12.6361.

[35] M. Nazari, M. Kurdi, H. Heerklotz, Classifying surfactants with respect to their effect on lipid membrane order, Biophys. J. 102 (2012) 498–506. doi:10.1016/j.bpj.2011.12.029.

[36] K. Tanhuanpaa, J. Virtanen, P. Somerharju, Fluorescence imaging of pyrene-labeled lipids in living cells, Biochim. Biophys. Acta. 1497 (2000) 308–320. doi:10.1016/S0167-4889(00)00068-9.

[37] H.J. Galla, E. Sackmann, Lateral diffusion in the hydrophobic region of membranes: use of pyrene excimers as optical probes, Biochim. Biophys. Acta. 339 (1974) 103–115. doi:10.1016/0005-2736(74)90336-8.

[38] T. Tharmalingam, C.T. Goudar, Evaluating the impact of high Pluronic F68 concentrations on antibody producing CHO cell lines, Biotechnol. Bioeng. 112 (2014) 832–7. doi:10.1002/bit.25491.

[39] D. Illinger, G. Duportail, Y. Mely, N. Poirel-Morales, D. Gerard, J.G. Kuhry, A comparison of the fluorescence properties of TMA-DPH as a probe for plasma membrane and for endocytic membrane, Biochim. Biophys. Acta - Biomembr. 1239 (1995) 58–66. doi:10.1016/0005-2736(95)00135-P.

[40] P. Somerharju, Pyrene-labeled lipids as tools in membrane biophysics and cell biology, Chem. Phys. Lipids. 116 (2002) 57–74. doi:10.1016/S0009-3084(02)00020-8.

[41] L. Piñeiro, M. Novo, W. Al-Soufi, Fluorescence emission of pyrene in surfactant solutions, Adv. Colloid Interface Sci. 215 (2015) 1–12. doi:10.1016/j.cis.2014.10.010.

[42] B. Neunstoecklin, M. Stettler, T. Solacroup, H. Broly, M. Morbidelli, M. Soos, Determination of the maximum operating range of hydrodynamic stress in mammalian cell culture, J. Biotechnol. 194 (2015) 100–109. doi:10.1016/j.jbiotec.2014.12.003.

[43] N. Ma, K.W. Koelling, J.J. Chalmers, Fabrication and use of a transient contractional flow

device to quantify the sensitivity of mammalian and insect cells to hydrodynamic forces, Biotechnol. Bioeng. 80 (2002) 428–437. doi:10.1002/bit.10387.

[44] W. Hu, R. Gladue, J. Hansen, C. Wojnar, J.J. Chalmers, The sensitivity of the dinoflagellate Crypthecodinium cohnii to transient hydrodynamic forces and cell-bubble interactions, Biotechnol. Prog. 23 (2007) 1355–1362. doi:10.1021/bp070306a.

[45] S.H. Mardikar, K. Niranjan, Observations on the shear damage to different animal cells in a concentric cylinder viscometer, Biotechnol. Bioeng. 68 (2000) 697–704. doi:10.1002/(SICI)1097-0290(20000620)68:6<697::AID-BIT14>3.0.CO;2-6.

[46] H. Kamaraju, K. Wetzel, W.J. Kelly, Modeling shear-induced CHO cell damage in a rotary positive displacement pump, Biotechnol. Prog. 26 (2010) 1606–1615. doi:10.1002/btpr.479.

[47] J.B. Sieck, T. Cordes, W.E. Budach, M.H. Rhiel, Z. Suemeghy, C. Leist, et al., Development of a Scale-Down Model of hydrodynamic stress to study the performance of an industrial CHO cell line under simulated production scale bioreactor conditions, J. Biotechnol. 164 (2013) 41–49. doi:10.1016/j.jbiotec.2012.11.012.

[48] J.D. Michaels, J.E. Nowak, A.K. Mallik, K.K. Koczo, D.T. Wasan, E.T. Papoutsakis, Analysis of cell-to-bubble attachment in sparged bioreactors in the presence of cell-protecting additives., Biotechnol. Bioeng. 47 (1995) 407–19. doi:10.1002/bit.260470402.

[49] M.-F.M.-F. Clincke, E. Guedon, F.T. Yen, V. Ogier, O. Roitel, J.-L. Goergen, Effect of Surfactant Pluronic F-68 on CHO Cell Growth , Metabolism , Production , and Glycosylation of Human Recombinant IFN- c in Mild Operating Conditions, Biotechnol.

Prog. 27 (2010) 181–90. doi:10.1002/btpr.503.

[50] A. Gigout, M.D. Buschmann, M. Jolicoeur, The fate of Pluronic F-68 in chondrocytes and CHO cells., Biotechnol. Bioeng. 100 (2008) 975–87. doi:10.1002/bit.21840.

[51] U. Adhikari, A. Goliaei, L. Tsereteli, M.L. Berkowitz, Properties of poloxamer molecules and poloxamer micelles dissolved in water and next to lipid bilayers: results from computer simulations, J. Phys. Chem. B. 120 (2016) 5823–5830. doi:10.1021/acs.jpcb.5b11448.

[52] C.R. White, J.A. Frangos, The shear stress of it all: the cell membrane and mechanochemical transduction, Philos. Trans. R. Soc. B Biol. Sci. 362 (2007) 1459–1467. doi:10.1098/rstb.2007.2128.

Chapter 4 – Rapid measurement of cell shear sensitivity to improve cell robustness and interfacial interactions in cell culture

4.1 Introduction

During scale-up of mammalian cell culture processes, the interfacial interactions between gas bubbles, cells, and media components can significantly impact bioreactor performance. Three major concerns which arise during this process are excessive foaming, cell damage from hydrodynamic shear or bubble bursting, and the maintenance of adequate mass transfer of oxygen and carbon dioxide [1–3]. Generally, scale-up strategies include maintaining constant impeller power input per volume (P/V) [4], volumetric gas flow per volume of liquid (vessel volumes per minute, vvm), mass transfer coefficient ($k_L a$), impeller to tank ratio (D_i/D_T), or impeller tip speed

from pilot (200 L) to production (15000 L) scale [5–7]. These parameters focus on the engineering features of the vessel, but do not specifically consider the interfacial effects on cells or foam. In addition, process development experiments must be done at-scale or in 5-L bioreactors.

Several techniques have been developed to measure shear sensitivity of cell culture (**Figure 4.1**). Each of these assays has certain strengths and limitations with respect to speed, accuracy, and practicality. Although the Couette viscometer [8–10] and microfluidic flow device [11–13] are highly quantitative in stressing cells with controlled hydrodynamic flows, comparable data with respect to bioreactor flows and stresses is scarce because models of bubble bursting energy dissipation have proven to be unreliable [14–16]. Therefore, it is difficult to correlate the values obtained from these assays to environmental stresses. On the other hand, the baffled shake flask and CCM assays quantify the relative shear sensitivity of the cell culture to obtain a trend depending on media composition, cell line, and other properties, and can be performed in high throughput experiments [17]. From the published literature, it is evident that the shear environment can be created in many different ways. Laminar or turbulent flows are used to generate shear and extensional stresses, and the culture's overall shear sensitivity is quantified by either the change in cell growth, viability, or lactase dehydrogenase (LDH) concentration [9,18]. These indirect measures correlate with the cells' ability to resist physical stress.

Three main factors contribute to cell damage during bioprocesses. First, the cell physiology, an intrinsic property, governs the cell's natural robustness. Although this property can be optimized by choosing cell lines with high mechanical stability, it is difficult to modify. Secondly, the shear environment, which originates from cell oxygen demand and the aeration/agitation strategy, determines the stress experienced by the culture. Lastly, media components have a large impact on cell sensitivity [19]. Chemically defined media for mammalian cell culture contains as

many as 50 different components, including inorganic salts, vitamins and amino acids, surfactant, buffer system, and a sugar source. In the production bioreactor, the culture also generates a large amount of protein, secondary metabolites, and waste/debris [20]. Many of these components are surface-active, and affect the mechanical stability of the cell membrane. While the surfactant Poloxamer 188 is the primary media additive which increases cell robustness, other components can also contribute to cell sensitivity. The media, cell physiology, and bioreactor environment during the fed-batch process can lead to significant variations in interfacial interactions.

		Time	Strengths	Limitations
Couette viscometer	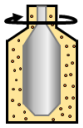	Minutes	• High throughput • Quantitative value	• Shear stress too low to induce damage
Microfluidic flow device	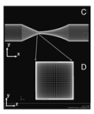	Minutes	• Quantitative value • Low volume/time	• Low throughput & difficult • Setup and device maintenance • Accuracy of model
Baffled shake flask		Hours/Days	• High throughput	• Large volume/time • Relative sensitivity value
CCM	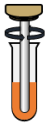	Minutes	• High throughput • Low volume/time	• Relative sensitivity value

Figure 4.1: Comparison of various assays used in measuring the shear sensitivity of cell culture.

Chapters 2 and 3 of this dissertation discussed fundamental interactions between surfactants and gas or cell interfaces. In the following two chapters, we will develop and apply methods to measure shear sensitivity, and demonstrate examples where the efficient use of surfactants can benefit mammalian cell culture processes. This chapter focuses on the development of the method and the effect of increased surfactant concentration on the interfacial interactions of

the culture. We also investigate the effects of surfactant on cell aggregation and foam stability of the cell suspension.

4.2 Materials and methods

4.2.1 Surfactants and chemicals

Poloxamer 188 was provided by BASF Corporation and used as received. Poloxamer stock solutions were prepared by dissolving solid flakes in purified MilliQ water (Millipore, Billerica, MA) to 100 g/L and sterilizing by filtration (0.22 μm, Millipore) before use. One good lot of P188 and one bad lot of P188 were used for all experiments, as determined in Chapter 2 of this dissertation. Sterile Antifoam Q7 (Dow Corning) was diluted to 15% stock solution prior to use.

4.2.2 Cell culture conditions and monitoring

A recombinant Chinese Hamster Ovary (CHO) cell line secreting a monoclonal antibody was used for experiments with cell culture. Cells were incubated at 37°C and 5% CO_2 with platform agitation at 125 rpm. The cells were passaged every 3-4 days with seed density of 3×10^5 cells/mL in 1 L shaker flasks (Corning Life Science, Tewksbury, MA) in Biogen's proprietary chemically defined media without Poloxamer 188. P188 was supplemented to the media prior to passage to ensure the same lot was used in every experiment. All cells used in experiments were in exponential growth phase. Cell viability and cell density were measured using the Trypan blue dye exclusion test with automated cell counter (ViCell XR, Beckman Coulter). LDH was measured using Cedex BioHT (Roche).

4.2.3 Cell sensitivity assays

The experimental set-up is shown in **Figure 4.2**. A concentric cylinder mixer (CCM) was used to measure the cell culture shear sensitivity A ServoDyne electronic mixer (Cole-Parmer, Vernon Hills, IL) equipped with a stainless-steel shaft with radius 4.75 mm was used to shear the cell suspension. 5 mL aliquot of cell suspension taken from the daily bioreactor sample was transferred to a glass test tube with inner radius 6.25 mm and centered with the steel shaft to form a gap distance 1.5 mm with solid-liquid contact length *L* of 5.5 cm. The shear time and rotational speed were varied using the ServoDyne controller. The sheared sample was analyzed with ViCell to determine the change in viability and viable cell density (VCD). Sample was then spun down and the supernatant analyzed with BioHT to quantify LDH concentration. LDH is an intracellular enzyme released upon cell lysis, and is used as a measure of cell damage. We calculated the normalized change in VCD after shearing in the CCM as a measure of cell sensitivity, given in Equation 1. VCD_i and VCD_f refer to the VCD concentration before and after shearing, respectively.

$$\Delta\text{VCD}(\%) = \left(\frac{VCD_f - VCD_i}{VCD_i} \right) \cdot 100\% \qquad \text{(Eq 1)}$$

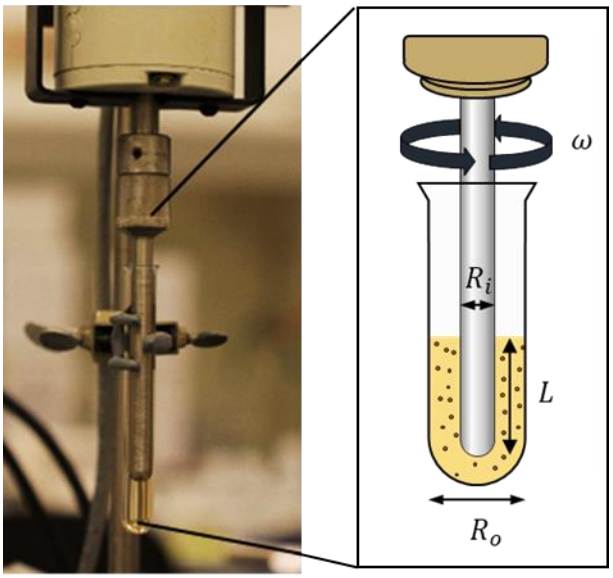

Figure 4.2: Schematic of the concentric cylinder mixer (CCM) assay to measure shear sensitivity.

4.2.4 Foam stability and cell aggregation experiments

Foam stability experiments were carried out in 100 mL glass graduated cylinders. A gas dispersion tube containing a sintered glass disc at the end with 70-100 µm diameter pores (Ace Glass, Inc., Vineland, NJ) was suspended down the center the graduated cylinder, leaving the bottom of the glass disc 2-4 mm above the bottom of the cylinder. A sample of cell suspension was transferred into the cylinder to a volume of 20 mL. The air sparge line connected to a G3Lab Universal mass flow controller (Finesse, Santa Clara, CA) was attached to the inlet of the dispersion rod. Air was introduced at a rate of 10 mL/min. The rise of the foam was recorded at specific volumes or time intervals. Foam generation was stopped after either 60 mL of foam head had been formed or after 30 minutes. The volume of the foam head was recorded for 1-2 hours. This process is shown in **Figure 4.3**.

Experiments to investigate the effects of surfactant on cell aggregation were done in 1 L shake flasks. Cell culture in exponential growth phase were seeded at 3×10^5 cells/mL, then supplemented with

the desired surfactant concentration. After 4 days of incubation at 37ºC and 125 rpm rotation, the flask was collected and observed.

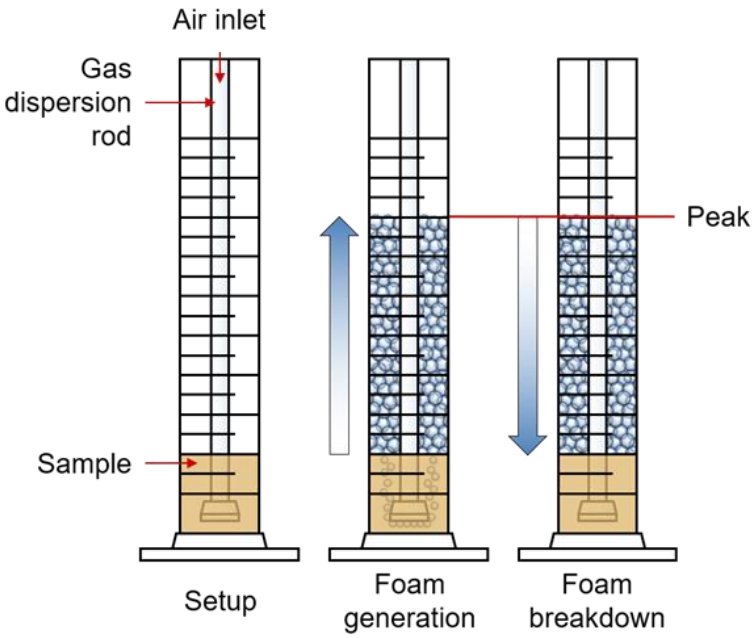

Figure 4.3: Experimental setup for foam stability during sparging. Air is sparged at a constant rate of 10 mL/min through a sintered glass frit through a cell suspension. Sparging is ceased when foam reaches 60 mL, and the breakdown is observed over a period of 2 hours.

4.3 Results and discussion

To characterize the effect of the dependent variables in the CCM assay, we quantified the VCD change after shearing the culture at various surfactant concentrations, shear rates, and shear times (**Figure 4.4**). In the first plot, the concentration dependence of shear sensitivity using a protective lot of P188 was compared with that of a bad lot of P188. The CCM was operated at 6000 RPM for 5 minutes. The high protective lot resulted in a steep rise in cell protection between 0 to 0.5 g/L P188, eventually reaching a plateau above 1 g/L. On the other hand, the majority of cells with the bad lot of P188 were killed at concentrations below 0.5 g/L, and a steep rise in cell protection was observed between 0.5 and 2 g/L. This result indicates that the CCM is highly

sensitive to small changes in cell protection efficiency, which could not be detected in small scale bioreactors [17]. Previously, the baffled shake flask (BSF) model was developed to screen for such inconsistencies in P188 protection, but our data show that the CCM can also accomplish this characterization with significantly lower sample volume and time [21–23].

In Figures 4.4B and C, we demonstrate a near linear dependence of cell sensitivity on both rotational speed of the mixer, and exposure time to shear. The slope of the cell sensitivity in Figure 4.4B depends on the shear time, and the slope in Figure 4.4C is a function of surfactant concentration. These trends allow us to establish the assay conditions to minimize experimental time while maintaining high resolution and precision of results. In this case, we have chosen 6000 RPM with a shear time of 5 minutes.

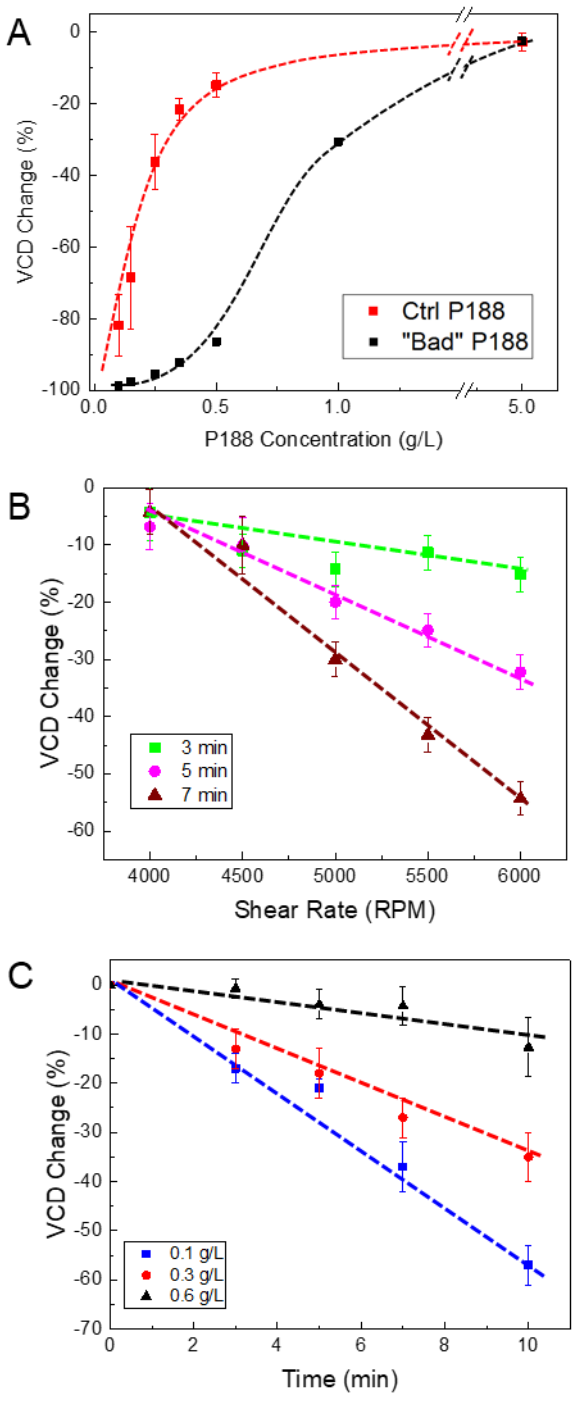

Figure 4.4: Change in VCD of cells after shearing in the CCM as a function of (A) surfactant concentration, (B) shear rate, and (C) exposure time to shear.

Because increased surfactant concentration results in higher cell robustness, we investigated whether cell growth was affected by higher P188 levels. We inoculated 1 L shake flasks with CHO cells in media supplemented with 1 to 10 g/L P188, and incubated them at standard growth conditions for 4 days. At the end of the 4 days, we analyzed the culture using the ViCell XR, and discovered no significant difference in both viability and VCD (data not shown) across the entire concentration range. However, slight differences in final LDH concentration were measured in the medium at the end of the 4 days (**Figure 4.5**). LDH is used as a measure of cell injury or lysis. Although no adverse effects on cell growth of increased P188 were observed during the exponential growth phase, there was a slight decrease in LDH concentration.

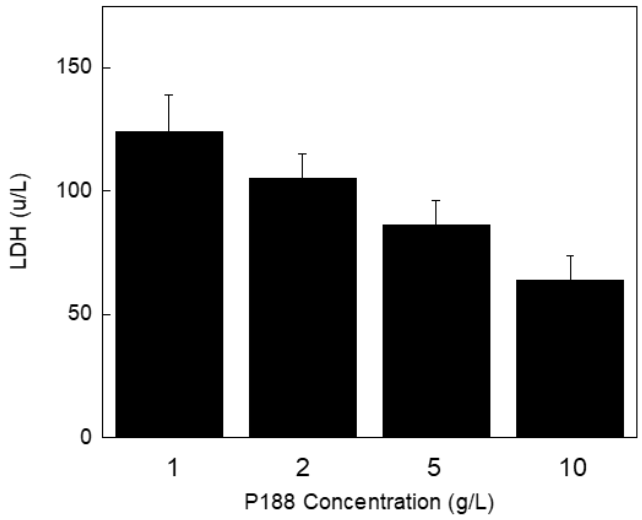

Figure 4.5: The LDH concentration in the medium after incubation of cells for 4 days with media at various P188 concentrations. Higher surfactant concentration results in lower rate of cell lysis, thus decreasing LDH concentration in the medium.

Another important observation was that cell aggregation and clumping were prevented at concentrations of P188 above 5 g/L (**Figure 4.6**). From 1-2 g/L P188, large aggregates of cells

were seen at the bottom of the flask, despite the viability and VCD of the culture being comparable. At 5 g/L P188, aggregation was not observed, indicating that the additional surfactant stabilized the single dispersed cells. Cell aggregation is generally undesirable, and can lead to early apoptosis or hinder cell growth [24]. Because similar VCD and viability were observed in all flasks, the cell aggregates likely consist of mostly dead cell debris.

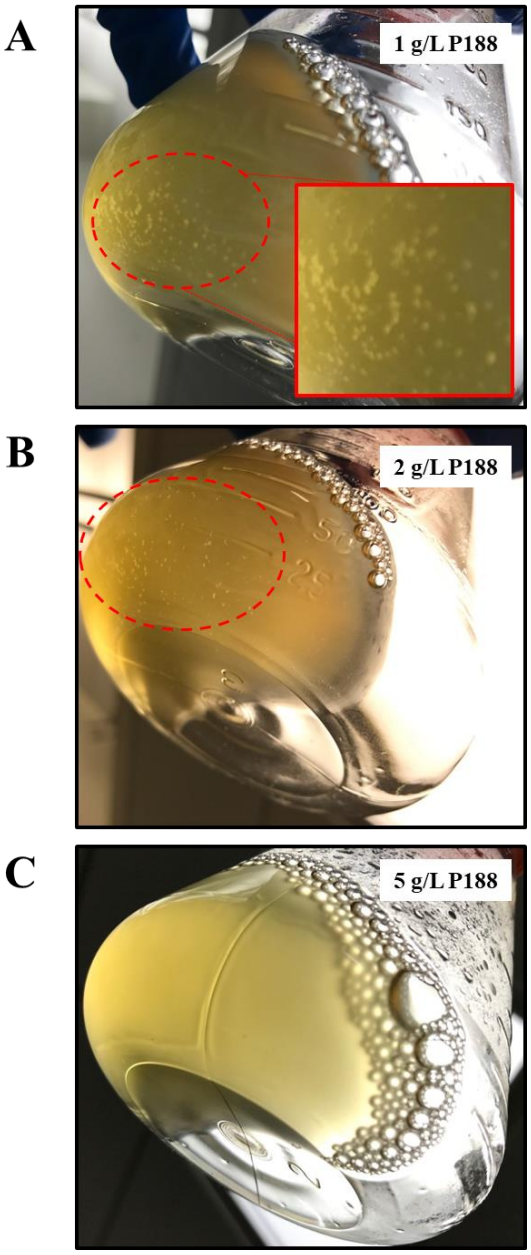

Figure 4.6: Stability of cell suspensions in media containing (A) 1 g/L, (B) 2 g/L, and (C) 5 g/L P188 after 4 days of incubation. Cells formed small aggregates in systems with 1 and 2 g/L P188, although cell growth was not affected.

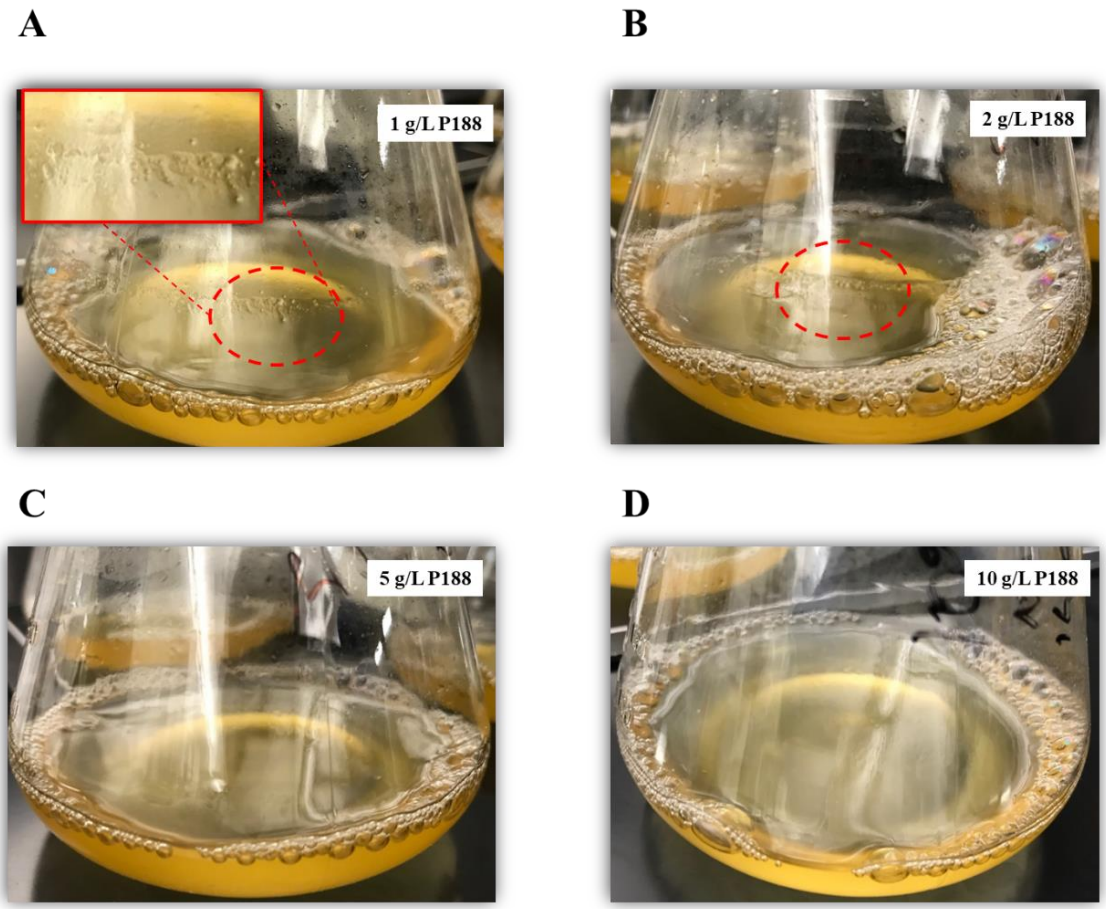

Figure 4.7: Images of the shake flask after 4 days of incubation with (A) 1 g/L, (B) 2 g/L, (C) 5 g/L, and (D) 10 g/L P188. In media containing 1-2 g/L P188, cells adhered to the walls of the flask, forming a ring.

We also observed the accumulation of deposits from cells adhered to the shake flask in the shape of a ring from systems of 1-2 g/L P188 in the medium (**Figure 4.7**). The presence of this ring as well as the cell aggregates indicates that a surface-active byproduct such as DNA accumulated in the medium during cell growth. DNA released upon cell death has been shown to cause cell-cell aggregation and adhesion to surfaces [25]. Some degree of cell death is expected to occur even during the growth phase. The lower LDH in the medium from **Figure 4.5** indicates that increasing the Poloxamer concentration decreases cell lysis during growth, which may also

decrease the amount of DNA released. The differences in cell death rate may be insignificant to cell growth, but they contribute to undesirable surface interactions. The formation of aggregates and adhesion to surfaces can lead to loss of cells during production, and may contribute to the foaming in the bioreactor. Additional surfactant can micellize the DNA, or adsorb to the cell interface to decrease hydrophobic interactions, thus preventing the factors leading to cell aggregation.

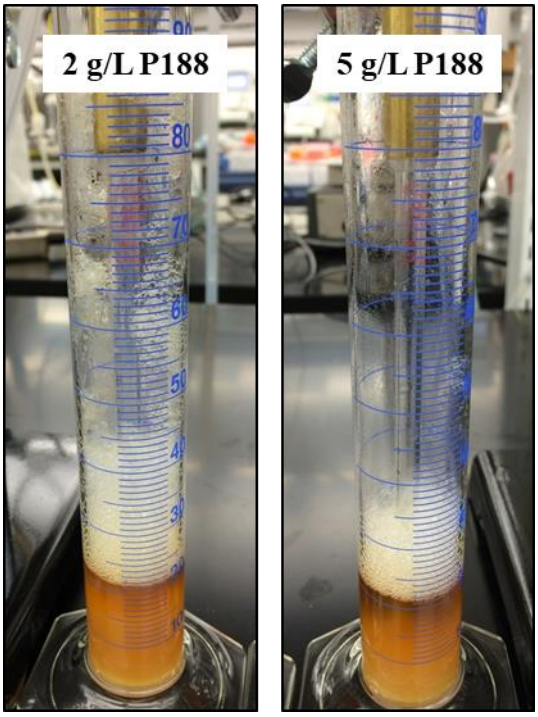

Figure 4.8: Foam stability of sample from production bioreactor with 2 g/L and 5 g/L P188. The sample with higher surfactant has lower foam stability, which results from decreased entrapment of protein and cell debris in the foam.

To demonstrate the effect of increased P188 on foamability, we designed an experiment to investigate foam stability of a sparged solution. In this experiment, shown schematically in **Figure 4.3**, we generate foam with a frit sparger, and measure the breakdown of foam over time. The

solution used was a cell culture sample taken from a late stage production bioreactor run. The sample with 5 g/L P188 showed decreased foam stability relative to the sample with 2 g/L P188 (**Figure 4.8**). This counterintuitive result may arise from two phenomena. First, as mentioned previously, higher surfactant may decrease DNA and LDH release into the medium, both of which contribute to foam stability. Second, the surfactant may have a detergency effect in the foam, decreasing hydrophobic interactions of proteins and cell debris in the thin films and letting them flow down freely along the foam lamellae and channels. When proteins and surface active particles become adsorbed to the interface and plateau borders of the thin films, they form Pickering foams, which can be extremely stable and difficult to break down [26,27]. The decreased adsorption of these particles leads to a "cleaner" foam stabilized primarily by surfactant molecules and micelles rather than a foam stabilized by protein and particles.

4.4 Conclusion

In this chapter, we demonstrate that the new concentric cylinder mixer (CCM) assay can be an efficient tool to quantify cell sensitivity with high accuracy and speed. This method can be used to not only screen surfactant batches for their protective quality, but also to determine the effects of different cell lines and media components on cell sensitivity. We also found that higher P188 concentration in the medium increased cell robustness, and improved the colloidal stability of cell particles during cultivation. The surfactant mitigates cell aggregation and adhesion to surfaces by decreasing cell lysis, which in turn decreases DNA release into the medium. Higher surfactant concentrations also decrease hydrophobic interactions. As a result, the system attains lower foamability, as the surface-active particles and proteins are excluded from the thin films. These results increase our understanding of the colloidal interactions during mammalian cell culture, and provide strong motivation to operate with increased P188 concentration in the

medium. The methods developed in this chapter, including the CCM and foam stability test, can be used to further improve and optimize interfacial interactions in production bioreactor operation. Future studies should elucidate the effects of process variables such as temperature shifts, pH, and media changes (perfusion) on cell sensitivity and foam stability.

Acknowledgements

We gratefully acknowledge financial support from Biogen (RTP, NC) We thank Dane Grismer for his contributions to this work.

4.1 References

[1] S.S. Mostafa, X. Gu, Strategies for improved dCO2 removal in large-scale fed-batch cultures, Biotechnol. Prog. 19 (2003) 45–51. doi:10.1021/bp0256263.

[2] F. Garcia-Ochoa, E. Gomez, Bioreactor scale-up and oxygen transfer rate in microbial processes: An overview, Biotechnol. Adv. 27 (2009) 153–176. doi:10.1016/j.biotechadv.2008.10.006.

[3] J. Varley, J. Birch, Reactor design for large scale suspension animal cell culture, Cytotechnology. 29 (1999) 177–205. doi:10.1023/A:1008008021481.

[4] S. Xu, L. Hoshan, R. Jiang, B. Gupta, E. Brodean, K. O'Neill, T.C. Seamans, J. Bowers, H. Chen, A practical approach in bioreactor scale-up and process transfer using a combination of constant P/V and vvm as the criterion, Biotechnol. Prog. (2017) 1–6. doi:10.1002/btpr.2489.

[5] F. Li, N. Vijayasankaran, A. Shen, R. Kiss, A. Amanullah, Cell culture processes for monoclonal antibody production, MAbs. 2 (2010) 466–479. doi:10.4161/mabs.2.5.12720.

[6] Z. Xing, B.M. Kenty, Z.J. Li, S.S. Lee, Scale-up analysis for a CHO cell culture process in large-scale bioreactors, Biotechnol. Bioeng. 103 (2009) 733–746. doi:10.1002/bit.22287.

[7] W.-S. Hu, J.G. Aunins, Large-scale mammalian cell culture, Curr. Opin. Biotechnol. 8 (1997) 148–153. doi:10.1016/S0958-1669(97)80093-6.

[8] J.F. Petersen, L. V. McIntire, E.T. Papoutsakis, Shear sensitivity of cultured hybridoma cells (CRL-8018) depends on mode of growth, culture age and metabolite concentration, J. Biotechnol. 7 (1988) 229–246. doi:10.1016/0168-1656(88)90054-5.

[9] S.H. Mardikar, K. Niranjan, Observations on the shear damage to different animal cells in a concentric cylinder viscometer, Biotechnol. Bioeng. 68 (2000) 697–704. doi:10.1002/(SICI)1097-0290(20000620)68:6<697::AID-BIT14>3.0.CO;2-6.

[10] O.T. Ramírez, R. Mutharasan, The role of the plasma membrane fluidity on the shear sensitivity of hybridomas grown under hydrodynamic stress., Biotechnol. Bioeng. 36 (1990) 911–920. doi:10.1002/bit.260360906.

[11] N. Gregoriades, J. Clay, N. Ma, K. Koelling, J.J. Chalmers, Cell damage of microcarrier cultures as a function of local energy dissipation created by a rapid extensional flow, Biotechnol. Bioeng. 69 (2000) 171–182. doi:10.1002/(SICI)1097-0290(20000720)69:2<171::AID-BIT6>3.0.CO;2-C.

[12] N. Ma, K.W. Koelling, J.J. Chalmers, Fabrication and use of a transient contractional flow device to quantify the sensitivity of mammalian and insect cells to hydrodynamic forces, Biotechnol. Bioeng. 80 (2002) 428–437. doi:10.1002/bit.10387.

[13] W. Hu, R. Gladue, J. Hansen, C. Wojnar, J.J. Chalmers, The sensitivity of the dinoflagellate Crypthecodinium cohnii to transient hydrodynamic forces and cell-bubble interactions, Biotechnol. Prog. 23 (2007) 1355–1362. doi:10.1021/bp070306a.

[14] P.L.L. Walls, O. McRae, V. Natarajan, C. Johnson, C. Antoniou, J.C. Bird, Quantifying the potential for bursting bubbles to damage suspended cells, Sci. Rep. 7 (2017) 1–9. doi:10.1038/s41598-017-14531-5.

[15] D. Dey, J.M. Boulton-Stone, A.N. Emery, J.R. Blake, Experimental comparisons with a numerical model of surfactant effects on the burst of a single bubble, Chem. Eng. Sci. 52 (1997) 2769–2783. doi:10.1016/S0009-2509(97)00083-3.

[16] J.R. Blake, J.M. Boulton-Stone, J.R. Blake, Gas bubbles bursting at a free surface, J. Fluid Mech. 254 (1993) 437–466.

[17] H. Peng, K.M. Hall, B. Clayton, K. Wiltberger, W. Hu, E. Hughes, J. Kane, R. Ney, T. Ryll, Development of small scale cell culture models for screening poloxamer 188 lot-to-lot variation, Biotechnol. Prog. 30 (2014) 1411–1418. doi:10.1002/btpr.1967.

[18] S.K.W. Oh, A.W. Nienow, M. Al-Rubeai, A.N. Emery, The effects of agitation intensity with and without continuous sparging on the growth and antibody production of hybridoma cells, J. Biotechnol. 12 (1989) 45–61. doi:10.1016/0168-1656(89)90128-4.

[19] M.-F.M.-F. Clincke, E. Guedon, F.T. Yen, V. Ogier, O. Roitel, J.-L. Goergen, Effect of Surfactant Pluronic F-68 on CHO Cell Growth , Metabolism , Production , and Glycosylation of Human Recombinant IFN- c in Mild Operating Conditions, Biotechnol. Prog. 27 (2010) 181–90. doi:10.1002/btpr.503.

[20] T. Klein, N. Heinzel, P. Kroll, M. Brunner, C. Herwig, L. Neutsch, Quantification of cell lysis during CHO bioprocesses: Impact on cell count, growth kinetics and productivity, J. Biotechnol. 207 (2015) 67–76. doi:10.1016/j.jbiotec.2015.04.021.

[21] B. Guan, A. Ali, H. Peng, W. Hu, L.R. Markely, S. Estes, S. Prajapati, Characterization of poloxamers by reversed-phase liquid chromatography, Anal. Methods. 8 (2016) 2812–2819. doi:10.1039/C5AY03311J.

[22] H. Peng, A. Ali, M. Lanan, E. Hughes, K. Wiltberger, B. Guan, S. Prajapati, W. Hu, Mechanism investigation for Poloxamer 188 raw material variation in cell culture, Biotechnol. Prog. 32 (2016) 767–775. doi:10.1002/btpr.2268.

[23] D. Chang, R. Fox, E. Hicks, R. Ferguson, K. Chang, D. Osborne, W. Hu, O.D. Velev, Investigation of interfacial properties of pure and mixed poloxamers for surfactant-mediated shear protection of mammalian cells, Colloids Surfaces B Biointerfaces. 156 (2017) 358–365. doi:10.1016/j.colsurfb.2017.05.040.

[24] J.A. Zanghi, W.A. Renner, J.E. Bailey, M. Fussenegger, The growth factor inhibitor suramin reduces apoptosis and cell aggregation in protein-free CHO cell batch cultures, Biotechnol. Prog. 16 (2000) 319–325. doi:10.1021/bp0000353.

[25] W.A. Renner, M. Jordan, H.M. Eppenberger, C. Leist, Cell-cell adhesion and aggregation: Influence on the growth behavior of CHO cells, Biotechnol. Bioeng. 41 (1993) 188–193. doi:10.1002/bit.260410204.

[26] S. Lam, K.P. Velikov, O.D. Velev, Pickering stabilization of foams and emulsions with particles of biological origin, Curr. Opin. Colloid Interface Sci. 19 (2014) 490–500. doi:10.1016/j.cocis.2014.07.003.

[27] E. Blanco, S. Lam, S.K. Smoukov, K.P. Velikov, S.A. Khan, O.D. Velev, Stability and viscoelasticity of magneto-pickering foams, Langmuir. 29 (2013) 10019–10027. doi:10.1021/la4014224.

Chapter 5 – Quantification of cell shear sensitivity in production bioreactors to minimize damage during scale-up of CHO cell culture

5.1 Introduction

Poloxamer 188 (P188) is routinely used in mammalian cell culture to protect cells from shear damage. Without the addition of shear protectants, the harsh environment in bioreactors from turbulent hydrodynamic flows and bubble-bursting would render cells nonviable and prevent production of biotherapeutics. Poloxamers are nonionic triblock copolymer surfactants with the general structure of hydrophobic poly(propylene oxide) (PPO) center molecular chain anchoring two hydrophilic poly(ethylene oxide) tails. Poloxamers are commercially available in a wide range of average molecular weights and hydrophilicities (ratio of PEO to PPO) [1] and are used in a variety of industries (cosmetics, consumer products, drug delivery), but Poloxamer 188 has proven to be the most effective in shear protection of cell culture [2]. Although inclusion of P188 in chemically defined media formulations is now standard for the biopharmaceutical industry, the concentration needed for adequate shear protection in manufacturing scale bioreactors remains cell-line and process dependent and is often determined on a semi-empirical basis [3]. This is partly attributed to our limited understanding of hydrodynamic shear in turbulent bioreactor systems, but also stems from a lack of fundamental knowledge on surfactant-cell interactions.

Prior research suggests that P188 protects cells via both physical and biophysical mechanisms. Physically, the surfactant mitigates cell damage in three modes. (1) P188 decreases interfacial tension, thermodynamically reducing cell-bubble adsorption [4–7]. Decreased adsorption of cells to bubbles prevents cells from concentrating at the top of the bioreactor, where constant "micro-explosions" from foam breakdown can damage cells [8–10]. (2) P188 stabilizes the foam layer, allowing for drainage of cells back into the bulk medium and delocalizing them

from the high shear bubble bursting region. Formation of a highly stable foam is generally undesirable in a bioreactor, but a small foam head can have beneficial effects [11]. Finally, (3) surfactants decrease the hydrodynamic force during bubble breakdown [12]. This decreases the energy dissipated per bubble, which in turn would limit cell damage.

P188 also protects cell culture from shear damage through biophysical interaction with cell membranes. This area is currently of high research interest due to implications of surfactant-cell interactions in drug delivery and therapeutics. Poloxamers have been shown to increase cell membrane bursting tension [13], decrease membrane fluidity [14,15], and seal membrane pores in injured cells [16,17]. P188 has also been shown to prevent cytoplasmic leakage in electroporated cells [18] and repair trypsin-damaged cells [19]. Furthermore, evidence of P188 incorporation into cell membranes and internal organelles over time suggests additional longer-term effects on cell metabolism or nutrient transport [20,21]. It is clear from these examples that P188 affects multiple interfaces and may have several modes of cell protection.

In biotherapeutic upstream process development, scale-up can span 6 orders of magnitude in volume, starting from 15 mL ambr® bioreactors to more than 15000 L on manufacturing scale. Media formulation and process conditions must be optimized to meet cellular metabolic demands, product quality characteristics, and maximize yield [22]. One group of such process conditions emerge from the shear environment experienced by the cell, which varies depending on the vessel size [23,24]. The level of shear experienced by cell culture in bioreactors can be minimized by optimizing the sparging regime, impeller geometry, and foam level; however, dissolved oxygen requirements and equipment constraints can restrict the freedom to vary these parameters.

The efficient use of shear protective additives such as P188 presents an alternative method to control cell shear damage [25]. P188 has a dose-dependent effect on cell robustness (i.e. higher

concentration, less cell damage), as shown in the previous chapter. It is impractical to use different levels of shear protectant for each volume scale, so media must be formulated to accommodate the harshest shear environment. This usually occurs at manufacturing scale, but unexpectedly high shear can also occur at intermediate scale with, for example, improperly sized pump or tubing [26]. Inadequate shear protectant can result in low cell viability, growth, productivity, and titer [27]. Increased P188 can result in higher foam formation, but intermediate levels (up to 5 g/L) have low impact on cell culture performance and product quality [3]. To determine the appropriate level of shear protectant in the media formulation, two quantities should be known: (1) the maximum energy dissipation or shear stress the culture will experience during scale up, and (2) the stress threshold the cell can withstand with no short-term and long-term negative impacts as a function of shear protectant. In practice, these two quantities are difficult to accurately determine experimentally [28]. Therefore, it is recommended to have excess rather than insufficient shear protectant. The goal of this work is to develop an efficient strategy to determine shear sensitivity of the culture prior to scale-up, and the appropriate level of shear protectant.

Several scale-down models have been proposed to simulate production scale stresses in benchtop experiments. Researchers have used shear sensitive particle sensors [29] or computational fluid dynamics (CFD) models [30] to characterize the hydrodynamic environment in large scale, and developed scale-down assays using microfluidics [31], thin capillary channels [29], rheometry/viscometry [32], and baffled shake flasks (BSF) [25] to stress the cells. These methods have various strengths and limitations in speed, accuracy, and efficiency. We have developed a concentric cylinder mixer (CCM) assay to rapidly characterize cell culture sensitivity using a laboratory mixer. This assay measures the relative shear sensitivity of culture quickly (5 min.) and with small volume (5 mL), enabling its use as an off-line analysis tool. The cell

sensitivity measured with the CCM can be correlated to the culture's performance in the bioreactor scale. Using this assay, we can develop sensitivity criteria for new processes, and supplement shear protective additives during media optimization to meet these requirements.

In this report, we demonstrate a strategy to optimize cell sensitivity in small scale bioreactors to minimize shear damage. We quantify the cell sensitivity by rapidly shearing the culture in the CCM, then tune the sensitivity by supplementing two different Poloxamers: P188 and P407. P188 increases cell protection, while a small amount of P407 reduces cell protection [33,34]. By correlating the culture's performance in the bioreactor with their measured sensitivity with the CCM, we can determine the sensitivity level at which we can expect shear damage to occur. We also show that P188 concentration decreases in the medium during the 14-day bioreactor batch, resulting in decreased cell protection. Our investigation presents an efficient approach to mitigate cell damage in bioreactors, and shows that shear damage can be easily controlled during the course of protein production by supplementing shear protectant.

5.2 Materials and methods

5.2.1 Surfactants and chemicals

P188 and P407 were provided by BASF Corporation and used as received. The physical properties of P188 and P407, as described by the manufacturer, are shown in Table I. Poloxamer stock solutions were prepared by dissolving solid flakes in purified MilliQ water (Millipore, Billerica, MA) to 100 g/L and sterilizing by filtration (0.22 μm, Millipore) before use. Antifoam Q7 (Dow Corning) was diluted to 15% stock solution prior to use. 0.15 M phosphate buffer saline (PBS) solution was prepared by dissolving PBS tablets (Sigma-Aldrich) in water according to supplier's instructions, then filtered before use. Triton X-100 (Sigma-Aldrich) was prepared as 10% w/v stock solution in MilliQ water.

Table 5.1: Physical properties of Poloxamers used in this study.

Surfactant	Average MW	PEO_x-PPO_y-PEO_x	HLB	%PEO
P188	8400	80-27-80	29	81.8
P407	12600	101-56-101	22	73.2

5.2.2 Quantification of P188 concentration using colorimetric assay

A colorimetric assay was used to quantify the concentration of P188 in the medium [35]. Briefly, cobalt thiocyanate stock solution was made by mixing 3 grams of $Co(NO_3)_2$ (Sigma-Aldrich) with 20 grams of NH_4SCN (Sigma-Aldrich) in 100 mL of MilliQ water. P188 standards from 0.5 to 2 g/L were prepared in both purified water and cell culture basal media to generate a standard curve. Then, an insoluble Poloxamer complex was formed by mixing a solution containing 200 µL P188 standard, 100 µL Cobalt thiocyanate stock solution, 200 µL ethyl acetate (Sigma Aldrich), and 80 µL of ethanol (VWR) in a 1.5 mL microcentrifuge tube. After vortexing for 30 seconds, the blue solution was centrifuged at 15000 g for 5 minutes to collect the precipitate, and the supernatant was discarded. The precipitate was washed with ethyl acetate and centrifuged 8 times, then dissolved in 2 mL acetone for UV/vis analysis. Absorbance was recorded at 622 nm to generate a linear standard curve, with no significant difference in slope between P188 in water and basal media. Solutions with unknown P188 concentration were analyzed with the same procedure. All solutions were analyzed in triplicate.

5.2.3 Cell culture expansion and fed-batch process

Bioreactor experiments were performed using two recombinant CHO cell lines (CHO-A and CHO-B) secreting monoclonal antibodies. Cells were incubated at 37°C and 5% CO_2 with

platform agitation at 75 rpm. The cells were passaged every 3-4 days with seed density of 3E5 cells/mL in 3 L shaker flasks (Corning Life Science, Tewksbury, MA) in Biogen's proprietary chemically defined media. All bioreactor studies were conducted in 5 L glass vessels (Applikon Biotechnology, Foster City, CA) with 2.5 L initial working volume. Reactors were seeded at cell densities of 10^6 cells/mL. Bioreactors were operated in fed-batch mode and controlled by TruBio DV controllers (Finesse Solutions, San Jose, CA).

In the fed-batch process, the nutrient feed amount was determined by measure of integrated biomass [36,37], which was calculated with bio-capacitance. The integrated bio-capacitance was determined from the area under the bio-capacitance curve and was estimated by using the trapezoid approximation method across a predetermined time interval (24 hours). The complex nutrient feed was then administered every 24 hours. Meanwhile, bolus glucose additions were fed to maintain the glucose concentration above 2 g/L at designated time points.

5.2.4 On-line and off-line monitoring of cell culture in bioreactors

Cell density and viability were measured daily by Vi-Cell XR (Beckman Coulter, Indianapolis, IN) automated cell counter using trypan blue dye exclusion. For metabolite analysis, supernatant was collected after centrifugation at 3000 rpm for 10 minutes. Glucose, glutamine, lactate, ammonium, potassium, sodium, and lactase dehydrogenase (LDH) in the broth were then measured using a Cedex BioHT (Roche Diagnostics GmbH, Mannheim, Germany). pH, pCO_2, and pO_2 were measured using a BioProfile pHOx analyzer (NOVA Biomedical, Waltham, MA). Osmolality was measured using an Auto Osmometer Model 3900 (Advanced Instruments, Norwood, MA).

5.2.5 Scale-down model of cell sensitivity using concentric shearing

A concentric cylinder mixer (CCM) was used to measure cell culture shear sensitivity. A ServoDyne electronic mixer (Cole-Parmer, Vernon Hills, IL) equipped with a stainless-steel shaft with radius 4.75 mm was used to shear the cell suspension. 5 mL of cell suspension taken from the daily bioreactor sample was transferred to a glass test tube with inner radius 6.25 mm and centered with the steel shaft to form a gap distance 1.5 mm with solid-liquid contact length L of 5.5 cm. 150 ppm antifoam stock solution was added to the suspension to prevent foam formation during shearing. Cells were sheared in the CCM for 5 minutes at 6000 rpm, then spun down and analyzed with BioHT to quantify LDH concentration. LDH is an intracellular enzyme released upon cell lysis, and is used as a measure of cell damage. A portion of the bioreactor sample was also completely lysed with Triton X-100 and analyzed to determine the total LDH concentration in the cell suspension. We calculated the normalized change in LDH after shearing in the CCM as a measure of cell sensitivity, given in Equation 1. LDH_i and LDH_f refer to the LDH concentration before and after shearing, respectively.

$$\text{Normalized } \Delta\text{LDH}(\%) = \left(\frac{LDH_f - LDH_i}{LDH_{lyse} - LDH_i} \right) \cdot 100\% \qquad \text{(Eq 1)}$$

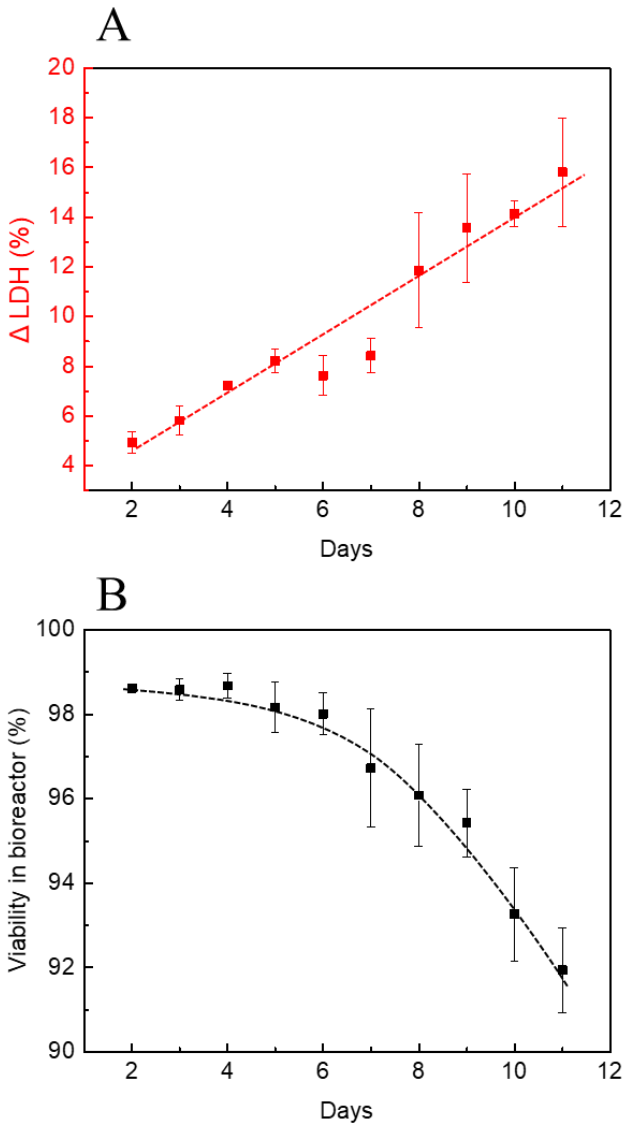

Figure 5.1*:* (A) CCM results in control bioreactor of CHO-A. Cell culture samples were taken daily and analyzed using the CCM to determine the normalized ΔLDH (%), which represents cell sensitivity. We observed a nohhear-linear relationship in cell sensitivity over time, steadily increasing throughout the bioreactor run. (B) The viability of cells in the control bioreactor. The viability declines throughout the bioreactor run, which results from natural cell death (apoptosis), shear damage, and other sources.

5.3 Results

5.3.1 Cell sensitivity changes during bioreactor operation

Initial results of the cell sensitivity over time are shown in Figure 5.1A. These CHO-A cells were taken from a pilot scale 315 L bioreactor grown in control conditions (2 g/L P188). Most notably, the measured Δ LDH (%) using the CCM increases linearly over time, indicating that the culture becomes more sensitive during the course of protein production. At inoculation, the sensitivity is ~5% Δ LDH, increasing more than three-fold to > 15% by harvest day. In Figure 1B, the viability of the cells in the bioreactor measured with trypan blue dye exclusion is shown. The observed viability decline starting on day 7 is typical of many cell culture processes – during the latter half of the process, cells tend to undergo apoptosis (programmed cell death). However, a portion of these cells may be necrotic, indicating premature cell death. The trypan blue viability assay does not distinguish between the two modes of cell death, as all cells which have lost structural integrity of the membrane (which occurs in both late stage apoptosis and necrosis) are stained and considered nonviable. Therefore, these interesting results warrant further experiments to determine if the increased cell sensitivity observed from Figure 5.1A partially contributes to the decreased viability in Figure 5.1B.

5.3.2 Poloxamer concentration in the medium

One possible cause for the observed increase in cell sensitivity over time is a decrease in P188 concentration. Previous studies have shown that CHO cells uptake P188 at a constant rate of 11.7 ± 6.7 μg/10^6 cells, independent of initial P188 concentration [20]. The internalization of P188 within cells decreases its concentration in the medium, making less surfactant available to protect subsequent generations of cells. To prove this hypothesis, we measured the concentration of P188

in the media of a pilot scale CHO-A seed train bioreactor over time (**Figure 5.2**). Cells from n-1 seed train are in exponential growth phase, so high viability is maintained. Also shown in Figure 5.2 is the calculated P188 concentration in the medium based on a P188 uptake rate of 11.7 μg/10^6 cells and the measured total cell density (TCD). We obtain strong agreement between theoretical and measured P188 concentration, indicating that internalization of surfactant by cells may strongly contribute to the decreased surfactant concentration in the medium.

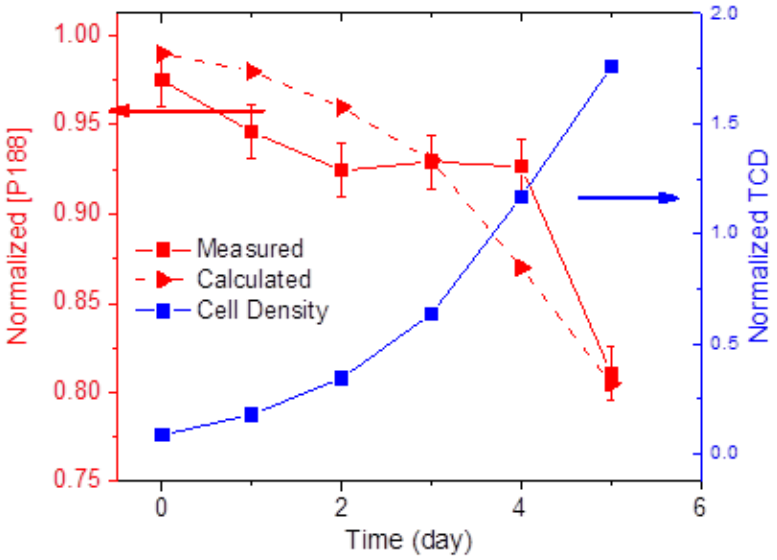

Figure 5.2*:* Concentration of P188 in the medium over time in a CHO-A seed train 315 L bioreactor. The measured P188 concentration (red solid line) shows a steep decrease as total cell density (TCD), shown in blue, increases. In dashed red, the predicted concentration based on a constant uptake rate of 11.7 μg/10^6 cells is shown. There is strong agreement between the predicted and measured P188 concentration, indicating that high cell growth may strongly contribute to P188 concentration decline.

5.2.1 Bioreactor experiments with increased cell shear protection

To determine the impact of high and low cell sensitivity on bioreactor performance, we performed two sets of studies in 5-L benchtop bioreactors with varying cell protection strategies.

In the first series, we added additional P188 to increase shear protection, while in the second, we added P407 to decrease cell shear protection. The list of conditions for both sets of experiments are given in **Table 5.2** and **Table 5.3**. We also tested two surfactant addition strategies: (1) supplementation in the initial basal media, or (2) fed into the bioreactor at set timepoints. The resulting cell sensitivity measurements with increased P188 are shown in Figure 5.3. The sensitivity of cells in the control bioreactor again increased during the process, while the culture with additional P188 in the basal medium displayed significantly higher cell robustness throughout the batch. The ΔLDH (%) in bioreactor with P188-A remains lower than in the control bioreactor, although it gradually increases (which may indicate that P188 concentration is decreasing). More interestingly, the bioreactor with P188 dosing strategy (P188-B) began with cell sensitivity comparable to control bioreactor, but the ΔLDH (%) drastically decreased upon addition of P188 on Day 5 (marked with arrow). This shows that the cell sensitivity can be tuned during the run by changing P188 concentration.

Table 5.2: Table of conditions in CHO-A experiments investigating bioreactor performance with increased P188.

Bioreactor	Poloxamer condition	Cell sensitivity strategy
Control	Initial: 2 g/L P188 Surfactant addition: None	Baseline
P188-A	Initial: 5 g/L P188 Surfactant addition: None	High cell protection at inoculation
P188-B	Initial: 2 g/L Surfactant addition: P188 on D5	Baseline cell protection at inoculation, increased protection at D5

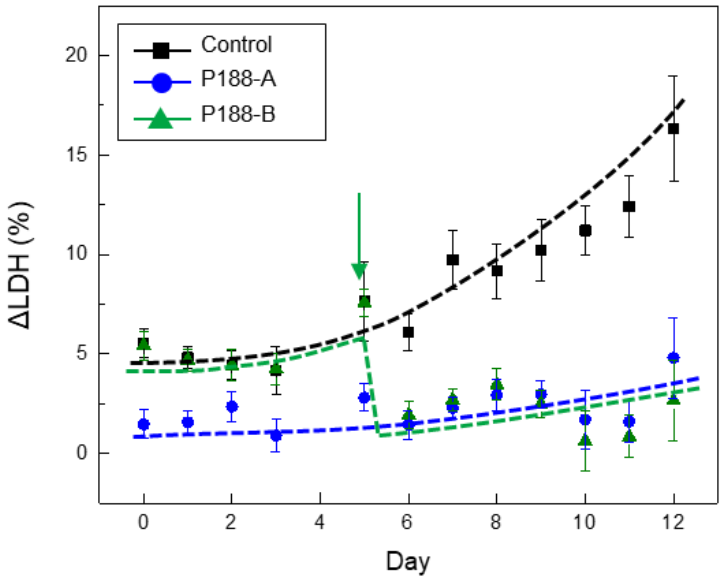

Figure 5.3: Results from CCM analysis comparing cell sensitivities for three bioreactors conditions: control, 5 g/L P188 in the basal media, and 2 g/L P188 in the basal with additional dosing of 3 g/L added on day 5 (indicated by the arrow).

The effects of increasing cell protection with P188 on total LDH concentration and cell viability are shown in **Figure 5.4**. Overall, both strategies resulted in approximately 40% reduced LDH concentration and ~10% increase in harvest viability. Both addition strategies had significant impact on the process performance.

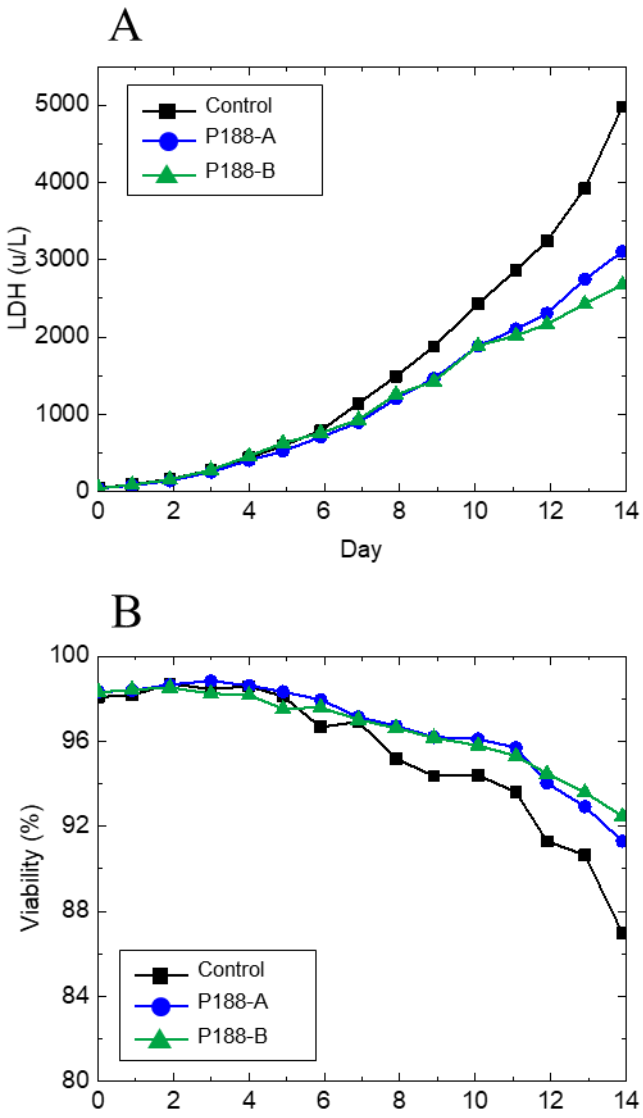

Figure 5.4*:* (A) LDH concentration and (B) cell viability of CHO-A in bioreactors comparing increased cell protection strategies. Both addition strategies resulted in significantly lower LDH concentration and harvest viability.

To investigate the effects of decreased cell protection on bioreactor performance, we supplemented P407 instead of P188 into the medium. These conditions are listed in **Table 5.3**. The goal of this set of experiments was to correlate the effects of increased cell sensitivity on the CCM with the resulting cell performance in the bioreactor. P407 is a high molecular weight surface

active Poloxamer, which decreases cell protection when introduced in small amounts [33]. The results of these experiments are shown in Figure 5.5. In condition P407-B, we initially started with 0.06 g/L P407 in the medium. The cell viability began to crash by Day 2, so we supplemented the medium with P188 on Day 4 to determine if we could recover the batch.

The cell sensitivity shown in **Figure 5.5**A displayed an unexpected trend. The P407 dosing strategy, P407-A, exhibited dramatic spikes in cell sensitivity immediately following addition of P407 on D5 and D10. However, this affect was short-lived, as the sensitivity dropped on the following days (D6 and D11). In P407-B, the P407 contamination was in the initial basal media at inoculation. The sensitivity of the culture started high (10% ΔLDH), resulting in cell damage. Because the viability rapidly declined to 80% on Day 4, we fed an additional 3 g/L P188 to investigate whether the increased sensitivity from P407 could be mitigated. The cell sensitivity immediately decreased after P188 addition, and the viability leveled off at ~80%. This indicates that the viability crash was prevented and the batch was successfully recovered. The increased cell sensitivity from high-molecular weight Poloxamer could be mitigated in the middle of the run using P188.

Table 5.3: Table of conditions in CHO-A experiments investigating bioreactor performance with P407. This surfactant makes the cell culture more sensitive and susceptible to shear damage.

Bioreactor	Poloxamer condition	Cell sensitivity strategy
Control	Initial: 2 g/L P188 Addition: None	Baseline
P407-A	Initial: 2 g/L P188 Addition: P407 on D5 and D10	Baseline cell protection at inoculation, decreased protection on D5 and D10
P407-B	Initial: 2 g/L P188 Addition: P188 on D4	Low cell protection at inoculation, Increased protection on D4

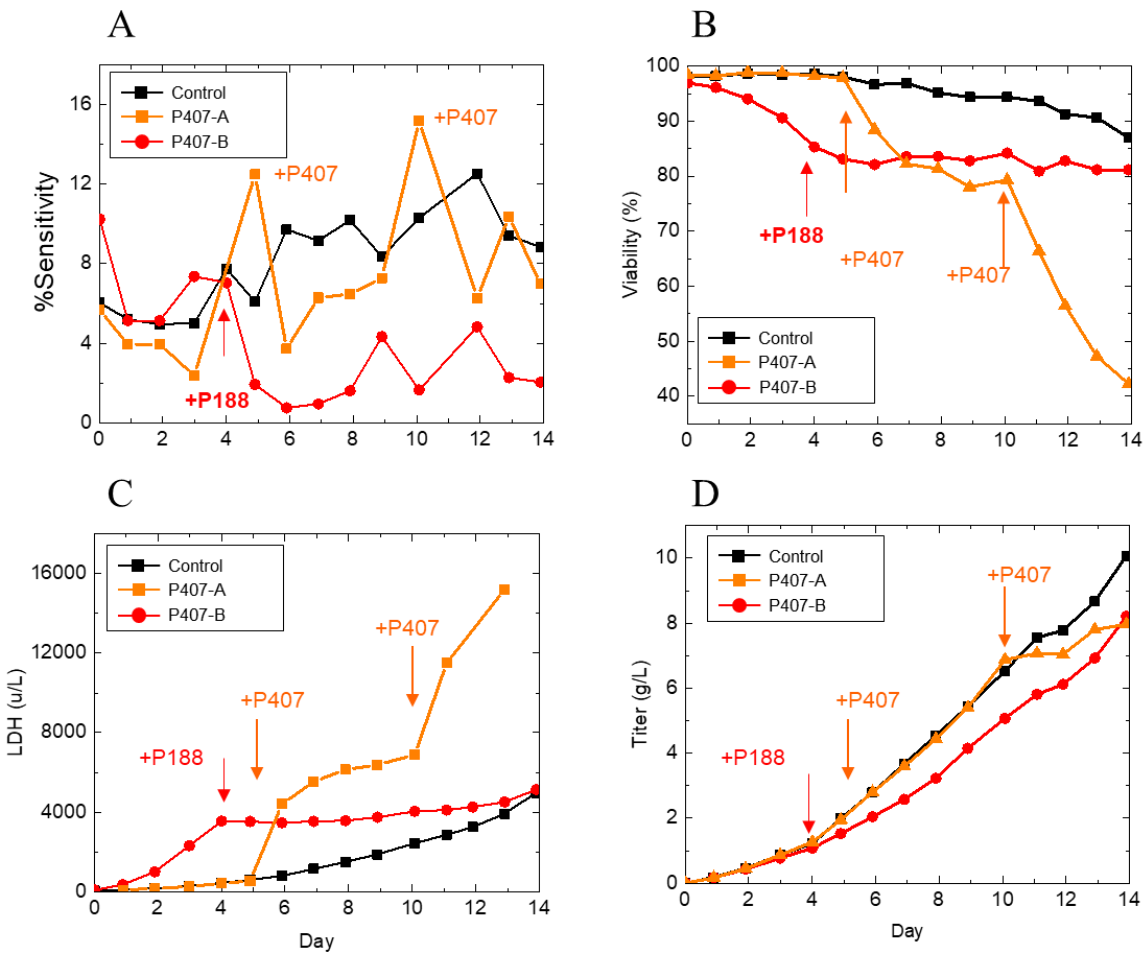

Figure 5.5*:* (A) Cell sensitivity, (B) cell viability, (C) LDH concentration, and (D) protein titer of CHO-A in 5-L benchtop bioreactors with high cell sensitivity induced through addition of P407. In P407-A bioreactor, P407 dosages on D5 and D10 resulting in sharp spikes in cell sensitivities, accompanied by viability drops and LDH increase. In P407-B, initial P407 in the medium resulted in high initial sensitivity. P188 was fed into this bioreactor on D4, leading to suppression of cell sensitivity. The viability and LDH of this bioreactor were preserved, but the titer did not recover.

Table 5.4*:* Table of conditions in experiments investigating effect of increased shear protection on higher shear environment. Sintered sparger (SS) produces small bubbles, which cause more cell damage than drilled hole sparger (DHS).

Bioreactor ID	Poloxamer condition
DHS-2G	2 g/L P188
SS-2G	2 g/L P188
DHS-5G	5 g/L P188
SS-5G	5 g/L P188

5.3.3 Bioreactor studies with varied shear environment

The previous set of experiments varied the shear protection of cells with relatively constant shear conditions (sparger, agitation rate, etc.). Next, we investigated the effect of increased shear environment on the cell performance by using different sparger designs. The table of conditions tested are listed in Table 5.4. These experiments were performed with CHO-B cell line in 5-L benchtop bioreactors. Drilled hole spargers (DHS) were used as the control-shear condition, while sintered spargers (SS) were used to induce a high-shear environment. Control (2 g/L) and high P188 concentration (5 g/L) were tested in both environments. Sintered spargers create micron sized bubbles, which significantly enhance mass transfer, but result in large energy dissipation during bubble breakdown due to high Laplace pressure. The data from these experiments are shown in Figure 5.6. The cell sensitivity (data not shown) was comparable between conditions with the same surfactant concentration, indicating that sensitivity depends only upon physiological and medium properties, and not on the external shear environment. The viability plot in **Figure 5.6**A shows similar trend between all conditions except SS-2G, the high shear environment with low shear protection. This condition also had 50% higher LDH upon harvest. In **Figure 5.6**B, there is almost no difference between DHS-5G and SS-5G, indicating that with high shear protection, the cells

are unaffected by the harsher environment. Therefore, the process has higher robustness, as the bioreactor performance is similar in both cases. Titer was comparable in all experiments except for SS-2G, which had lower titer.

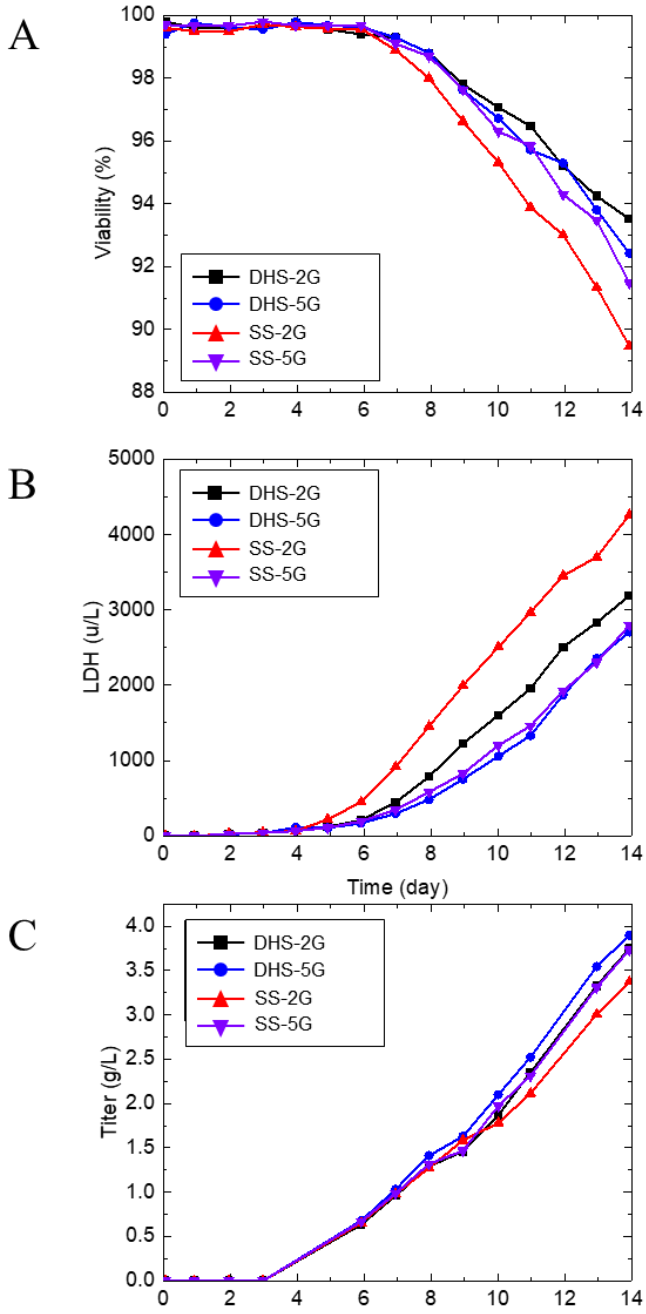

Figure 5.6: (A) Viability, (B) LDH concentration, and (C) protein titer in bioreactor experiments varying shear environment with different spargers. Sintered sparger (SS) with 2 g/L P188 results in high shear damage. With 5 g/L P188, the high shear environment has little effect on the bioreactor performance.

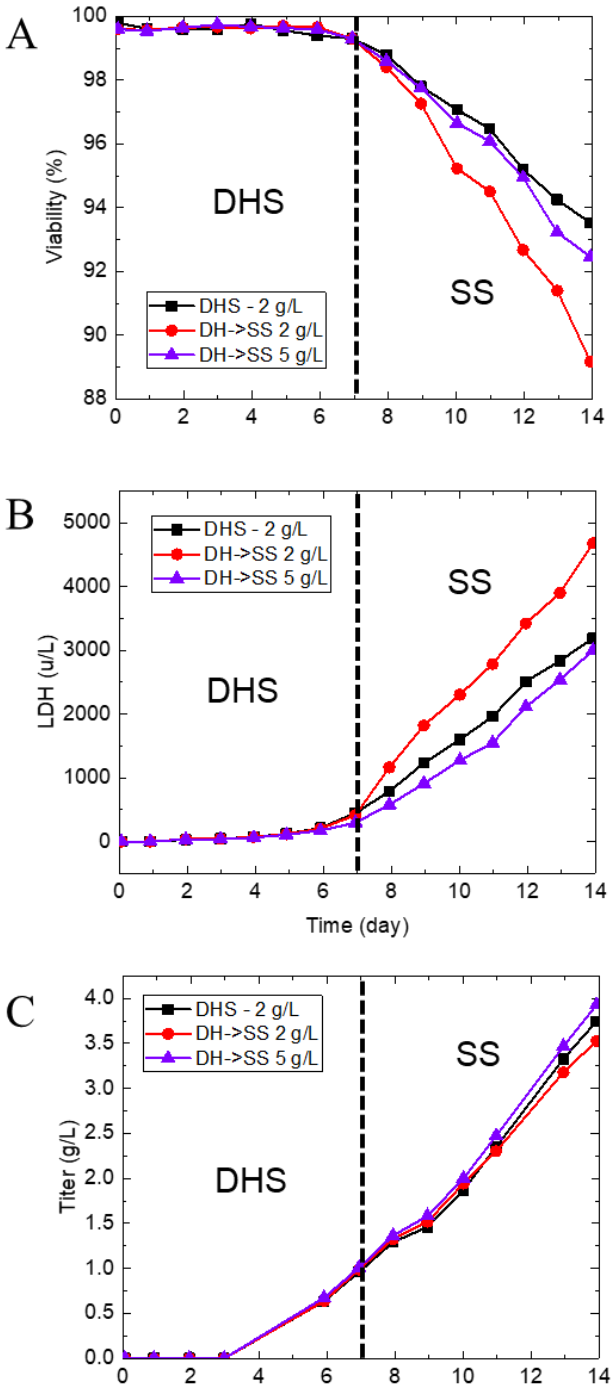

Figure 5.7*:* (A) Viability, (B) LDH concentration, and (C) protein titer in bioreactor experiments with process insult on D7. Sintered sparger (SS) with 2 g/L P188 results in high shear damage. With 5 g/L P188, the insult has little effect on the bioreactor performance.

In the final set of bioreactor experiments, we switched from DHS to SS on Day 7 of the batch. These conditions model a change in shear environment during the process, such as a restricted tubing or clamp. Bioreactors were set up with both drilled hole and sintered spargers, and the mass flow controllers switched from DHS to SS on Day 7. The results of this experiment are shown in **Figure 5.7**. After switching from DHS to SS, the culture with 2 g/L P188 had steeper viability decline and LDH increase, indicating some cells experienced shear damage. With 5 g/L P188, the culture performed similar to control. Therefore, the process change had virtually no effect on them.

5.4 Discussion

In this study, we used the CCM as a shear sensitivity assay to identify a process deficiency in shear protection. We then increased or decreased the shear sensitivity of the culture in benchtop bioreactors by supplementing P188 and P407, respectively. By correlating the measured shear sensitivity of the resulting culture with their performance in the bioreactors, we observed that at above 10% ΔLDH, CHO-A experienced adverse effects in cell growth and viability in bioreactor environment. The sensitivity can be adjusted by supplementing the culture with P188 either initially in the basal medium, or fed during the bioreactor run, to keep the sensitivity below 10%.

In our initial cell sensitivity measurements over time **(Figure 5.1**A), the observed linear increase in sensitivity was an unexpected and alarming result. Because the CCM does not output a quantitative shear rate, it is difficult to compare to other published cell sensitivity data, such as studies using flow-focusing microfluidics [31] and rheometers [32]. However, exact bioreactor shear rates are also difficult to characterize, as they require accurate computational fluid dynamics

(CFD) models and vary by scale and geometry [30]. Therefore, even quantitative methods can be inaccurate or unreliable in predicting scale-up damage. We obtained a relative sensitivity trend with the CCM, but bioreactor experiments were needed to evaluate whether the increased sensitivity contributes to the viability decline (**Figure 5.1**B), or is negligible factor in cell health. Trypan blue dye exclusion stains all cells which have compromised membranes, including both cells damaged by shear, and naturally apoptotic cells.

Our bioreactor experiments with higher P188 concentration showed that the increased sensitivity contributed to higher cell damage, even in the 5-L scale (**Figure 5.3** and **Figure 5.4**). While comparing the LDH curves in Figure 5.4, it appears that the LDH begins to deviate on Day 7. The control bioreactor continues to increase with steeper LDH slope than bioreactors with increased P188. The shear sensitivity at this time point is ~10% ΔLDH (**Figure 5.3**). Therefore, adverse effects on cell performance were observed above 10% ΔLDH. Supplementation of P188 to maintain below 10% ΔLDH results in high robustness of the cell culture.

Addition of P407 had a strong effect on cell sensitivity, which resulted in decreased cell viability, higher LDH concentration, and lower protein titer. One surprising observation was that P407 only temporarily increased the shear sensitivity (**Figure 5.5**A). The samples in P407-A were sampled for measurement with the CCM directly following P407 dosing, resulting in the dramatic spike in cell sensitivity. On the following day, the sensitivity dipped back down. We hypothesize that the most fragile cells were damaged or killed by the bioreactor environment the same day that P407 was added. Therefore, when the subsequent sample was taken on the next day, the highly sensitive cell population did not contribute to the measurement, giving the appearance that cell sensitivity had decreased. This suggests the presence of a cell robustness distribution (inverse of cell sensitivity), which is illustrated schematically in **Figure 5.8.** We hypothesize that adding P188

or P407 shifts the cell robustness distribution higher or lower, respectively. The cells experience stress from the bioreactor environment, which is shown as the red dashed line. The cell population which cannot withstand the shear environment experiences adverse effects, denoted by yellow shading.

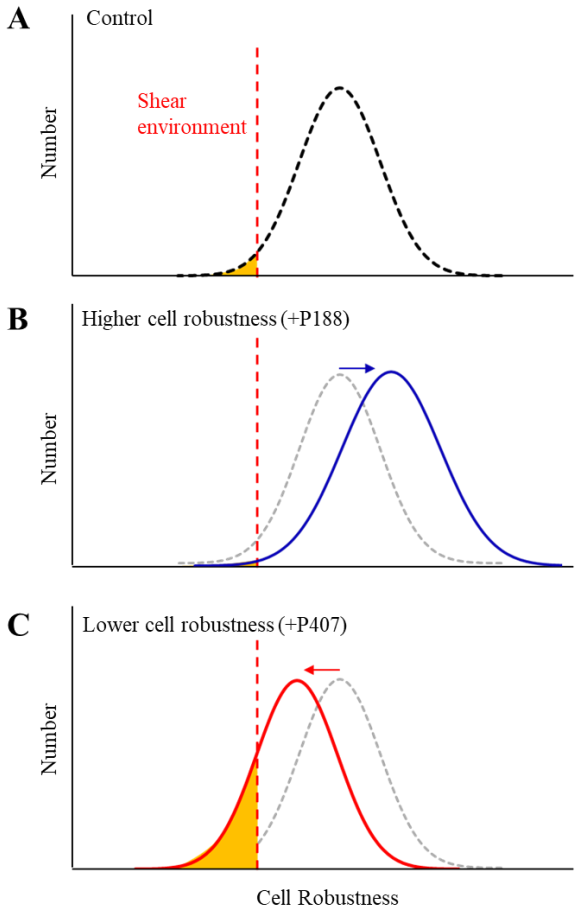

Figure 5.8: Schematic illustrating our hypothesis of cell robustness distribution and the effects of P188 and P407. (A) Cell population has a distribution of cell robustness. The level of shear experienced by the cells is indicated by the vertical dashed line. If the environment is sufficiently harsh, the population shaded in yellow may experience negative effects. (B) P188 adds additional cell robustness, shifting the distribution higher, while (C) P407 makes the cells more sensitive, shifting the robustness distribution lower, resulting in higher cell damage.

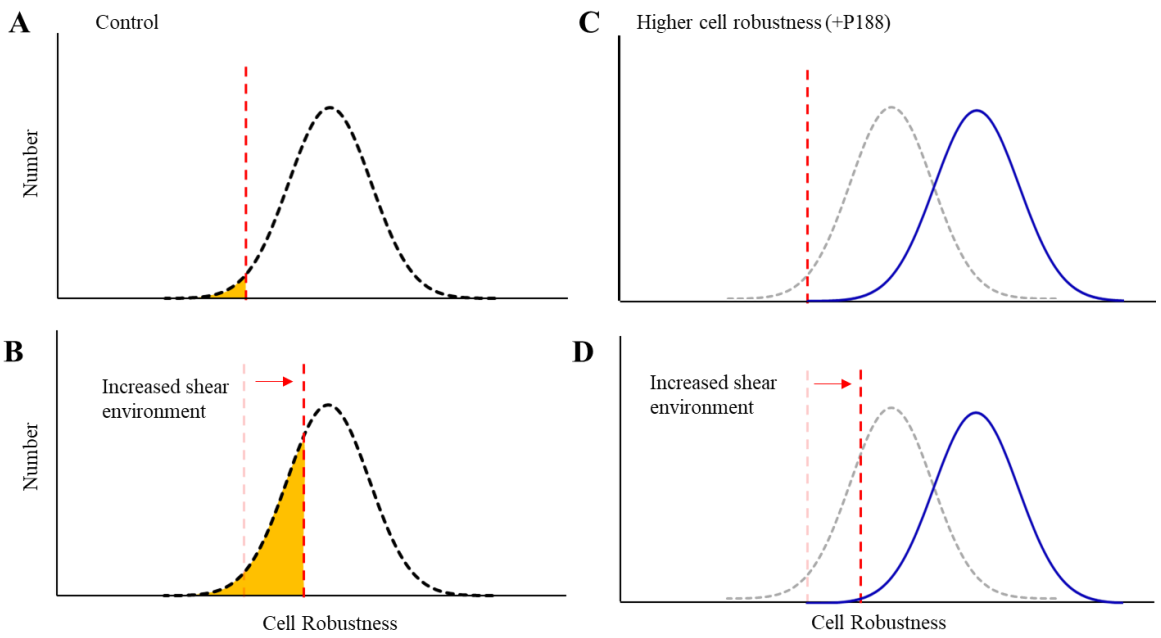

Figure 5.9: Schematic illustrating our hypothesis on the role of changing the shear environment on cell population. In (A)-(B), increasing the shear environment results in larger affected cell population. With higher cell protection (C)-(D), the additional shear does not affect the cell population.

The last set of bioreactor experiments varied the shear environment by changing the sparger geometry. Sintered spargers create micron-sized bubbles, which have higher gas entrance velocity damage and bubble bursting damage [38] Cell culture with additional P188 did not experience any negative effects with the harsher environment, while cells with lower cell protection experienced cell damage, evidenced by lower viability and increased LDH concentration **(Figure 5.6**). In our model of cell sensitivity distribution, the harsher environment shifts the stress higher, affecting a greater portion of the cell population **(Figure 5.9**A-B). If the cells have high robustness as in **Figure 5.9**D, the shift in shear environment does not have any affect. The ideal shear protection strategy is therefore to supplement P188 to maintain cell robustness above the shear in the environment.

5.5 Conclusion

In this work, we have shown that the CCM can be used as a tool to quantify the relative shear sensitivity of cell culture. By taking daily bioreactor samples for off-line CCM analysis, we determined that cell sensitivity increased during the bioreactor process, which resulted in shear damage to the culture in the latter half of the batch. We proved that supplementation of culture with additional P188 either in the initial batch media or midway through the run could rapidly suppress the cell sensitivity, effectively mitigating shear damage. Furthermore, we showed that higher P188 concentration increased the process robustness to withstand a high shear environment, which we induced by using sintered sparger. The results from this investigation demonstrate the potential of using CCM as a tool for process development, and show that P188 can be used as a lever for enhancing process robustness when shear damage is a concern. We have also developed a hypothesis for cell robustness distribution in cell population, which contributes to our understanding of cell damage in bioreactors.

Acknowledgements

We gratefully acknowledge financial support from Biogen (RTP, NC) We thank Kevin Chang, Vivian Shen, Marshall Bowden, and Alex Vaca for their contributions to this work.

5.6 References

[1] P. Alexandridis, V. Athanassiou, S. Fukuda, T.A. Hatton, Surface Activity of Poly(ethylene oxide)-block-Poly(propylene oxide)-block-Poly(ethylene oxide) Copolymers, Langmuir. 10 (1994) 2604–2612.

[2] D.W. Murhammer, C.F. Goochee, Structural features of nonionic polyglycol polymer molecules responsible for the protective effect in sparged animal cell bioreactors, Biotechnol. Prog. 6 (1990) 142–148. doi:10.1021/bp00002a008.

[3] T. Tharmalingam, C.T. Goudar, Evaluating the impact of high Pluronic F68 concentrations on antibody producing CHO cell lines, Biotechnol. Bioeng. 112 (2014) 832–7. doi:10.1002/bit.25491.

[4] D. Chattopadhyay, J.F. Rathman, J.J. Chalmers, Thermodynamic approach to explain cell adhesion to air-medium interfaces., Biotechnol. Bioeng. 48 (1995) 649–58. doi:10.1002/bit.260480613.

[5] J.D. Michaels, J.E. Nowak, A.K. Mallik, K.K. Koczo, D.T. Wasan, E.T. Papoutsakis, Analysis of cell-to-bubble attachment in sparged bioreactors in the presence of cell-protecting additives., Biotechnol. Bioeng. 47 (1995) 407–19. doi:10.1002/bit.260470402.

[6] F. Bavarian, L.S. Fan, J.J. Chalmers, Microscopic Visualization of Insect Cell-Bubble Interactions. I: Rising Bubbles, Air-Medium Interface, and the Foam Layer, Biotechnol. Prog. 7 (1991) 140–150. doi:10.1021/bp00008a009.

[7] J.J. Chalmers, F. Bavarian, Microscopic visualization of insect cell-bubble interactions. II: The bubble film and bubble rupture, Biotechnol. Prog. 7 (1991) 151–158. doi:10.1021/bp00008a010.

[8] E.T. Papoutsakis, Fluid-mechanical damage of animal cells in bioreactors, Trends Biotechnol. 9 (1991) 427–437.

[9] E.T. Papoutsakis, Media additives for protecting freely suspended animal cells against agitation and aeration damage, Trends Biotechnol. 9 (1991) 316–24. doi:10.1016/0167-7799(91)90102-N.

[10] S. Goldblum, Y.K. Bae, W.F. Hinkj, J. Chalmers, W.F. Hink, J. Chalmers, Protective Effect of Methylcellulose and Other Polymers on Insect Cells Subjected to Laminar Shear Stress, Biotechnol. Prog. 6 (1990) 383–390. doi:10.1021/bp00005a011.

[11] B. Junker, Foam and its mitigation in fermentation systems., Biotechnol. Prog. 23 (2007) 767–84. doi:10.1021/bp070032r.

[12] D. Dey, J.M. Boulton-Stone, A.N. Emery, J.R. Blake, Experimental comparisons with a numerical model of surfactant effects on the burst of a single bubble, Chem. Eng. Sci. 52 (1997) 2769–2783. doi:10.1016/S0009-2509(97)00083-3.

[13] Z. Zhang, M. Al-Rubeai, C.R. Thomas, Effect of Pluronic F-68 on the mechanical properties of mammalian cells, Enzyme Microb. Technol. 14 (1992) 980–983. doi:10.1016/0141-0229(92)90081-X.

[14] O.T. Ramírez, R. Mutharasan, The role of the plasma membrane fluidity on the shear sensitivity of hybridomas grown under hydrodynamic stress., Biotechnol. Bioeng. 36 (1990) 911–920. doi:10.1002/bit.260360906.

[15] O.T. Ramirez, R. Mutharasan, Effect of serum on the plasma membrane fluidity of hybridomas: an insight into its shear protective mechanism, Biotechnol. Prog. 8 (1992) 40–50.

[16] S. Yasuda, D. Townsend, D.E. Michele, E.G. Favre, S.M. Day, J.M. Metzger, Dystrophic heart failure blocked by membrane sealant poloxamer, Nature. 436 (2005) 1025–1029. doi:10.1038/nature03844.

[17] V. Sharma, K. Stebe, J.C. Murphy, L. Tung, Poloxamer 188 decreases susceptibility of artificial lipid membranes to electroporation., Biophys. J. 71 (1996) 3229–41. doi:10.1016/S0006-3495(96)79516-4.

[18] S.A. Maskarinec, J. Hannig, R.C. Lee, K.Y.C. Lee, Direct observation of poloxamer 188 insertion into lipid monolayers, Biophys. J. 82 (2002) 1453–1459. doi:10.1016/S0006-3495(02)75499-4.

[19] T. Tharmalingam, H. Ghebeh, T. Wuerz, M. Butler, Pluronic enhances the robustness and

reduces the cell attachment of mammalian cells, Mol. Biotechnol. 39 (2008) 167–177. doi:10.1007/s12033-008-9045-8.

[20] A. Gigout, M.D. Buschmann, M. Jolicoeur, The fate of Pluronic F-68 in chondrocytes and CHO cells., Biotechnol. Bioeng. 100 (2008) 975–87. doi:10.1002/bit.21840.

[21] M.-F.M.-F. Clincke, E. Guedon, F.T. Yen, V. Ogier, O. Roitel, J.-L. Goergen, Effect of Surfactant Pluronic F-68 on CHO Cell Growth , Metabolism , Production , and Glycosylation of Human Recombinant IFN- c in Mild Operating Conditions, Biotechnol. Prog. 27 (2010) 181–90. doi:10.1002/btpr.503.

[22] W.-S. Hu, J.G. Aunins, Large-scale mammalian cell culture, Curr. Opin. Biotechnol. 8 (1997) 148–153. doi:10.1016/S0958-1669(97)80093-6.

[23] W. Hu, C. Berdugo, J.J. Chalmers, The potential of hydrodynamic damage to animal cells of industrial relevance: current understanding., Cytotechnology. 63 (2011) 445–60. doi:10.1007/s10616-011-9368-3.

[24] S. Xu, L. Hoshan, R. Jiang, B. Gupta, E. Brodean, K. O'Neill, T.C. Seamans, J. Bowers, H. Chen, A practical approach in bioreactor scale-up and process transfer using a combination of constant P/V and vvm as the criterion, Biotechnol. Prog. (2017) 1–6. doi:10.1002/btpr.2489.

[25] H. Peng, K.M. Hall, B. Clayton, K. Wiltberger, W. Hu, E. Hughes, J. Kane, R. Ney, T. Ryll, Development of small scale cell culture models for screening poloxamer 188 lot-to-lot variation, Biotechnol. Prog. 30 (2014) 1411–1418. doi:10.1002/btpr.1967.

[26] H. Kamaraju, K. Wetzel, W.J. Kelly, Modeling shear-induced CHO cell damage in a rotary positive displacement pump, Biotechnol. Prog. 26 (2010) 1606–1615. doi:10.1002/btpr.479.

[27] J. Wu, Insights into protective effects of medium additives on animal cells under fluid stresses: the hydrophobic interactions., Cytotechnology. 22 (1996) 103–9. doi:10.1007/BF00353929.

[28] P.L.L. Walls, O. McRae, V. Natarajan, C. Johnson, C. Antoniou, J.C. Bird, Quantifying

the potential for bursting bubbles to damage suspended cells, Sci. Rep. 7 (2017) 1–9. doi:10.1038/s41598-017-14531-5.

[29] B. Neunstoecklin, M. Stettler, T. Solacroup, H. Broly, M. Morbidelli, M. Soos, Determination of the maximum operating range of hydrodynamic stress in mammalian cell culture, J. Biotechnol. 194 (2015) 100–109. doi:10.1016/j.jbiotec.2014.12.003.

[30] T.K. Villiger, B. Neunstoecklin, D. Karst, E. Lucas, M. Stettler, H. Broly, M. Morbidelli, M. Soos, Experimental and CFD Physical Characterization of Animal Cell Bioreactors: From Micro- to Production Scale, Biochem. Eng. J. 131 (2017) 84–94. doi:10.1016/j.bej.2017.12.004.

[31] N. Ma, K.W. Koelling, J.J. Chalmers, Fabrication and use of a transient contractional flow device to quantify the sensitivity of mammalian and insect cells to hydrodynamic forces, Biotechnol. Bioeng. 80 (2002) 428–437. doi:10.1002/bit.10387.

[32] S.H. Mardikar, K. Niranjan, Observations on the shear damage to different animal cells in a concentric cylinder viscometer, Biotechnol. Bioeng. 68 (2000) 697–704. doi:10.1002/(SICI)1097-0290(20000620)68:6<697::AID-BIT14>3.0.CO;2-6.

[33] D. Chang, R. Fox, E. Hicks, R. Ferguson, K. Chang, D. Osborne, W. Hu, O.D. Velev, Investigation of interfacial properties of pure and mixed poloxamers for surfactant-mediated shear protection of mammalian cells, Colloids Surfaces B Biointerfaces. 156 (2017) 358–365. doi:10.1016/j.colsurfb.2017.05.040.

[34] H. Peng, A. Ali, M. Lanan, E. Hughes, K. Wiltberger, B. Guan, S. Prajapati, W. Hu, Mechanism investigation for Poloxamer 188 raw material variation in cell culture, Biotechnol. Prog. 32 (2016) 767–775. doi:10.1002/btpr.2268.

[35] H. Ghebeh, A. Handa-Corrigan, M. Butler, Development of an assay for the measurement of the surfactant pluronic F-68 in mammalian cell culture medium., Anal. Biochem. 262 (1998) 39–44. doi:10.1006/abio.1998.2750.

[36] Y.-M. Huang, W. Hu, E. Rustandi, K. Chang, H. Yusuf-Makagiansar, T. Ryll, Maximizing productivity of CHO cell-based fed-batch culture using chemically defined

media conditions and typical manufacturing equipment, Biotechnol. Prog. 26 (2010) 1400–1410. doi:10.1002/btpr.436.

[37] A. Zhang, V.L. Tsang, B. Moore, V. Shen, Y.M. Huang, R. Kshirsagar, T. Ryll, Advanced process monitoring and feedback control to enhance cell culture process production and robustness, Biotechnol. Bioeng. 112 (2015) 2495–2504. doi:10.1002/bit.25684.

[38] Y. Liu, F. Li, W. Hu, K. Wiltberger, T. Ryll, Effects of bubble-liquid two-phase turbulent hydrodynamics on cell damage in sparged bioreactor, Biotechnol. Prog. 30 (2014) 48–58. doi:10.1002/btpr.1790.

Chapter 6 – Summary and outlook

6.1 Summary

The use of shear-protective additives in large-scale animal cell culture has been a standard industry practice for more than half a century [1]. However, complete fundamental knowledge of the colloidal interactions in the bioreactor taking place between cells, bubbles, proteins, and surfactants is still lacking. The biopharmaceutical industry continues to advance processes towards higher cell density, productivity and yield, using innovative feed strategies, process analytical technologies, and cell line engineering [2–4]. During the implementation of these advances, interfacial interactions will become increasingly important and may eventually become a bottleneck in bioprocessing. The main objectives of this dissertation were to (1) improve our understanding of the mechanisms of surfactant-mediated cell protection in relation to surface activity and interfacial phenomena, and (2) develop methods to quantify and mitigate cell damage in mammalian cell culture processes. As we discuss in the background knowledge presented in Chapter 1, efficient control of the interfacial interactions during bioprocesses can mitigate scale-up challenges such as excessive foaming and hydrodynamic shear damage.

Chapter 2 of this dissertation explored the surface activity of pure and mixed Poloxamer systems in correlation to their protective effects on cell culture. A small amount of Poloxamer 407 (P407) was added to Poloxamer 188 (P188) to model a high molecular weight (HMW) contaminant which caused cell damage in a 15000 L manufacturing scale batch. Using surface tensiometry and foam stability experiments, we determined that the P407 is highly surface active, preferentially adsorbing to the gas-liquid interface. This phenomenology suggests that P407 disrupts cell protection by excluding P188 from either the gas interface, the cell interface, or both. To determine which mechanism is dominant, we showed that both P407 and P188 exhibit similar

cell-to-bubble attachment rates, which suggests that the surfactant adsorption at the vapor-liquid interface is not the dominant mode of protection [5]. Subsequently, in Chapter 3, we investigated the effect of this surfactant system on the cell membrane interface. Using fluorescence anisotropy and excimer fluorescence ratio to probe the lateral and rotational cell membrane fluidity, we showed that cells with lower membrane fluidity (i.e. higher membrane order) also had low shear sensitivity (i.e. high shear resistance). This trend was consistent across different Poloxamer types, Poloxamer concentration, as well as with two CHO cell lines. Moreover, we demonstrated that adding a small amount of P407 (0.1 g/L) to a cell suspension containing P188 (2 g/L) resulted in a drastic and immediate increase in both cell membrane fluidity and cell shear sensitivity. This provides strong evidence that surfactant primarily protects cells from shear damage by adsorbing to and reinforcing their plasma membrane. Our data suggests that the effectiveness of the additive in cell protection is a function of its ability to increase membrane order.

In Chapter 4, we report the development of a rapid and efficient method to quantify the shear sensitivity of cell cultures using a concentric cylinder mixer (CCM). By means of characterizing the culture's shear sensitivity as a function of shear rate, exposure time, and surfactant composition, we observed that increased P188 concentration had the additional benefits of (1) stabilizing the cell suspension and preventing aggregation and adhesion of cells to surfaces and (2) decreasing foam stability of protein and Pickering foams during the cell death phase of the production bioreactor. These observations provide strong motivation to increase surfactant concentration in the medium. In Chapter 5, we explored several strategies of tuning the cell sensitivity and shear damage in an industrial CHO cell bioprocess using different Poloxamers and sparger designs. We showed that the CCM could be used to monitor cell shear sensitivity of the culture as an off-line analysis tool and found that cell sensitivity increased during the production

process. Increase in P188 concentration resulted in an immediate decrease in cell sensitivity, and robustness against higher shear environments. With an optimized media formulation, the cell culture viability was increased by 10% and lactase dehydrogenase (LDH) concentration was decreased by 40% at the end of the process.

6.2 Impact and future outlook

Although shear-induced damage is not an immediate bottleneck in the majority of current bioprocesses, the negative impact of recent Poloxamer lot-to-lot variations on the mammalian cell biotechnology industry has exposed gaps in the fundamental knowledge of colloidal interactions between bioparticles and revealed potential areas for improvement in the field [6]. Despite the industry shift towards chemically defined media components, processes are still susceptible to raw material variation due to the use of polymeric compounds with inherent molecular weight polydispersity. In addition, application of surfactants may be underutilized in both upstream and downstream processing; for example, recent studies have used surfactants to stabilize concentrated feed media solutions [7], and to precipitate proteins for enhanced recovery and separation [8]. These examples demonstrate that there is a large space for further research and innovation by applying fundamental colloidal principles to complex bioprocessing systems.

Prior to our research, agreement on the primary mechanism of surfactant-mediated cell protection has been split between surfactant interaction with gas bubbles, and surfactant interaction with the cell membrane interface. We have collected significant evidence that surfactant-cell interactions are primarily responsible for the observed increase in cell robustness. To our knowledge, we are the first to demonstrate that the surfactant's capacity to protect cell culture correlates with its ability to increase cell membrane order, while comparing two types of surfactants with similar cell-bubble attachment rates. This knowledge may lead to a shift in

paradigm in the biotechnology industry. Since the mechanical properties of the cell membrane are a function of the membrane fluidity, the cell robustness can either be tuned by adsorption of surface active compounds, or through cell line engineering. As the currently used Poloxamers eventually will reach the limit of their efficacy [9], improved surfactants will be needed to further push the limits of cell culture processes. To accomplish this, structure-performance relationships should be developed to formulate design principles for future new cell protective compounds. While we hypothesize that Poloxamer 188 is more effective than Poloxamer 407 in protecting cells due to its high hydrophilicity, further studies using a wide range of molecular weights and hydrophilicities are necessary to expand these insights.

In addition to Poloxamers, additional classes of compounds should also be investigated. Ideally, candidates should be well-defined molecules to avoid inconsistent molecular weight distributions. This precludes compounds such as polyvinyl alcohol, methylcellulose, and polyvinyl pyrrolidone, which have been previously studied for use as cell protectants, because they are all susceptible to raw material variability [10–12]. In a recent effort to find an alternative shear protectant, researchers screened small-molecule surfactants based on their surface activities (dynamic surface tension) and cell-bubble attachment rates [13]. In light of our findings, we propose that future studies should also focus on the compounds' interaction with the cell membranes. The methods we have developed, including the CCM and pyrene excimer fluorescence ratio, enable means to execute such experiments with high throughput efficiency. We envision a comprehensive strategy that begins with choosing a highly robust cell clone with strong intrinsic mechanical stability. Next, an additive with optimal surfactant-cell interactions would be selected based on a set of predetermined screening criteria (cytotoxicity, cell membrane fluidity, surface tension, etc.). As a result, shear damage would be minimized during subsequent process

development and scale-up of this cell line, enabling high gas flow rates and agitation speeds to meet mass transfer and nutritional demands of the high-density cell culture.

Our studies have also revealed that the origins and the role of bioreactor foam stability are insufficiently understood and still rely heavily on empirical practice. This gap in knowledge is partially attributed to the rapid rate at which biotechnology has developed, but also comes from the complexity and inherent variability in animal cell culture. Variations in hydrodynamic flow, bubble dispersion, vessel geometry, and media composition can all lead to unpredictable foam generation rates. The current state-of-the-art in foam control for bioprocesses relies on 'as-needed' dosages of particle-in-oil antifoam emulsions [14]. This strategy can be subjective and inconsistent, with variable amounts of antifoam added to each batch. It is clear that our understanding and control of the colloidal interactions during bioreactor operation have not progressed at the same rate as our understanding of molecular processes within cells. Alternative strategies such as physical defoaming with temperature gradients, mechanical breakdown, sonication, and electric field have been explored in research, but further studies are needed to improve antifoaming efficiency and gain industry acceptance [15].

A

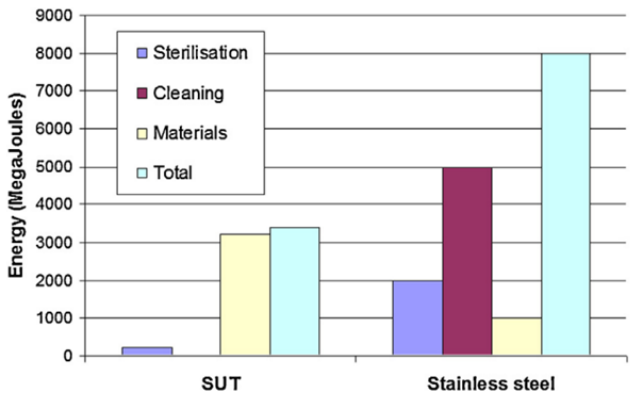

B

Category	Parameter	SUT (% of change)
Utility requirements	Water consumption	−87
Materials	Cleaning materials	−95
Consumables	Plastics disposal	+5
Labour	Labour headcount	−21
Space	Facility footprint	−38
Electricity	Electricity consumption	−30
	HVAC operations	−29
Steelwork	Stainless steel	−62
Carbon	CO_2 emissions	−25.5

Figure 6.1: (A) Comparison between energy costs of traditional stainless-steel bioreactor tanks and single use technologies (SUT) for biopharmaceutical production. (B) Environmental impact of SUT compared to traditional processing equipment [16].

The research in this dissertation was focused on investigating the interfacial interactions in traditional stirred-tank bioreactors made from stainless steel. In recent years, however, the biomanufacturing industry has begun to shift towards single-use technologies (SUT). These technologies use vessels that are composed of pre-sterilized polymer bags with plug-and-play probes. They are becoming increasingly popular due to their flexibility, low short-term cost, and sustainability (**Figure 6.1**) [16]. They are also ideal to meet rapid process development demands for clinical trials. Although the principles and concepts developed in this work also apply to SUTs, the introduction of this new technology results in additional considerations and complexities in the colloidal and interfacial interactions of the system. For example, leachable compounds from these

SUTs have been of major concern in terms of cytotoxicity [17], but they can also have undesirable implications in the system's interfacial interactions. Thus, one would need to investigate a number of interfacial and cell-surfactant interactions in SUTs in order to achieve fundamental understanding of the principles of their operation. This exciting and evolving field will undoubtedly continue to progress at an exponential rate, providing numerous opportunities for therapeutic and research innovations. We hope that the results of this dissertation will contribute to this expanding field, and ultimately enable further bioprocess intensification.

Acknowledgements

The authors gratefully acknowledge Biogen (Research Triangle Park, NC) for financial support of this study. We also thank Douglas Osborne, Kevin Chang, An Zhang, Kelly Wiltberger, Weiwei Hu and Dane Grismer for all of their discussion and support.

6.3 References

[1] H.E. Swim, R.F. Parker, Effect of Pluronic F68 on Growth of Fibroblasts in Suspension on Rotary Shaker, Exp. Biol. Med. 103 (1960) 252–254.

[2] W. Hu, C. Berdugo, J.J. Chalmers, The potential of hydrodynamic damage to animal cells of industrial relevance: current understanding., Cytotechnology. 63 (2011) 445–60. doi:10.1007/s10616-011-9368-3.

[3] F.M. Wurm, Production of recombinant protein therapeutics in cultivated mammalian cells., Nat. Biotechnol. 22 (2004) 1393–1398. doi:10.1038/nbt1026.

[4] A.A. Shukla, U. Gottschalk, Single-use disposable technologies for biopharmaceutical manufacturing, Trends Biotechnol. 31 (2013) 147–154. doi:10.1016/j.tibtech.2012.10.004.

[5] D. Chang, R. Fox, E. Hicks, R. Ferguson, K. Chang, D. Osborne, et al., Investigation of interfacial properties of pure and mixed poloxamers for surfactant-mediated shear protection of mammalian cells, Colloids Surfaces B Biointerfaces. 156 (2017) 358–365. doi:10.1016/j.colsurfb.2017.05.040.

[6] H. Peng, A. Ali, M. Lanan, E. Hughes, K. Wiltberger, B. Guan, et al., Mechanism investigation for Poloxamer 188 raw material variation in cell culture, Biotechnol. Prog. 32 (2016) 767–775. doi:10.1002/btpr.2268.

[7] P. Hossler, S. Mcdermott, C. Racicot, J.C.H. Fann, Improvement of mammalian cell culture performance through surfactant enabled concentrated feed media, Biotechnol. Prog. 29 (2013) 1023–1033. doi:10.1002/btpr.1739.

[8] S.I. Cheng, D.C. Stuckey, Protein recovery from surfactant precipitation, Biotechnol.

Prog. 27 (2011) 1614–1622. doi:10.1002/btpr.671.

[9] J.J. Chalmers, Mixing, aeration and cell damage, 30+ years later: What we learned, how it affected the cell culture industry and what we would like to know more about, Curr. Opin. Chem. Eng. 10 (2015) 94–102. doi:10.1016/j.coche.2015.09.005.

[10] J.D. Michaels, J.E. Nowak, A.K. Mallik, K. Koczo, D.T. Wasan, E.T. Papoutsakis, Interfacial properties of cell culture media with cell-protecting additives, Biotechnol. Bioeng. 47 (1995) 420–430. doi:10.1002/bit.260470403.

[11] D.W. Murhammer, C.F. Goochee, Scaleup of Insect Cell Cultures: Protective Effects of Pluronic F-68, Nat. Biotechnol. 6 (1988) 1411–1418.

[12] E.T. Papoutsakis, Media additives for protecting freely suspended animal cells against agitation and aeration damage, Trends Biotechnol. 9 (1991) 316–24. doi:10.1016/0167-7799(91)90102-N.

[13] W. Hu, J.J. Rathman, J.J. Chalmers, An investigation of small-molecule surfactants to potentially replace pluronic F-68 for reducing bubble-associated cell damage, Biotechnol. Bioeng. 101 (2008) 119–27. doi:10.1002/bit.21872.

[14] S. Xu, R. Jiang, R. Mueller, N. Hoesli, T. Kretz, J. Bowers, et al., Probing lactate metabolism variations in large-scale bioreactors, Biotechnol. Prog. (2018) 1–11. doi:10.1002/btpr.2620.

[15] B. Junker, Foam and its mitigation in fermentation systems., Biotechnol. Prog. 23 (2007) 767–84. doi:10.1021/bp070032r.

[16] A.G. Lopes, Single-use in the biopharmaceutical industry: A review of current technology

impact, challenges and limitations, Food Bioprod. Process. 93 (2015) 98–114. doi:10.1016/j.fbp.2013.12.002.

[17] M. Hammond, L. Marghitoiu, H. Lee, L. Perez, G. Rogers, Y. Nashed-Samuel, et al., A cytotoxic leachable compound from single-use bioprocess equipment that causes poor cell growth performance, Biotechnol. Prog. 30 (2014) 332–337. doi:10.1002/btpr.1869.